INFORMATION TO USERS

This manuscript has been reproduced from the microfilm master. UMI films the text directly from the original or copy submitted. Thus, some thesis and dissertation copies are in typewriter face, while others may be from any type of computer printer.

The quality of this reproduction is dependent upon the quality of the copy submitted. Broken or indistinct print, colored or poor quality illustrations and photographs, print bleedthrough, substandard margins, and improper alignment can adversely affect reproduction.

In the unlikely event that the author did not send UMI a complete manuscript and there are missing pages, these will be noted. Also, if unauthorized copyright material had to be removed, a note will indicate the deletion.

Oversize materials (e.g., maps, drawings, charts) are reproduced by sectioning the original, beginning at the upper left-hand corner and continuing from left to right in equal sections with small overlaps. Each original is also photographed in one exposure and is included in reduced form at the back of the book.

Photographs included in the original manuscript have been reproduced xerographically in this copy. Higher quality 6" x 9" black and white photographic prints are available for any photographs or illustrations appearing in this copy for an additional charge. Contact UMI directly to order.

UMI

A Bell & Howell Information Company
300 North Zeeb Road, Ann Arbor MI 48106-1346 USA
313/761-4700 800/521-0600

ESTIMATING CROP YIELDS BY INTEGRATING THE FAO CROP SPECIFIC WATER BALANCE MODEL WITH REAL-TIME SATELLITE DATA AND GROUND-BASED ANCILLARY DATA

by

Curt Andrew Reynolds

A Dissertation Submitted to the Faculty of the

DEPARTMENT OF AGRICULTURAL AND BIOSYSTEMS ENGINEERING

In Partial Fulfillment of the Requirements
For the Degree of

DOCTOR OF PHILOSOPHY

In the Graduate College

THE UNIVERSITY OF ARIZONA

1 9 9 8

THE UNIVERSITY OF ARIZONA ®
GRADUATE COLLEGE

As members of the Final Examination Committee, we certify that we have read the dissertation prepared by Curt Andrew Reynolds

entitled Estimating Crop Yields by Integrating the FAO Crop Specific Water Balance Model with Real-time Satellite Data and Ground-based Ancillary Data

and recommend that it be accepted as fulfilling the dissertation requirement for the Degree of Doctor of Philosophy

Muluneh Yitayew — Date 4/2/98

Donald C. Slack — Date 4/2/98

Alfredo Huete — Date 4/2/98

Charles F. Hutchinson — Date 4/2/98

Margaret S. Petersen — Date 4/2/98

Final approval and acceptance of this dissertation is contingent upon the candidate's submission of the final copy of the dissertation to the Graduate College.

I hereby certify that I have read this dissertation prepared under my direction and recommend that it be accepted as fulfilling the dissertation requirement.

Dissertation Director — Date 4/16/98

Muluneh Yitayew

STATEMENT BY AUTHOR

This dissertation has been submitted in partial fulfillment of requirements for an advanced degree at The University of Arizona and is deposited in the University Library to be made available to borrowers under rules of the Library.

Brief quotations from this dissertation are allowable without special permission, provided accurate acknowledgment of source is made. Requests for permission for extended quotation from or reproduction of this manuscript in whole or in part may be granted by the copyright holder.

SIGNED: Curt A. Reynolds

ACKNOWLEDGEMENTS

I would like to express my sincere gratitude to my major advisor, Dr. Muluneh Yitayew, for his constant assistance, guidance, and advice throughout my graduate education. I also wish to thank my graduate committee members consisting of Dr. Donald C. Slack, Dr. Alfredo Huete, Dr. Charles F. Hutchinson, and Prof. Margaret Petersen, for their sagacious advice.

I am also very grateful to the Department of Agricultural and Biosystems Engineering for giving me the opportunity to start and finish a Ph.D. program. I am especially grateful to Drs. Slack and Yitayew who made it possible by providing the initial two years of financial support. Similarly, I wish to acknowledge financial support received from the NASA Earth System Science Fellowship and from the American Geophysical Union through the Horton Research Grant.

I also wish to thank the Office of Arid Lands Studies and Dr. Charles Hutchinson for their assistance in helping me find a research topic related to Early Warning Systems. I especially would like to thank Eric Pfirman for his technical support and quick troubleshooting abilities during the course of this study.

Special thanks are extended to the many people and organizations who provided office accommodation, data, or advice during various phases of this research. In particular, I would like to thank the Regional Centre for Services in Surveying, Mapping, and Remote Sensing for allowing me to base my research in their Nairobi office for more than one year. Likewise, I would like to thank Drs. Compton Tucker and Chris Justice at the NASA Goddard Space Flight Center for their advice and cooperation while I participated in the Graduate Student Summer Program sponsored by the Universities Space Research Program. Finally, I would like to thank the Kenya Meteorological Department, Kenya Ministry of Agriculture, Kenya Department of Resource Surveys and Remote Sensing, FEWS-Nairobi office, and Rene Gommes and Fred Snijders from the FAO-Rome for their kind cooperation in providing data.

In closing, I wish to thank my family and friends for their patience and encouragement during the years I studied at the University of Arizona.

TABLE OF CONTENTS

TABLE OF CONTENTS-*Continued*

LIST OF ILLUSTRATIONS

LIST OF ILLUSTRATIONS-*Continued*

LIST OF TABLES

LIST OF SYMBOLS AND ACRONYMS

AEZ	Agro-Ecological Zones
AGRHYMET	Agro-Hydrometeorology program based in Niamey, Niger, and serving CILSS member countries
AgRISTARS	Agriculture and Resources Inventory Surveys Through Aerospace Remote Sensing, USDA
AISC	Assessment and Information Services Center, NESDIS, NOAA
ARS	Agricultural Research Service, USDA
ARTEMIS	Africa Real Time Environmental Monitoring Information System, FAO
ASAL	Arid and Semi-Arid Lands
AVHRR	Advance Very High Resolution Radiometer satellite sensor
BATS	Bioshpere-Atmosphere Transfer Scheme for vegetation Classification
CBS	Central Bureau of Statistics, GoK
CCD	Cold Cloud Duration
CPC	Climate Prediction Center, NOAA
CILSS	Comite Permanent Inter-Estats Lutte Contre la Secheresse dans le Sahel(Burkino Faso, Cape Verde, Chad, Gambia, Guinea-Bissau, Mali, Mauritania, Niger, and Senegal)
CPSZ	Crop Production System Zone
CSWB	Crop Specific Water Balance
D	Soil water deficit, mm or mm/dekad
DEM	Digital Elevation Model
DMC	Drought Monitoring Centre, UNDP, Nairobi, Kenya
DP	Deep percolation, mm

LIST OF SYMBOLS AND ACRONYMS-*Continued*

DRSRS	Department of Resources Surveys and Remote Sensing, Government of Kenya
D	Soil water deficit, mm/dekad
D_{rz}	Depth of root zone, m
EDC	EROS Data Center, USGS, Sioux Falls, South Dakota
EGP	End of Growing Period, dekad
EMC	Environmental Modeling Center, NOAA
ENSO	El Niño/Southern Oscillation
EOS	Earth Observing System
EROS	Earth Resources Observation Systems
ESA	European Space Agency
ET_a	Actual crop evapotranspiration, mm/day or mm/dekad
ET_m	Maximum crop evapotranspiration, mm/day or mm/dekad
EU	European Union
EW/CCA	Early Warning and Crop Condition Assessment
EWS	Early Warning Systems
FAO	Food and Agricultural Organization, UN
FAS	Foreign Agriculture Service, USDA
FC	Field Capacity of the soil, mm/m
FCCAD	Foreign Crop Condition Assessment Division, FAS, USDA
FEWS	Famine Early Warning System, USAID
GAC	Global Area Coverage, (approximately 7.6 by 7.6 kilometer resolution near the equator)

LIST OF SYMBOLS AND ACRONYMS-*Continued*

GDD	Growing Degree Days
GIEWS	Global Information and Early Warning System, FAO
GIMMS	Global Inventory Monitoring and Modeling Studies, GSFC, NASA
GIS	Geographic Information Systems
GoK	Government of Kenya
GPI	Global Precipitation Index
GSFC	Goddard Space Flight Center, NASA, Greenbelt, Maryland
GTS	Global Telecommunication System
HRPT	High Resolution Picture Transmission ground receiving station
IDA	Image Display Analysis software
IGAD	Intergovernmental Authority on Development (Djibouti, Ethiopia, Eritrea, Kenya, Somalia, the Sudan, and Uganda), formerly the Intergovernmental Authority of Drought and Desertfication (IGADD)
IGT	IDA GIS Tools software
ITCZ	Inter-Tropical Convergence Zone
KMD	Kenya Meteorological Department, Nairobi, Kenya
K_c	Crop Coefficient
K_y	Yield reduction factor
LAC	Local Area Coverage, (approximately 1.1 by 1.1 kilometer resolution at the equator)
LACIE	Large Area Crop Inventory Experiment, USDA
LAI	Leaf Area Index

LIST OF SYMBOLS AND ACRONYMS-*Continued*

LGP	Length of Growing Period, dekad
MAD	Maximum Allowable Depletion, percent
MARS	Monitoring Agriculture with Remote Sensing Project, European Union
MoA	Ministry of Agriculture, Kenya
MODIS	Moderate Imaging Spectroradiometer
NASA	National Aeronautics and Space Administration
NCPB	National Cereals and Produce Board, GoK
NDVI	Normalized Difference Vegetation Index
NESDIS	National Environmental Satellite Data and Information Service, NOAA
NIR	Near Infrared
NOAA	National Oceanic and Atmospheric Administration
OFDA	Office of United States Foreign Disaster Assistance
P_a	Actual Precipitation, mm or mm/dekad
P_{eff}	Effective Precipitation, mm
PET	Potential Evapotranspiration
POES	Polar-Orbiting Operational Environmental Satellites
PWP	Permanent Wilting Point, mm/m
ρ_n	Near-infrared reflectance
ρ_r	Red reflectance
RAW	Readily Available Water, mm

LIST OF SYMBOLS AND ACRONYMS-*Continued*

RCSSMRS	Regional Centre for Services in Surveying, Mapping, and Remote Sensing, Nairobi, Kenya
RFE	Rainfall Estimate, mm/dekad
RO	Runoff, mm or mm/dekad
S	Soil moisture content in the root zone, mm
SADC	Southern African Development Community (Angola, Botswana, Lesotho, Malawi, Mauritius, Mozambique, Namibia, South Africa, Swaziland, Tanzania, Zambia, and Zimbabwe)
SAVI	Soil Adjusted Vegetation Index
SEDI	Satellite Enhanced Data Interpolation
SGP	Start of Growing Period, dekad
SPOT	French Satellite Probatoire d'Observation de la Terre
T_{base}	Base Temperature, degrees Celsius
T_{max}	Maximum Temperature, degrees Celsius
T_{min}	Minimum Temperature, degrees Celsius
UN	United Nations
UNDP	United Nations Development Programme, UN
USAID	United States Agency for International Development
USDA	United States Department of Agriculture
USGS	United States Geological Survey
VAST	Vegetation Analysis in Space and Time software
W	Water Requirements of Crop, mm/dekad
WHC	Water Holding Capacity, mm

LIST OF SYMBOLS AND ACRONYMS-*Continued*

WINDISP3	Windows-based IDA software
WMO	World Meteorological Organization, UN
WR	Maximum Plant Water Requirement, mm
WRSI	Water Requirement Satisfaction Index
WWW	World Wide Web
Y_a	Actual Yield, kg/ha or metric tons/ha
Y_m	Maximum Yield, kg/ha or metric tons/ha

ABSTRACT

The broad objective of this research was to develop a spatial model which provides both *timely* and *quantitative* regional maize yield estimates for real-time Early Warning Systems (EWS) by integrating satellite data with ground-based ancillary data. The Food and Agriculture Organization (FAO) Crop Specific Water Balance (CSWB) model was modified by using the real-time spatial data that include: dekad (ten-day) estimated rainfall (RFE) and Normalized Difference Vegetation Index (NDVI) composites derived from the METEOSAT and NOAA-AVHRR satellites, respectively; ground-based dekad potential evapo-transpiration (PET) data and seasonal estimated area-planted data provided by the Government of Kenya (GoK).

A Geographical Information System (GIS) software was utilized to: drive the crop yield model; manage the spatial and temporal variability of the satellite images; interpolate between ground-based potential evapo-transpiration and rainfall measurements; and import ancillary data such as soil maps, administrative boundaries, etc.. In addition, agro-ecological zones, length of growing season, and crop production functions, as defined by the FAO, were utilized to estimate *quantitative* maize yields.

The GIS-based CSWB model was developed for three

different resolutions: agro-ecological zone (AEZ) polygons; 7.6-kilometer pixels; and 1.1-kilometer pixels. The model was validated by comparing model production estimates from archived satellite and agro-meteorological data to historical district maize production reports from two Kenya government agencies, the Ministry of Agriculture (MoA) and the Department of Resource Surveys and Remote Sensing (DRSRS).

For the AEZ analysis, comparison of model district maize production results and district maize production estimates from the MoA (1989-1997) and the DRSRS (1989-1993) revealed correlation coefficients of 0.94 and 0.93, respectively. The comparison for the 7.6-kilometer analysis showed correlation coefficients of 0.95 and 0.94, respectively. Comparison of results from the 1.1-kilometer model with district maize production data from the MoA (1993-1997) gave a correlation coefficient of 0.94. These results indicate the 7.6-kilometer pixel-by-pixel analysis is the most favorable method. Recommendations to improve the model are finer resolution images for area planted, soil moisture storage, and RFE maps; and measuring the actual length of growing season from a satellite-derived Growing Degree Day product.

1. INTRODUCTION

Drought is a common occurrence in Africa and often leads to widespread famine. In response to the human suffering associated with droughts, several regional and national Early Warning Systems (EWS) have been established in Africa to provide advance warning of droughts that may cause temporary or prolonged food shortages. Most of the EWS stations operating today can provide national governments with *qualitative* assessments of crop conditions from real-time satellite data, but operational models that provide *quantitative* assessments for specific crops are still in a very early stage of development at this time.

Utilizing remote sensing methodologies to estimate and forecast crop yields on a national and regional scale is becoming increasingly more important for both developed and developing countries as most agricultural monitoring still relies heavily on agricultural field reports. Such field reports are often subjective, costly, and prone to large errors due to incomplete ground observations, inaccuracies from estimating crop area, poor crop yield assessment techniques, or inadequate networks. In addition, national crop yields in Africa may be intentionally reported inaccurately for a variety of social, political, or economic

reasons. In contrast, estimating regional crop yields by integrating crop yield models with real-time satellite technology gives the potential to estimate regional yields by non-biased, analytical, empirical, and spatial methods. While estimating regional crop yield based on real-time satellite technology will also have errors, at least these models have the potential to be more objective than subjective ground surveys. Crop yield models integrated with real-time satellite data also have the potential to improve in the future as satellite technologies improve.

1.1 Statement of Problem

The Africa Real-time Environmental Monitoring Information System (ARTEMIS) was established by the Food and Agriculture Organization (FAO) in the late 1980s to develop and distribute satellite images to regional EWS stations (Hielkema, et al, 1986; Hielkema, 1991). ARTEMIS is basically an automated satellite system that provides rainfall and vegetation cover data on a dekad (ten-day) and monthly basis for agriculture crop assessment. ARTEMIS uses the geostationary METEOSAT satellite, operated by the European Space Agency (ESA), to estimate rainfall. It also uses the polar-orbiting Advanced Very High Resolution Radiometer (AVHRR), operated by the U.S. National Oceanic

and Atmospheric Administration (NOAA), to monitor vegetation growth by utilizing a Normalized Difference Vegetation Index (NDVI).

ARTEMIS data are commonly used by EWS stations to determine *qualitative* regional vegetation anomalies by subtracting the current NDVI image from the average historical NDVI image of the same month. The underlying assumption is that vegetation greenness is related to rainfall (Henricksen and Durkin, 1985 and 1986; Malo and Nicholson, 1990; Davenport and Nicholson, 1993; Justice, et al, 1986; Justice, et al, 1991). For many years, *qualitative* crop conditions from the NDVI archive (from 1981-present) has helped EWS stations in Africa to determine the relative severity of drought, making the NDVI archive one of the most important remote sensing databases for monitoring the response of vegetation to weather conditions in Africa. However, current NDVI satellite-derived products cannot yet provide governments with *quantitative* assessments.

Accordingly, operational models that provide *quantitative* crop yield estimates for specific crops are one of the tools most needed by regional and government decision-makers. Eilerts (1993) states that, despite advances in satellite technology, remote sensing data

provided to EWS stations cannot yet answer the two questions most frequently asked by government officials: "How many people are affected?" and "How much food is needed?" These *quantitative* questions cannot be answered at this time largely because (Hutchinson, 1991; and Hutchinson, et al, 1993):

- *Qualitative* NDVI assessment techniques cannot answer *quantitative* crop yield questions.
- A direct relationship between NDVI and crop yield does not exist.
- A single crop assessment method does not exist due to mixture of vegetation within each pixel.
- Complex crop yield models with numerous parameters make development of operational models difficult.
- Trade-off between spatial scale and temporal frequency of satellites causes technical problems.

Even though the use of vegetation indices is one of the most widely used concepts to separate, within a given pixel, the percent of vegetation cover and soil, only *qualitative* crop yield models on a regional scale have been developed from spectral vegetation indices. The main problem associated with estimating yields from vegetation indices is that the exact relationship between vegetation indices and crop yield is not yet known. In addition, each pixel from low spatial resolution satellite data measures a mixture of vegetation greenness that makes it difficult to discriminate and monitor the growth of one crop.

The main problem associated with scale of satellite data is the trade-off that exists between temporal frequency and spatial resolution of satellite data. For example, the higher spatial resolution satellites, such as the United States Landsat series (30-80 meters) and the French SPOT series (10-20 meters), can distinguish specific crops. But these satellites cannot easily monitor seasonal plant growth because cloud cover during the growing season often prevents data collection at the time of their infrequent orbits (every 16-26 days). In contrast, the NOAA-AVHRR satellites have high temporal frequency (at least once daily), but specific crop condition assessments from these satellites are limited because their lower spatial resolution (1000-4000 meters) prevents distinguishing specific crops or determining the size of fields for area-planted estimates.

1.2 Definition of Objectives

The ground-based FAO Crop Specific Water Balance (CSWB) model utilizes agro-meteorological data to estimate crop condition at a specific site, but remote sensing data in combination with a GIS have not yet been incorporated into the model to estimate national crop yields (Hutchinson, et al, 1993). Therefore, the main objective of this research was to develop a model that integrates the FAO CSWB model

with real-time satellite data and ground-based ancillary data. GIS software was used to:

- Drive the crop yield model.
- Manage and measure the spatial and temporal variability of each parameter within the crop yield model.
- Interpolate between ground-based potential evapotranspiration and rainfall measurements.
- Integrate ground-based data with real-time satellite data
- Import ancillary data such as soil maps, administrative boundaries, and agro-meteorological stations, etc.

The main purpose for introducing real-time satellite data into the ground-based CSWB model is to provide *timely* and *quantitative* regional maize yield estimates at the end of each growing season. An objective and timely methodology can benefit national governments in determining how much food to import or export at the end of the growing season, long before food stocks are depleted and a food-shortage crisis occurs. It also is envisaged that the GIS-based crop yield model developed by this research can later be extended to estimate crop yields for other crops and applied to larger regions within Africa such as Intergovernmental Authority on Development (IGAD) or the Southern Africa Development Community (SADC) member countries.

The specific research objectives are:

1. Modify the FAO CSWB model by introducing real-time satellite data.

2. Develop an analytical and spatial model to estimate *quantitative* maize yields at the end of each growing season.

3. Utilize a common and affordable GIS to manage the temporal and spatial changes of model parameters.

4. Statistically validate the real-time crop yield model by comparing model yield estimates from archived satellite data to reported maize yields from two Kenya government agencies.

5. Develop an operational GIS-based crop yield model that can be enlarged for other countries or extended to other crops.

1.3 Scope of Study

Kenya was chosen as the initial region of analysis because the climate and agriculture within Kenya are diverse and representative of the IGAD region (Figure 1.1).

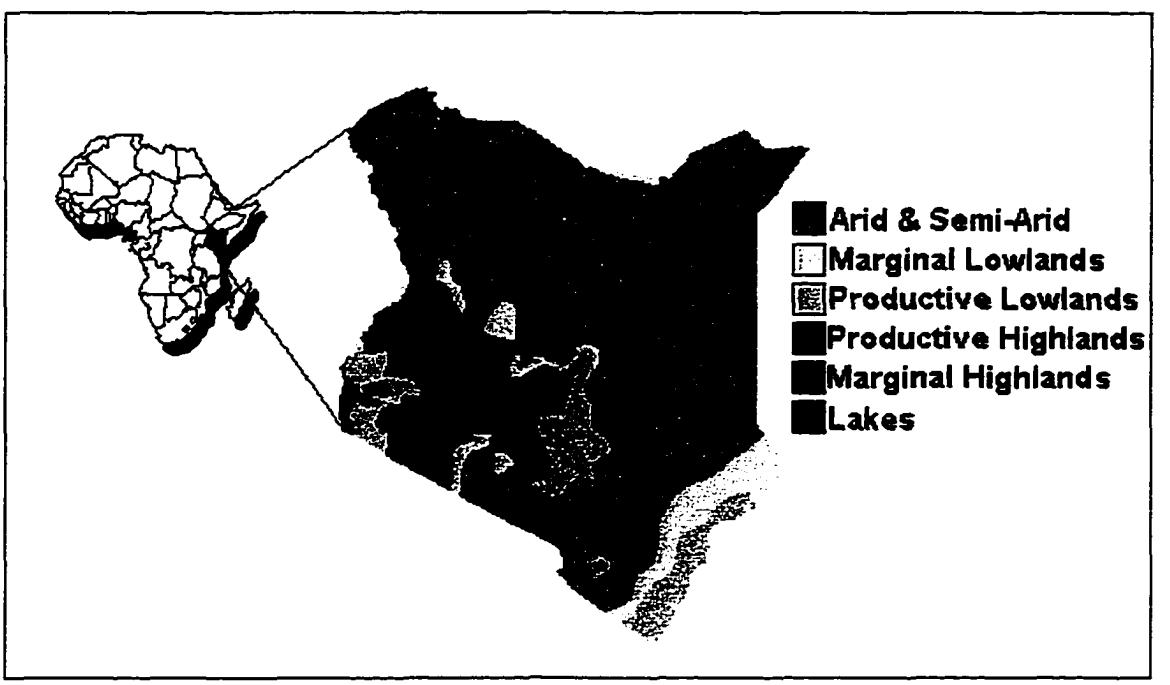

Figure 1.1. Crop Productivity Zones in Kenya

Some 75 percent of the land area in Kenya is classified as arid and semi-arid lands (ASAL). The remaining land area is at higher elevations where the bulk of cereals and grains are grown in small landowner plots under rain-fed conditions.

In addition, Kenya was chosen as the region of study because:

1. The Regional Centre for Surveying, Mapping, and Remote Sensing (RCSSMRS) is based in Nairobi, Kenya, and serves the IGAD region with early warning and remote sensing data. Presently, RCSSMRS processes real-time NDVI composites with Local Area Coverage (1.1-kilometer resolution)for the IGAD region (Figure 1.2).

2. A soil classification image for Kenya with a 1:1 million scale (1-kilometer resolution) was developed by the FAO (Kassam, et al, 1993a and 1993b).

3. Ground-based crop yield, production figures, and agro-meteorological data are available in Kenya due to the relative high level of development and stability of the country.

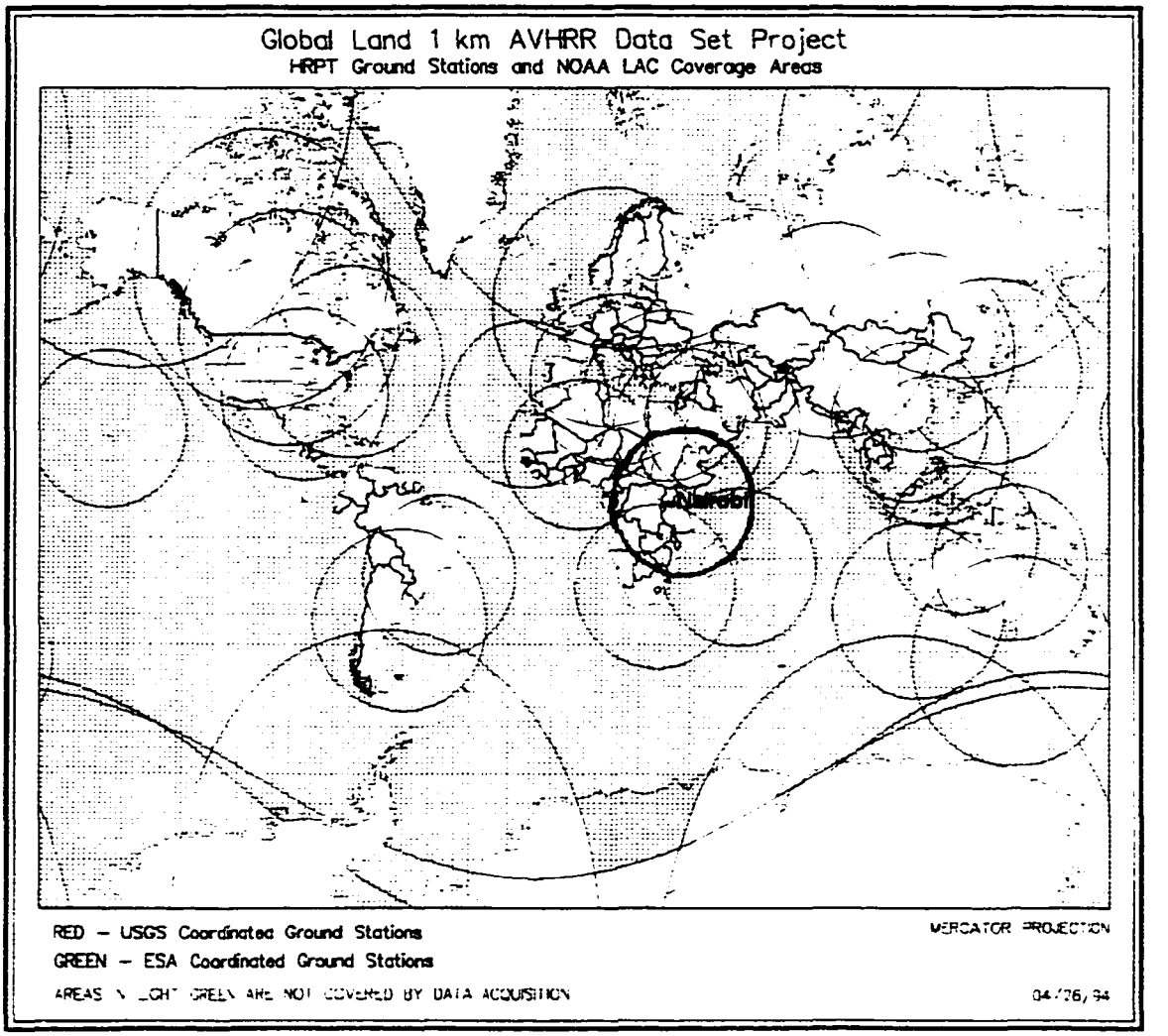

Figure 1.2. Location of HRPT Stations for Receiving LAC (1.1-kilometer resolution) Data from NOAA-AVHRR Satellite Series (from Eidenshink and Faundeen, 1996)

The FAO CSWB model was chosen because it is an operational ground-based model commonly used in Africa which can be integrated with crop production functions to provide *quantitative* crop yield estimates (Negre, 1994, and Gommes, 1983). A water balance model is simple, but a physically sound approach to monitor crop growth during the growing

season. Water balance growth models are based on ground agro-meteorological data, and require large amounts of input data. They have also been proven to be accurate and easily operational when compared to other crop growth models such as growth-simulation or statistical-regression models (FAO, 1986), largely because water is the major driving force for crop yield reductions during periods of drought. However, water balance models have been largely neglected in most crop yield models integrated with remote sensing data, even though the water balance method is one of the most reliable methods for analyzing ground-based agro-meteorological data.

Maize (*Zea mays*) was chosen as the crop to be analyzed because maize is the major staple food in East Africa, and it is the major grain imported as food aid during years of drought and famine. Also, *quantitative* maize yields can be predicted by introducing water versus crop yield functions in the CSWB model as described by Gommes (1983). Crop production functions were originally defined by Stewart and Hagan (1973), Stewart, et al, (1975), and later developed by the FAO (Doorenbos and Kassam (1979), with specific crop production functions for Katumani maize in Kenya developed by Stewart and Hash (1982).

RFE and NDVI data were chosen for integration into the CSWB model because they are the most common tools used by

EWS stations. With advent of RFE images in the mid-1990s, it became possible to estimate crop yields by integrating real-time RFE and NDVI images into the CSWB model. At present, the Famine Early Warning System (FEWS) project, sponsored by the United States Agency for International Development (USAID), provides an historical archive of the following real-time and dekad image composites on their home page (FEWS, 1998):

- Estimated rainfall (RFE)
- Normalized Difference Vegetation Index (NDVI)

These images are archived by the EROS Data Center and have a 7.6-kilometer spatial resolution with Hammer-Aitoff projections.

Utilizing a GIS software is implicit for running the model and for estimating agricultural crop yields because GIS permits the capture, storage, manipulation, and display of spatial data. These GIS functions are ideal for monitoring and estimating national agriculture yields and total production because several different types of geographic information must be monitored during the cropping season.

The GIS software chosen for this study is IDA GIS Tools (IGT), which is available free of charge from the FAO, and can be used on any DOS- or Windows-based personal computer

(Hoefsloot, 1996). IGT was chosen because it was specifically developed to provide GIS capabilities for EWS stations and ARTEMIS satellite images are typically stored at these stations in Image Display Analysis (IDA) format. Since IGT is completely compatible with IDA format images, only one GIS archive in IDA format must be maintained by EWS stations. Running the FAO crop yield model with another GIS software would require two separate digital archives, one for IDA images and another for the GIS. Therefore, other GIS software programs were purposely not chosen to spare EWS stations from having to maintain two separate digital archives or from purchasing expensive computer software and hardware.

Three spatial resolutions were chosen to run the GIS-based CSWB model; large agro-ecological (AEZ) polygons, 7.6-kilometer and 1.1-kilometer pixels. AEZ polygons were chosen as the coarsest resolution to take advantage of the Crop Production System Zone (CPSZ) database developed by the FAO (van Velthuizen, et al, 1995). A 7.6-kilometer database was chosen because this resolution is commonly used by EWS stations from Cold Cloud Duration (CCD) images re-projected from METEOSAT images with 5-km resolution and Normalized Difference Vegetation Index (NDVI) images re-projected from NOAA-AVHRR images with Global Area Coverage (GAC, or 4-km

resolution). The moderate resolution of 1.1-kilometer was chosen as the finest resolution because:

- Real-time dekad NDVI composites with LAC (1.1-kilometer) resolution are available for Kenya from the Department of Resource Surveys and Remote Sensing (DRSRS) and the RCSSMRS.
- Digital Elevation Models (DEM), soils, vegetation, and dekad NDVI composites with 1-kilometer resolution are available from the Global 1-KM Data Set Project (Eidenshink, and Faundeen, 1996).
- Soil images with 1-kilometer resolution have been developed by the FAO (Kassam, et al, 1993).

The period of analysis for this study is from 1989-1997. The starting year of 1989 was chosen because this is when the ARTEMIS archive begins. Nine years of data provides a sufficient sample size for determining the accuracy of the model because approximately 30 out of 41 districts within Kenya produce maize each year. Therefore, a total sample size of approximately 270 maize producing district estimates were available to give an indication of whether the model can be used in the future with relative confidence.

2. LITERATURE REVIEW

2.1 Agriculture Monitoring by Remote Sensing

One of the first attempts to apply satellite data to agricultural crop production was the Large Area Crop Inventory Experiment (LACIE) program from 1974-1980, a cooperative project of the United States Department of Agriculture (USDA), National Oceanic and Atmospheric Administration (NOAA), and National Aeronautics and Space Administration (NASA). The main objective of LACIE was to develop an experimental wheat production forecast program using Landsat data, and in the later years, the program was extended to other crops. The LACIE program revealed that using Landsat data for agricultural monitoring had two disadvantages: large amounts of data were stored, and cloud cover during the growing season often prevented data collection at a particular area because Landsat passed the same area only once every 18-days (Lecompte, 1989).

In the early 1980s, the Agriculture and Resources Inventory Surveys Through Aerospace Remote Sensing (AgRISTARS) program of the USDA-Agricultural Research Service (ARS) followed the LACIE program. AgRISTARS, through its Early Warning and Crop Condition Assessment Program (EW/CCA), pioneered early research associated with using NOAA's Advance Very High-Resolution Radiometer (AVHRR)

satellite (Boatwright and Whitehead, 1986). The EW/CCA project was one of eight AgRISTARS projects, and it recognized the AVHRR-NOAA satellite series was more useful for agricultural crop assessment because of its frequent orbits (at least once daily). The AVHRR-NOAA satellite series is still very popular today for crop condition assessments. Another major accomplishment of the EW/CCA program included the development of crop-yield reduction models based on crop-stress indicators, and the program explored the effects of cloud contamination, canopy structure, solar zenith angle, scan angle, and spectral characteristics of soils and vegetation

In the 1980s, remote sensing crop assessment projects in the United States shifted from a national to an international scale as all models developed by the EW/CCA project were transferred to the Foreign Crop Condition Assessment Division (FCCAD) of the Foreign Agriculture Service (FAS) within the USDA. FCCAD was established as an outgrowth from the LACIE program with the primary purpose of assessing and monitoring crop conditions in selected areas of the world, with the ultimate goal of quantifying crop assessments. The use of GIS was also highly recommended by this program for monitoring crop growth (Philipson and Teng, 1988).

In the early 1980s, the United States Agency for International Development (USAID) and the Office of U.S. Foreign Disaster Assistance (OFDA) also began to provide national and international agencies with brief, *qualitative* reports on the potential impact of weather variability on food crops. Initial work was conducted through the Assessment and Information Services Center (AISC) of the NOAA/National Environmental Satellite Data and Information Service (NOAA/NESDIS)(Johnson, et al, 1987a and 1987b; Sakamoto and Steyaert, 1987). Later, in 1985, USAID initiated several Famine Early Warning System (FEWS) projects in Africa as a response to the 1984-1985 famine in the Sahel region and Horn of Africa. The goals of USAID-sponsored FEWS project were to assist in targeting food aid and to provide government decision-makers with early warning of famine. To accomplish this, the FEWS project cooperated with the Global Information and Early Warning System (GIEWS) project of FAO to start the automated ARTEMIS satellite system that presently provides both RFE and NDVI data to regional Early Warning Systems (EWS) stations.

Simultaneously, many national and sub-regional EWS stations were also started on the African continent during the 1980s and 1990s. The three most notable regional programs in Africa are the:

1. *Agro-Hydrometeorology (AGRHYMET)* program: based in Niamey, Niger, which serves all Permanent Inter-State Committee on Drought Control (CILSS) member countries of Burkino Faso, Cape Verde, Chad, Gambia. Guinea-Bissau, Mali, Mauritania, Niger, and Senegal.

2. *Intergovernmental Authority on Development (IGAD)* regional remote sensing center at Nairobi, Kenya, which serves the member countries of Djibouti, Ethiopia, Eritrea, Kenya, Somalia, the Sudan, and Uganda; and the Drought Monitoring Centre (DMC) which also serves East Africa and is based in the Kenya Meteorological Department (KMD) at Nairobi.

3. *Southern African Development Community (SADC)* remote sensing center at Harare, Zimbabwe, which monitors the member countries of Angola, Botswana, Lesotho, Malawi, Mauritius, Mozambique, Namibia, South Africa, Swaziland, Tanzania, Zambia, and Zimbabwe.

These regional systems are supplied with RFE and NDVI satellite-derived products from the FEWS and ARTEMIS projects, and collect, store, and analyze ground-based information from local government agencies to determine the severity of drought. The results are then reported to national and international organizations.

Crop yield estimation by using remote sensing technologies also became more important on the European continent in the late 1980s, with the implementation of the Monitoring Agriculture with Remote Sensing (MARS) project. The purpose of the MARS project is to monitor agricultural seasonal conditions over member countries of the European Union (EU) and to make *quantitative* yield estimates at regional and national scales. Integrating a crop yield

model with real-time remote sensing data and a GIS (50-kilometer resolution), has been the main methodology of the MARS program (Vossen and Ruks, 1995).

2.2 Crop Growth Models

2.2.1 Ground-based Models

Baier (1977) classified ground-based crop-weather models in three categories; crop-growth simulation models, empirical-statistical models, and crop-weather analysis models. Crop-weather analysis models are the most widely used models for remote sensing purposes and yield forecasting because a limited number of parameters is required and fairly accurate results can be obtained (Barret, 1979; FAO, 1986a; Motha and Heddinghaus,1986; Horie, et al, 1992).

In crop-growth simulation models, the impact of physical (meteorological) variables is related to specific biological (plant) responses. These dynamic models are usually developed as precise and complicated research tools and cannot be used for operational crop assessments. They often require detailed data sets using very sophisticated and unconventional parameters.

The empirical-statistical models use regression techniques to relate specific weather variables to historical crop yields. They give good results for average

or near average conditions, but one major drawback is that they are often location-specific and may not reflect real conditions in extreme weather situations. In addition, these models may not be applicable to yield forecasting because the regression coefficients usually change with cultivars, crop-growth stage, and environment (Horie, et al, 1992).

In crop-weather, or simplified plant-process models, detailed physiological processes are replaced by simple relationships that describe crop-growth patterns. These models are often a combination of crop-growth simulation models and statistical-regression models. The FAO Crop Specific Water Balance (CSWB) Model is considered to be within the crop-weather category since the dynamic soil water balance equation is combined with a statistical calibration yield function to estimate crop yields.

2.2.2 Remote Sensing Approaches

For remote sensing models, Hatfield (1983), Wiegand, et al (1986), and Horie, et al (1992) note that researchers have basically developed simplified crop growth models based on spectral and thermal inputs, and biomass accumulations as affected by incident and intercepted photosynthetically-active radiation. Water balance models are also included in

this category, but they have not been extensively used for remotely sensed crop yield models, even though ground-based soil moisture models had higher correlation coefficients than growth-simulation or statistical-regression models (Baier and Robertson, 1968).

Integrating traditional ground-based crop yield models with real-time remote sensing data has become more popular, with several recent studies utilizing a GIS to account for the spatial and temporal variability of each crop yield parameter (Thornton, et al, 1997, Thornton, et al, 1995, and Vossen and Ruks, 1995). The main differences between these studies are generally related to the use of different satellite platforms, spatial scales, time increments, crop yield models, ground-based data, and GIS software that present different operational problems and final model results.

Crop yield models tend to vary from being simple (few input parameters) and easily operational, to being complex (many input parameters) and serving only as unique research tools that are impractical to operate on a real-time basis. In addition, GIS software programs tend to range from being inexpensive and featuring a small range of utilities, to being very expensive and requiring computer hardware not commonly available in developing countries.

The different satellite platforms tend to determine the spatial scale and time steps of the models, with a few researchers beginning to develop specific crop assessment models that utilize Local Area Coverage (LAC) from the NOAA-AVHRR satellite (Gallo and Flesch, 1989, and Quarmby, et al, 1993). LAC data provide the advantages of high temporal frequency (daily coverage) and moderate (1.1-kilometer) spatial resolution, but collecting and processing LAC data in Africa is typically done regionally which often makes these data sets not easily available.

2.3 FAO Crop Specific Water Balance Model (CSWB)

The FAO CSWB model was developed by Frère and Popov (1979) of the FAO (1986a) and was specifically designed for real-time operation. The CSWB model utilizes ground-based agro-meteorological data to estimate crop condition, and when combined with crop production functions the model can estimate yields. The CSWB model has five major components for calculating *quantitative* yield reductions:

- Real-time input data.
- Reference data such as soil images, administrative boundaries, etc.
- Water balance model.
- Crop yield function.
- Crop yield and production outputs.

The many spatial data sets and parameters used in the CSWB model make the use of GIS an ideal procedure for estimating regional agricultural yields. The water balance component of the CSWB model is described in this chapter, and the real-time input data, GIS reference data, yield functions, and output products are described in Chapter 3.

The CSWB model is a book-keeping method that accounts for water gained or lost by recording the cumulative water stress of a specific crop for each time increment over the entire growing season. The water balance, or budget, of the specific crop is calculated in time increments, usually dekad time periods, where each month is comprised of three dekads; the first two are exactly 10 days in length, and the third dekad has either 8, 9, 10, or 11 days, depending on the number of days in the specific month. The use of ten-day time increments is a compromise between time scales of one month and one day. One month is usually too long a period for agricultural analysis because four weeks may hide significant agro-meteorological events such as dry spells one or two weeks long, and using one-day periods can lead to excessive data processing when dealing with a large number of stations.

The fundamental equation used by the CSWB model is the water balance equation expressed as:

$$dS/dt = P_a - (ET_m + RO + DP) \quad (2.1)$$

where, dS/dt = change of soil moisture in the root zone with respect to each dekad, mm/dekad
P_a = actual observed precipitation, mm/dekad
Et_m = maximum crop evapotranspiration, mm/dekad
RO = runoff, mm/dekad
DP = deep percolation, mm/dekad

Extensive research has been conducted for each term in equation (2.1), and various methods can be used to measure or calculate their values. The main parameter monitored is not the amount of rain, but the soil moisture, S, within the root zone because plants derive their water from the soil. Estimating soil moisture contributes to accuracy of the water balance model (Gommes, 1983; Baier and Robertson, 1968).

No account is typically taken for effective rainfall in the CSWB model,

$$P_{eff} = P_a - (RO + DP) \quad (2.2)$$

where, P_{eff}= Effective rainfall, mm

because deep percolation and runoff are initially assumed zero. However, after the plant's root zone has reached water holding capacity, the remaining rainfall is considered as runoff or deep percolation. Therefore, the effective precipitation is typically assumed to be 100 percent of the actual precipitation so that precipitation, maximum crop evapotranspiration, and soil moisture reserve are the

fundamental parameters considered, reducing equation (2.1) to:

$$S_i = S_{i-1} + P_a - ET_m \qquad (2.3)$$

where, S_i = soil moisture reserve at the end of the i^{th} time interval, mm/dekad
S_{i-1} = soil moisture reserve at the end of the previous i^{th} time interval, mm/dekad

The water balance equation (2.3) allows the continuous monitoring of the soil moisture during the growing season by determining the cumulative water balance of rainfall, P_a, less maximum crop water use, ET_m. Insufficient rainfall during the growing season implies a soil moisture deficit for one or more dekads from planting to maturity. Hence, the final aim of the water balance model is to account for the plant's water consumption during the entire growing season, and to determine whether the rainfall was adequate for maximum growth.

In equation (2.3), the maximum crop evapotranspiration, ET_m, is the water requirement for the crop, defined as:

$$ET_m = K_c * PET \qquad (2.4)$$

where, K_c = crop coefficient
PET = potential evapotranspiration, mm/dekad

The potential evapotranspiration, PET, in equation (2.4), is calculated from the FAO-Penman equation defined by

Doorenbos and Pruitt (1977). PET is the reference evapotranspiration, defined as the maximum quantity of water that is transpired and evaporated by a uniform cover of short grass.

Calculating PET requires agro-meteorological measurements of temperature, wind speed, relative humidity, and sunshine. If actual ten day values of temperature, sunshine, wind speed, etc., are not available, then average or normal values may be used to estimate PET. The original work by Frère and Popov (1979) used "normal" PET values which is an acceptable method for running the CSWB model during the growing season since PET is subject to minor variations during each dekad and its fluctuations are dampened over a ten-day period. However, one problem with using normal PET values is that the actual PET is typically underestimated during dry spells.

Crop coefficient values, K_c in equation (2.4), are estimated from the length of the growing period (LGP), as described by Doorenbos and Pruitt (1977) and Doorenbos and Kassam, (1979). Developing a set of crop coefficient curves for estimating the seasonal water requirements is accomplished by knowing the precise length of the growing season for a given location and estimating the relative length of each crop stage.

Doorenbos and Kassam (1979) define the stages of maize development and the respective crop coefficients that relate maize water requirements to the reference evapotranspiration (PET) as follows:

- Initial stage: 0.3-0.5 (15 to 30 days),
- Development stage: 0.7-0.85 (30 to 45 days),
- Mid-season stage: 1.05-1.2 (30 to 45 days),
- Late season stage: 0.8-0.9 (10 to 30 days),
- Harvest stage: 0.55-0.6 (final day)

When estimating crop yields, the length of the vegetative phase (or development stage) must be especially known so that the high water requirements during the critical flowering phase (during the mid-season stage) are not underestimated. The high water requirements during the flowering phase (approximately 3 dekads) is due to the large size of the crop, and K_c values during this time will be greater than 1.0 and may reach 1.1 to 1.2 (FAO, 1986).

The soil moisture content, S_i and S_{i-1} in equation (2.3), is the water stored in the plant's root zone. Soil moisture is assumed zero at the beginning of the growing season. If S_i is greater than the readily available water-holding capacity (RAW) of the soil, then the soil has a water surplus. RAW is defined as:

$$\mathbf{RAW = WHC * MAD = D_{rz} * (FC - PWP)/100 * MAD} \qquad \mathbf{(2.5)}$$

where, RAW = Readily available water, mm
MAD = Maximum allowable depletion, percent

WHC = Maximum water holding capacity, mm
D_{rz} = Depth of root zone, m
FC = Field capacity of the soil, mm/m
PWP = Permanent wilting capacity, mm/m

If S_i from equation (2.3) is less than 0, the soil has a water deficit. Soil water deficits are very important for calculating the Water Requirement Satisfaction Index (WRSI), which is the final output from the CSWB model.

The WRSI is the *qualitative* index (i.e. good, average, poor) of the CSWB model that assesses the amount of water already received by the crop during any time of the season. It is calculated as follows:

$$WRSI = 100*(1-\frac{\Sigma|D|}{WR}) \qquad (2.6)$$

where, D = water deficit, mm/dekad
WR = total seasonal plant water requirement, mm
WRSI = water requirement satisfaction index

The water deficit, D, is set equal to zero whenever S_i from equation (2.3) is zero or positive, and D is set equal to S_i whenever S_i is negative. The values of D are then summed and divided by the total seasonal water requirement of the plant to calculate the WRSI. When the WRSI is equal to 100, it indicates no water stress and good crop yields, while a WRSI of 50 corresponds to poor crop yields or crop

failures. Intermediate WRSI values are indicated in Table 2.1.

Table 2.1. Water Requirement Satisfaction Index

WRSI	*Qualitative* Assessment	*Quantitative* Assessment (% yield)
100	Very good	>100
95-99	Good	90-100
80-94	Average	50-90
60-79	Mediocre	20-50
50-59	Poor	10-20
<50	Complete failure	<10

The WRSI index from the CSWB model gives a *qualitative* assessment of crop condition, but combining the water balance model with crop yield functions can give *quantitative* yields (Gommes, 1983). Crop yield functions are based on empirical water balance studies and were originally defined by Stewart and Hagan, (1973) and Stewart, et al (1975); and later developed by the FAO (Doorenbos and Kassam, 1979).

Crop yield functions are useful for estimating yields because they relate water stress to yield reduction, as follows:

$$1 - \frac{Y_a}{Y_m} = K_y\left(1 - \frac{ET_a}{ET_m}\right) \qquad (2.7)$$

where, Y_a = Actual yield, kg/ha
Y_m = Maximum yield, kg/ha

ET_a = Actual evapotranspiration, mm/day, of a crop with a limit in water supply
ET_m = Maximum evapotranspiration, mm/day, of a crop with no limit in water supply
K_y = Yield reduction factor

Solving equation (2.7) in terms of Y_a and assuming K_y = 1.5 allows one to calculate *quantitative* yields as shown in equation (2.8)

$$Y_a = 1.5(ET_a/ET_m)Y_m - 0.5Y_m \qquad (2.8)$$

Equation (2.8) is commonly called the crop yield function.

The maximum reference yield, Y_m from equations (2.7) and (2.8), will in an indirect way, account for other local farm factors which affect yield, such as:

- Inputs: use of fertilizers, pesticides, herbicides, etc.
- Technology and management: traditional cultivars or high-yielding cultivars, fallow periods, soil conservation measures, types of crop, planting distance, planting dates, manual labor or mechanized, etc.
- Market orientation: subsistence or commercial production
- Land holding: small fragmented or large consolidated
- Income level: low or high
- Prices: tend to affect area planted and mix of crops, rather than yields
- Government policies: taxes or subsidies

Therefore, Y_m from equation (2.8), varies locally depending on agricultural and soil management practices. To quantify Y_m from local data, the FAO (1986) recommends that maximum yields for a given crop not be estimated from yields

produced at an experiment station or by a single farmer, but rather be estimated from yields reported at village, district, or provincial level.

It should be noted that unforeseen events, such as disease, pests, or changed governmental policies may cause discrepancies between modeled yields and actual yields. However, yields affected by pests and diseases often cannot be modeled, and Hassan (1997) notes that droughts, not pests, are the prevailing factor contributing to reduced yields for most agro-ecological zones in Kenya.

The yield reduction value, K_y from equation (2.7), tends to be linear, allowing the CSWB model to be combined with a crop yield function to predict crop yields for a particular field or region. While the intensity of water stress, or the K_y yield reduction factor, is different for each phenological stage of crop development (i.e., vegetative, flowering, yield formation, and ripening periods), K_y values have been empirically determined for an entire season. The literature indicates seasonal K_y values ranging from 1.2 (Doorenbos and Kassam, 1979) to 1.5 (Gommes and Houssiau, 1982), with Stewart and Hash (1982) and Gommes and Houssiau (1982) recommending a K_y value of 1.5 for East Africa.

A *quantitative* crop yield estimate is the final output product derived after the water balance equation is combined with the yield function, but the final crop yield output hides the fact that a complex analysis and large amount of data were integrated together to obtain the yield estimate.

The water balance model combined with the crop yield function can be used to forecast crop yields and total production, where forecasting differs from estimating when the model is run in advance of harvest, usually several months, to predict yields of a particular crop. Forecasting requires running the model with average or "normal" rainfall and PET values. These normal values can be replaced later with actual rainfall and PET values as the growing season progresses. In contrast, estimating crop yields requires use of actual rainfall and PET values during the growing season with a final yield estimate made at the end of the season.

The forecast yields can be expected to improve during later stages of the growing season as normal rainfall and PET values are replaced with actual real-time rainfall and PET values. Also, normal estimates tend to over-estimate crop yields because normal rainfall estimates are more regularly distributed than actual rainfall.

In summary, the FAO CSWB model uses the following assumptions for simplification and operational use:

1. Dekad is the time step interval.

2. Crop coefficients are estimated for a crop based on the average growing season length for a particular region.

3. Deep percolation and runoff are neglected after the soil root zone is filled with water.

4. Plant root depth is assumed constant during the growing season, and soil water holding capacity is estimated from soil texture. If soil texture data is not available, soil water holding capacity is assumed.

5. Crop yield functions enable the water balance to estimate *quantitative* crop yields.

6. Normal PET and normal rainfall values can be used for missing agrometeorological measurements when estimating crop yields.

7. Crop yield estimates are obtained from actual dekad rainfall and PET measurements during the growing season

8. Crop yields can be forecasted by running the model in advance with normal PET and rainfall values.

The literature further indicates that the following problems are associated with the CSWB model:

1. Remote sensing data have not yet been incorporated into the CSWB model (Hutchinson, 1993).

2. Good point estimates of crop yields are obtained near agrometeorological stations, but area-wide estimates are often less realistic (FAO, 1989).

3. Regional variations caused by non-weather factors, such as soil fertility, pests, disease, etc. are not accounted for in the CSWB model (FAO, 1989), but are

indirectly accounted for by crop production functions (FAO, 1986).

4. Obtaining real-time ground-based agro-meteorological data is often difficult for operational use.

5. Use of normal PET values, in absence of real-time agrometeorological data, tend to underestimate yields during dry periods (FAO, 1986)

6. Length of growing period is estimated by calendar days and not by thermal days.

7. Excess precipitation may lead to reduced yields (Frère and Popov, 1979).

By integrating the CSWB model with real-time remote sensing data and GIS software, this research will assist to solve model limitations associated with items (1-5), and no attempt will be made to address items (6) and (7). However, after a GIS-based CSWB model is developed by this study, item (6) could be improved by introducing a Growing Degree Day (thermal day) product derived from geo-stationary satellite data. The model could also address item (7) by introducing polynomial crop production functions as described by Solomon (1985). Polynomial crop production functions quantitatively relate crop yield reductions to excess water based upon empirical experiments.

3. METHODOLOGY

3.1 Description of Kenya Study Area

3.1.1 Physical Geography and Administrative Units

Kenya straddles the equator and is bounded by Lake Victoria to the northwest, Mount Kilimanjaro to the southwest, Lake Turkana to the north, and the Indian Ocean to the southeast (Figure 3.1). From the coast to Lake Victoria, the land rises gradually, with the exception of the Great Rift Valley that dissects the country from north to south. Several Rift Valley lakes such as Magadi, Naivashsa, Nakuru, Baringo, and Turkana lie within the trough of the rift. To the east of the Rift Valley, lies the Aberdares mountain range and Mount Kenya, the highest summit of the country. The largest river in Kenya is the Tana that drains off the slopes of Mount Kenya and the Aberdares, and empties into the Indian Ocean.

The principal climatic features affecting agricultural productivity divide the country into approximately three regions (Figure 1.1):

1. *Arid and Semi-Arid lands (ASAL)* located in low altitude areas which form 75% of Kenya's surface area and are unfavorable for rain-fed crop production;

2. *Productive Highlands* which form the largest agriculture region, a triangular-shaped plateau originating near the Nairobi capital and extending

east to Mount Kenya and west to Lake Victoria and Mount Elgon;

3. *Productive Lowlands* which form coastal agricultural bands along lake Victoria and the Indian Ocean.

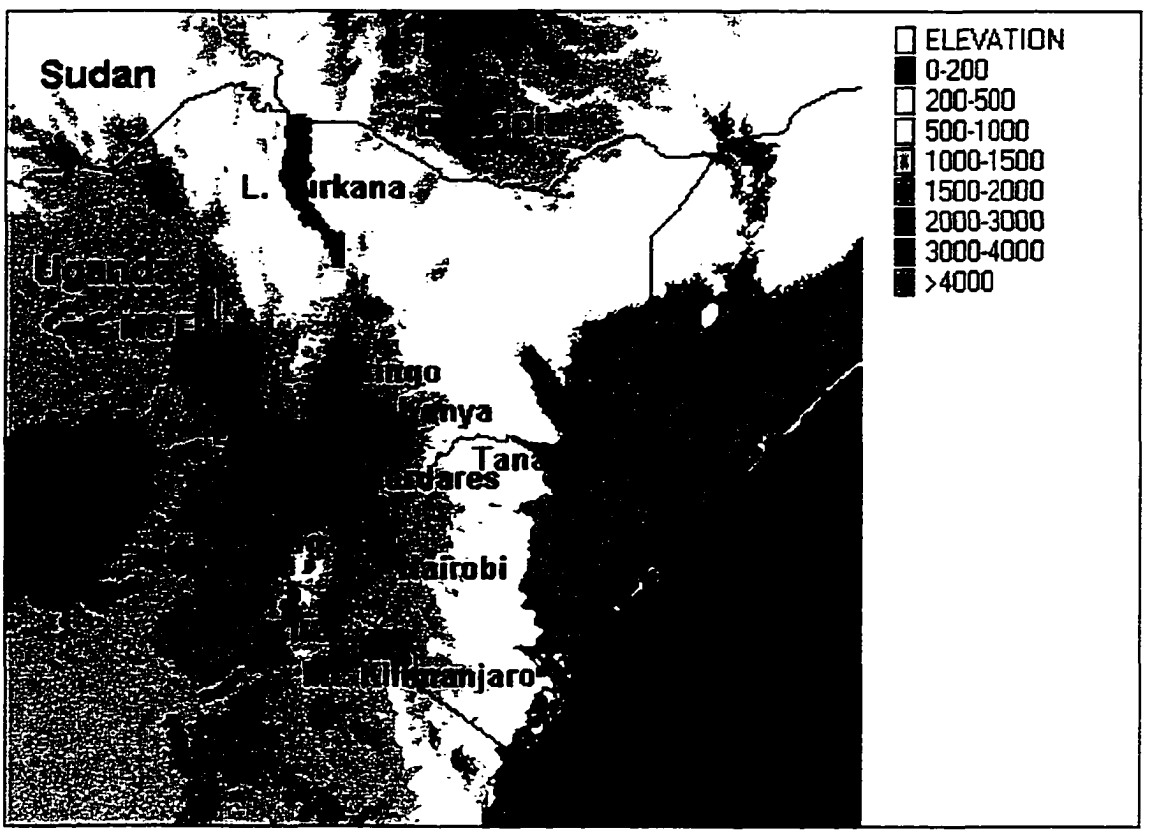

Figure 3.1. Digital Elevation Model (DEM) of Kenya Showing Major Geographical Features

3.1.2 Rainfall

Kenya's climate is largely influenced by its equatorial location. With the equator passing through approximately the center of the country, temperature and solar radiation have little seasonal variation. However, Kenya's tropical

location provides a largely bimodal rainfall pattern which is closely linked to the convergence of global wind patterns in the tropics. The location of global winds convergence is the Inter-tropical Convergence Zone (ITCZ), and rainfall is associated with this zone where air rises in a broad band.

The ITCZ moves seasonally north and south with the sun, reaching its farthest north point (23^0 20′ N) on June 21 and its farthest south point (23^0 20′ S) on December 21. Thus, the sun and the ITCZ pass over Kenya twice annually, approximately in April and November, creating the southeast (colloquially "long rains") and northeast (colloquially "short rains") monsoons, respectively. The exact time when the ITCZ passes over Kenya is complicated by yearly changes in the location and temperatures of ocean currents and by surface features of the earth, such as mountain ranges, large land masses, etc.

In April, the ITCZ is moving north, and the predominant winds from the southeast carry large amounts of moisture from the Indian Ocean. The influx of moisture from the ocean produces a large band of clouds so rainfall during this time tends to cover a large area and may last for several days at a time. In November, the ITCZ is moving south, and the predominant winds are from the northeast. These winds often carry less moisture than the April-May

monsoon because they pass over a generally arid landmass across Ethiopia and Somalia. Thus, the short rains are likely to be more variable, produce less rain, and be of shorter duration than the monsoons generated from the Indian Ocean.

Rainfall is also caused by orographic lifting in Kenya's highlands, with rainfall tending to increase with increasing elevation and rainfall variability tending to decrease with increasing elevation. Thus, rains generated from orographic lifting are inclined to be more reliable than storms and thunderstorms generated by the ITCZ.

The onset of rains tends to be earlier in high altitude areas than in low altitude areas. Correspondingly, the length of the rainy season and growing period are longer in higher elevation areas. The onset of rainfall for the entire country is critical for determining crop yields because wet years tend to start early and have longer growing periods, producing higher crop yields (Stewart, 1988). Similarly, vegetation growth is a response to rainfall, and vegetation biomass extends both temporally and spatially during years of good rainfall, as shown by Eiden, et al, (1991). In addition, Ropelewski and Halpert, (1987) have shown that increased rainfall occurs in northern Kenya during the second half of the short rainy season due to a

teleconnection signal from the El Niño-Southern Oscillation (ENSO) phenomenon (Figure 3.2).

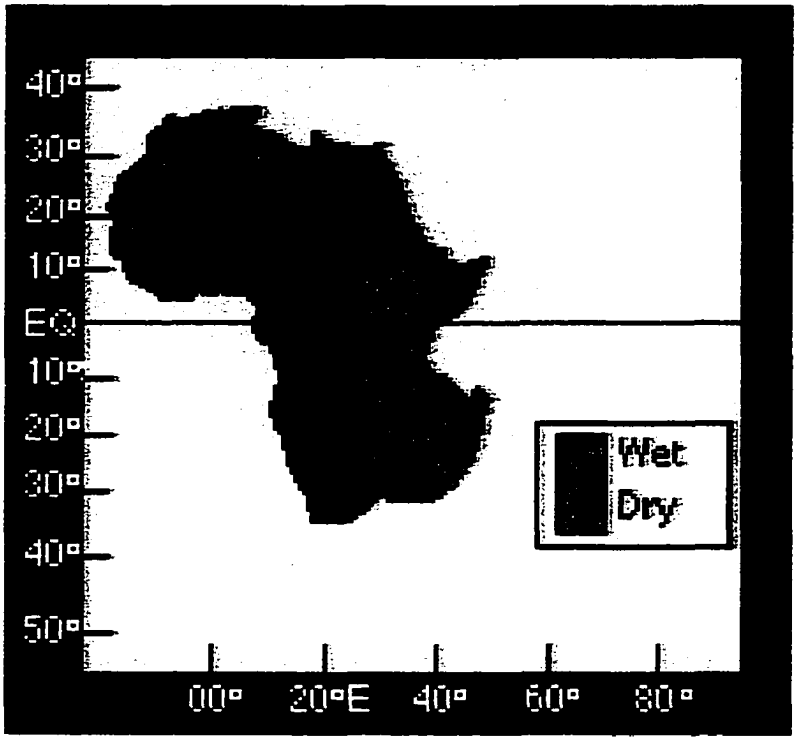

Figure 3.2. ENSO Teleconnections in Africa during December-February (adapted from Ropelewski and Halpert, 1987).

3.1.3 Maize Production

Maize (*Zea Mays*) is one of the major food crops in East Africa, and it is the principle cereal crop grown and consumed in Kenya. Weather, especially drought, has the greatest influence on maize production. Maize is grown mainly under rain-fed conditions in East Africa, in areas ranging from temperate (1000-2500 meters) to tropic (sea level to 1000 meters) during the period when daily mean daily temperatures are above 15°C (40°F) and frost-free. For maximum production, a medium maturity crop requires between 500 to 800 mm of rainfall, depending on the climate.

The average length of the growing period for maize in East Africa is 120-140 days. However, due to its wide elevation adaptations, some varieties of maize may take up to 300 days from sowing to maturation, and 90-100 days for most early warm varieties to mature. So successful cultivation depends on matching the correct seed varieties to the average length of growing period of the region. Table 3.1 summarizes growing season lengths and thermal days for maize within different agro-ecological zones (Kassam, et al, 1993a and 1993b; Hassan, 1997).

Table 3.1. Calendar Days and Thermal Days for Maize (from Hassan, 1997, and Kassam, et al., 1993a and 1993b)

Crop	Growth Cycle (days)	24-hour mean temp.	Agroclimatic Zone (from Hassan,1997)	Thermal Days
Maize (lowland)	70-90	> 20.0		
	90-110	> 20.0	Semi-Arid	1767
	110-130	> 20.0	Lowland Tropics	2124
Maize (highland)	120-140	17.5-20.0	Dry Transitional	1829
	140-180	17.5-20.0	Moist mid-altitude	2461
	180-200	17.5-20.0	Moist Transitional	2063
	200-220	15.0-17.5	Highland Tropics	2066
	220-280	15.0-17.5		
	280-300	15.0-17.5		

Following Kenya's independence in 1963, the agricultural sector performed reasonably well during the first two decades, except in drought years. In the 1960s and 1970s, yields in Kenya increased due to better seed varieties developed by the Green Revolution and due to expansion of area planted. However, yields have largely remained constant since the early 1980s, with yields tending to be lower in the low-altitude areas (1 ton/ha) and higher in the high-altitude areas (3 tons/ha).

In addition, area planted in Kenya has not increased significantly during the last two decades. The maximum area

harvested in 1976 was 1.59 million hectares and the average area planted in the 1990s has been around 1.3 million hectares (Figure 3.3).

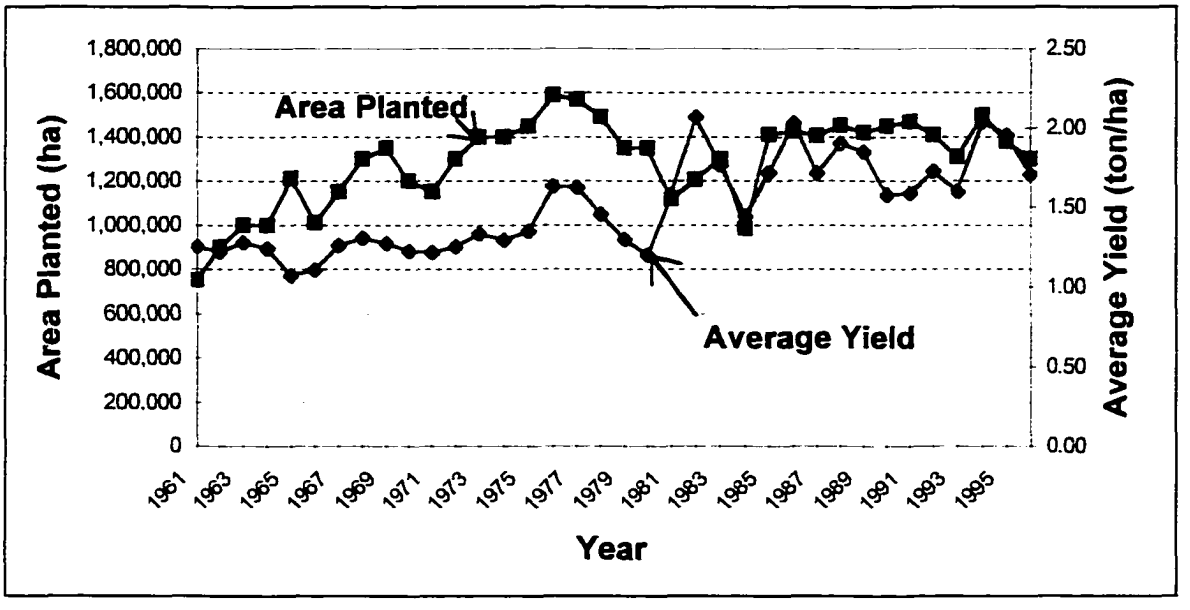

Figure 3.3. Estimated Maize Area Planted and Average Yield from 1961-1996 (from FAO 1997)

Most of the increase in maize production for Kenya has been overshadowed by a rapid increase in population, with Kenya experiencing a gradual decline in production/capita for the past two decades (Figure 3.4). Kenya began to experience maize deficits in the 1980s, even during years of good rains. Despite the bumper harvest of 1994, there was still a maize deficit requiring importation of maize. Because of maize deficits even during years of good rainfall, as well as the high variability of rainfall caused by ITCZ and ENSO effects, Kenya must closely monitor maize

production every year. During the 1989-1997 study period of this research, total maize production was poor during 1990-1993, and 1996-1997, and above average during 1989, 1994 and 1995 (Figure 3.4).

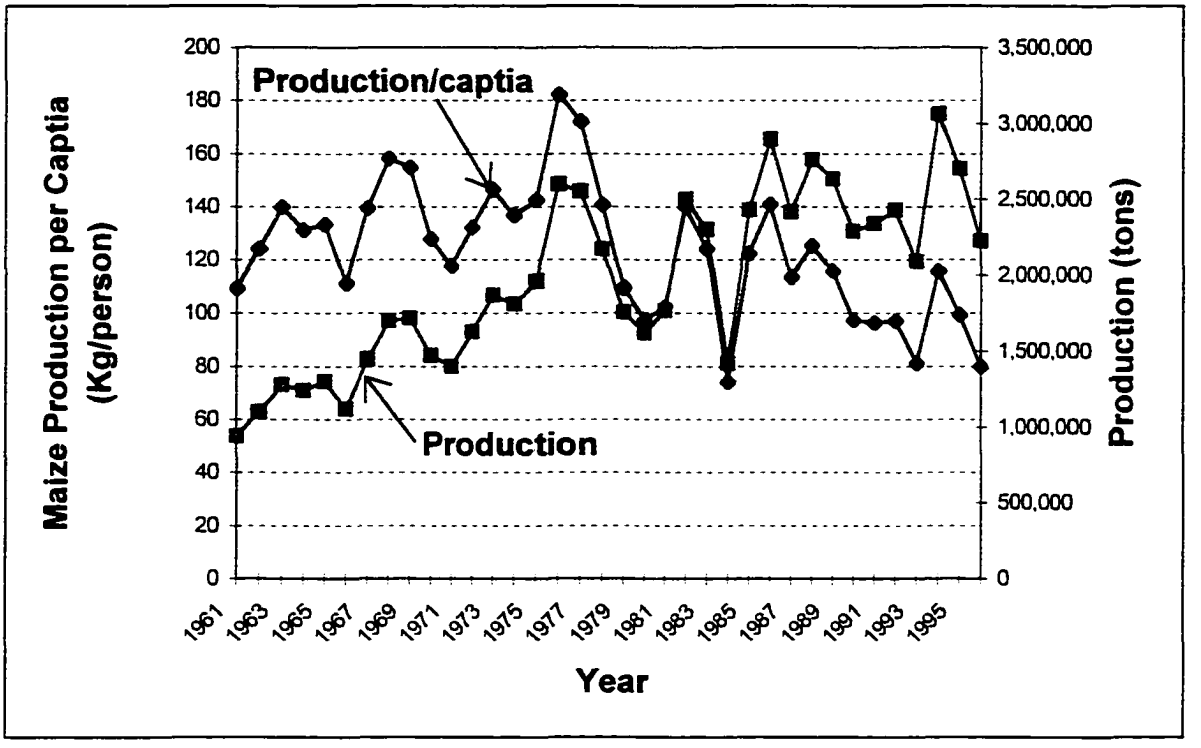

Figure 3.4. Kenya Maize Production and Maize Production per Capita from 1961-1996 (from FAO, 1997)

3.2 Geographic Information System Databases

The use of Geographic Information System (GIS) in agriculture and natural resource management has grown exponentially over the past decade due to the proliferation of GIS software and reduced prices in computer hardware (Hutchinson, et al, 1993). GIS software permits the capture,

storage, manipulation, and display of spatial data, and GIS is ideal for determining regional agriculture yields by managing several different types of geographic information during the cropping season.

The GIS utilized for this research is IGT which was specifically designed to give GIS capabilities for the DOS-based IDA program (Pfirman and Hoefsloot, 1995, and Hoefsloot, 1996). IDA was originally developed in the late 1980s for EWS stations to analyze and process time series of ARTEMIS satellite images. The DOS-based IDA program was later upgraded to a Windows-based program called WINDISP3 (Pfirman and Hogue, 1997). Recently, the DOS-based IGT program has been upgraded to a Windows environment by incorporating several IGT functions into WINDISP3 (Pfirman, 1998).

The original spatial input data are derived from the following spatial formats:

1. *Maps:* administrative boundaries, soil type, agro-ecological zones, etc.

2. *Images:* RFE and NDVI images derived from real time satellite information.

3. *Point data:* rainfall and potential evapotranspiration data collected from ground-based stations.

4. *Tabular data:* estimated crop area planted per district, crop production estimates, etc..

The DOS-based IGT and the Windows-based WINDISP3 programs were utilized to process the spatial data for this research as described in detailed by the meta-data information in Appendix I. The final spatial databases, batch files, and programs required to run the GIS-based CSWB model are included on the CD-ROM, Appendix IV. All of the archived images are in IDA format, and have a common Geographic projection, also referred to as Latitude\Longitude or Platte Carré projections.

3.3 Research Methodology for Estimating Maize Production

As noted earlier, the FAO CSWB model can be summarized as having five major components:

- Real-time input data.
- Reference data.
- Water balance model.
- Crop yield function.
- Crop yield and production outputs.

The research methodology to develop the modified GIS-based CSWB model also comprises of these same five components, and a final statistical analysis step for validating the model for future operation. A flow chart illustrating the research methodology to estimate crop yields from real-time satellite data and ground-based ancillary data is presented in Figure 3.5. A brief

description of each of the five major components of the GIS-based CSWB model is presented in the remaining sections of this chapter.

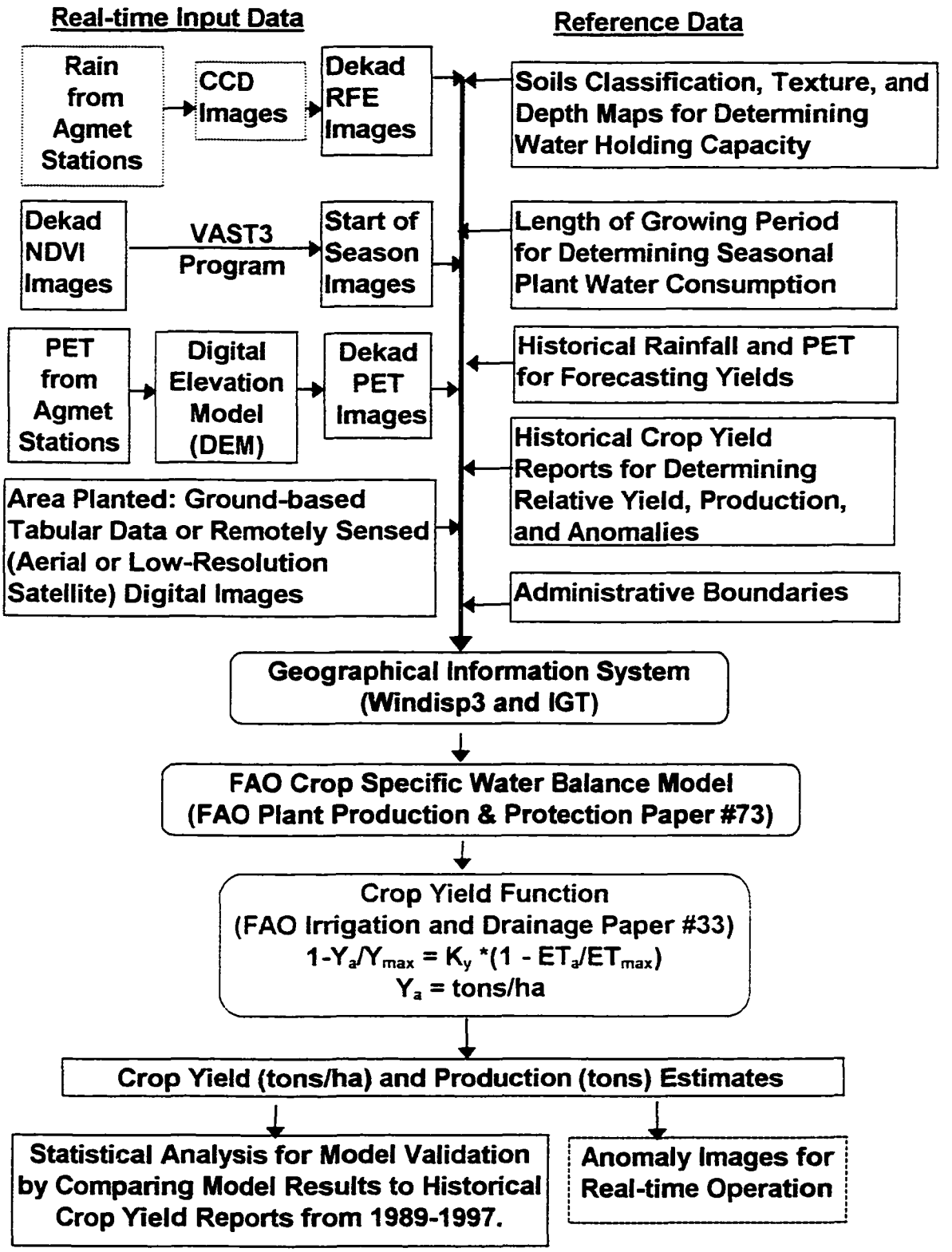

Figure 3.5. Flowchart Illustrating Research Methodology

3.4 Reference Data

Most of the ground-based reference data for the AEZ polygon analysis was provided by the Crop Production System Zones (CPSZ) database for the IGAD region (van Velthuizen, et al, 1995). Many of these same data bases were used for the pixel-by pixel analysis.

The following reference databases were used within the model for estimating crop yields:

1. *Administrative boundaries:* from the CPSZ database.
2. *Agro-ecological zones:* from the CPSZ database.
3. *Average LGP for maize:* from the CPSZ database.
4. *Readily extracted soil moisture storage:* from the CPSZ database for the AEZ Polygon Analysis; FAO Digital Soils World Map, FAO 1995 for 7.6-km Pixel-by-Pixel Analysis; and Kenya Soil Classification image for the 1.1-km Pixel-by Pixel Analysis (Kassam, et al, 1993a).
5. *Historical average crop yield data:* from the CPSZ database.
6. *Average dekad RFE images:* by averaging nine years (1989-1997) of RFE images or by interpolating from another historical agmet data set.
7. *Average dekad PET images:* by averaging nine years (1989-1997) of PET images or by interpolating from another historical agmet data set.

3.4.1 Administrative Boundaries

Kenya's administrative boundaries defined eight provinces and 41 districts following Independence in 1963

(Figure 3.6). However, administrative boundaries have changed drastically since 1991, with a total of 68 districts created to date. Presently, some of the new boundaries have not yet been defined or surveyed. The progressive creation of new districts is shown in Table 3.2.

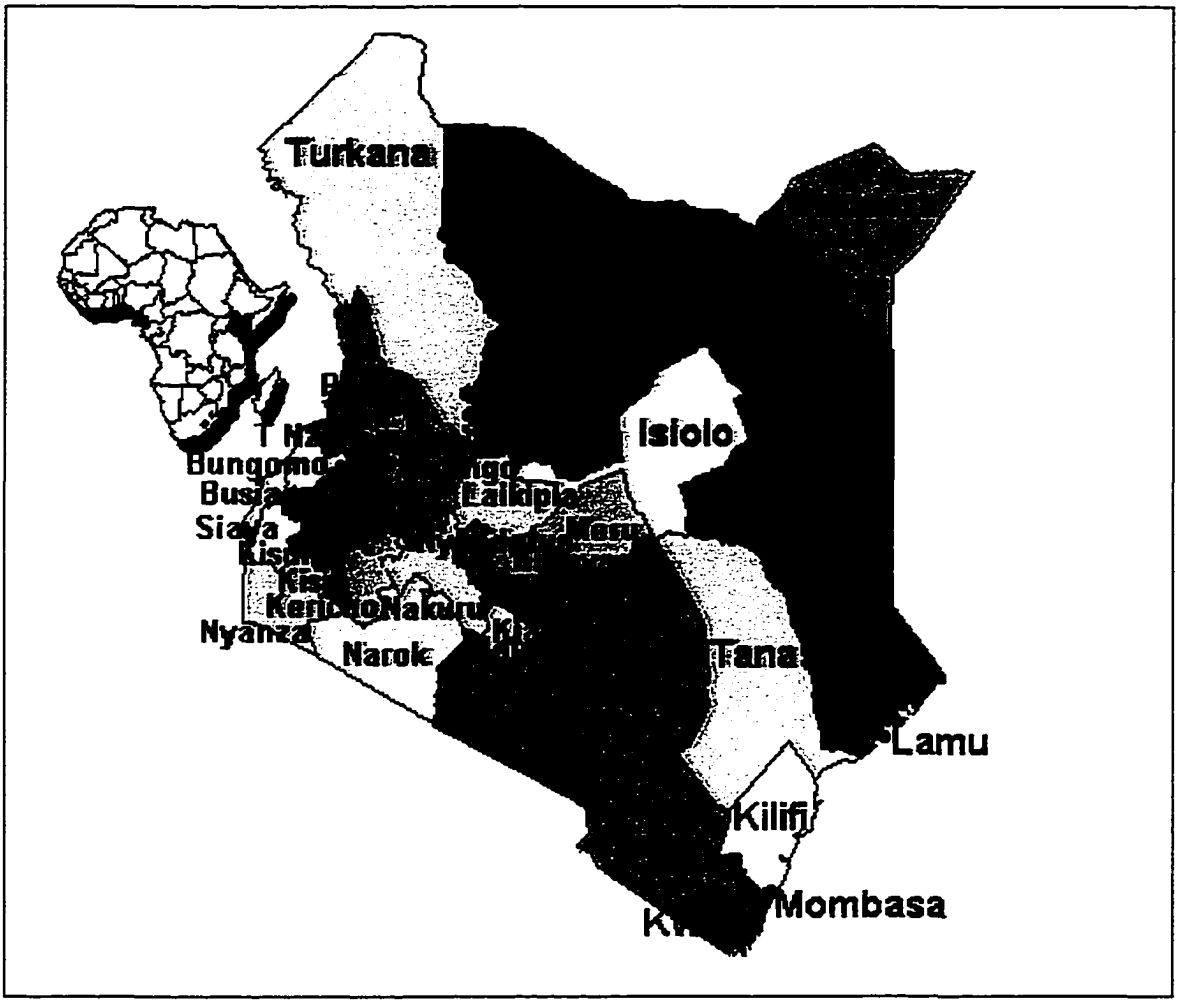

Figure 3.6. Kenya Districts in 1989.

Table 3.2. Recent Divisions of Kenya Districts (adapted from FEWS, 1997)

Province	Pre-1991	No	1991	1993	1995	1996	1997	1998
Western	Busia	1	Busia	Busia	Busia	Busia	Busia	Busia
	Bungoma	2	Bungoma	Bungoma	Bungoma	Bungoma	Bungoma	Bungoma
Western				Mt Elgon	Mt Elgon	Mt Elgon	Mt Elgon	Mt Elgon
					Teso	Teso	Teso	Teso
Western	Kakamega	3	Kakamega	Kakamega	Kakamega	Kakamega	Kakamega	Kakamega
					Lugai	Lugari	Lugari	Lugari
			Vihiga	Vihiga	Vihiga	Vihiga	Vihiga	Vihiga
Nyanza	Siaya	4	Siaya	Siaya	Siaya	Siaya	Siaya	Siaya
Nyanza	Kisumu	5	Kisumu	Kisumu	Kisumu	Kisumu	Kisumu	Kisumu
Nyanza	S. Nyanza	6	Homa Bay	Homa Bay	Homa Bay	Homa Bay	Homa Bay	Homa Bay
						Rachuonyoo	Rachuonyoo	Rachuonyoo
			Migori	Migori	Migori	Migori	Migori	Migori
					Suba	Suba	Suba	Suba
				Kuria	Kuria	Kuria	Kuria	Kuria
Nyanza	Kisii	7	Kisii	Kisii	Kisii	Kisii	Kisii	Kisii Central
							Gucha	Kisii South
			Nyamira	Nyamira	Nyamira	Nyamira	Nyamira	Kisii North
R. Valley	Turkana	8	Turkana	Turkana	Turkana	Turkana	Turkana	Turkana
R. Valley	West Pokot	9	W. Pokot	W. Pokot	W. Pokot	W. Pokot	W. Pokot	W. Pokot
R. Valley	Trans Nzoia	10	Trans Nzoia	Trans Nzoia	T. Nzoia	T. Nzoia	T. Nzoia	T.Nzoia
R. Valley	Nandi	11	Nandi	Nandi	Nandi	Nandi	Nandi	Nandi
R. Valley	Uasin Gishu	12	Uasin Gishu	Uasin Gishu	U. Gishu	U. Gishu	U. Gishu	U. Gishu
R. Valley	Elgeyo Marakwet	13	E Marakwet	E Marakwet	Elgeyo	Elgeyo	Elgeyo	Elgeyo
					Marakwet	Marakwet	Marakwet	Marakwet
R. Valley	Baringo	14	Baringo	Baringo	Baringo	Baringo	Baringo	Baringo
					Koibatek	Koibatek	Koibatek	Koibatek
R. Valley	Samburu	15	Samburu	Samburu	Samburu	Samburu	Samburu	Samburu
R. Valley	Kericho	16	Kericho	Kericho	Kericho	Kericho	Kericho	Kericho
			Bomet	Bomet	Bomet	Bomet	Bomet	Bomet
R. Valley	Nakuru	17	Nakuru	Nakuru	Nakuru	Nakuru	Nakuru	Nakuru
R. Valley	Laikipia	18	Laikipia	Laikipia	Laikipia	Laikipia	Laikipia	Laikipia
R. Valley	Narok	19	Narok	Narok	Narok	Narok	Narok	Narok
					Trans Mara	T. Mara	T. Mara	T. Mara
R. Valley	Kajiado	20	Kajiado	Kajiado	Kajiado	Kajiado	Kajiado North	Kajiado N
							Kajiado South	Kajiado S.

Table 3.2. (cont.) Recent Divisions of Kenya Districts (FEWS, 1997)

Province	Pre-1991	No	1991	1993	1995	1996	1997	1999
Central	Nyandarua	21	Nyandarua	Nyandarua	Nyandarua	Nyandarua	Nyandarua	Nyandarua
Central	Nyeri	22	Nyeri	Nyeri	Nyeri	Nyeri	Nyeri	Nyeri
Central	Kirinyaga	23	Kirinyaga	Kirinyaga	Kirinyaga	Kirinyaga	Kirinyaga	Kirinyaga
Central	Muranga	24	Muranga	Muranga	Muranga	Muranga	Muranga	Muranga
							Maragwa	Maragwa
Central	Kiambu	25	Kiambu	Kiambu	Kiambu	Kiambu	Kiambu	Kiambu
				Thika	Thika	Thika	Thika	Thika
Eastern	Marsabit	26	Marsabit	Marsabit	Marsabit	Marsabit	Marsabit	Marsabit
					Moyale	Moyale	Moyale	Moyale
Eastern	Isiolo	27	Isiolo	Isiolo	Isiolo	Isiolo	Isiolo	Isiolo
Eastern	Meru	28	Meru	Meru	Meru	Meru	Meru	Meru Central
			T. Nithi	T. Nithi	T. Nithi	T. Nithi	T. Nithi	Meru South
								Tharaka
				Nyambene	Nyambene	Nyambene	Nyambene	Meru North
Eastern	Embu	29	Embu	Embu	Embu	Embu	Embu	Embu
						Mbeere	Mbeere	Mbeere
Eastern	Machakos	30	Machakos	Machakos	Machakos	Machakos	Machakos	Machakos
			Makueni	Makueni	Makueni	Makueni	Makueni	Makueni
Eastern	Kitui	31	Kitui	Kitui	Kitui	Kitui	Kitui	Kitui
				Mwingi	Mwingi	Mwingi	Mwingi	Mwingi
N. Eastern	Mandera	32	Mandera	Mandera	Mandera	Mandera	Mandera	Mandera
N. Eastern	Wajir	33	Wajir	Wajir	Wajir	Wajir	Wajir	Wajir
N. Eastern	Garissa	34	Garissa	Garissa	Garissa	Garissa	Garissa	Garissa
Coast	Tana River	35	Tana River	Tana River	Tana River	Tana River	Tana River	Tana River
Coast	Lamu	36	Lamu	Lamu	Lamu	Lamu	Lamu	Lamu
Coast	Taita	37	Taita	Taita	Taita	Taita	Taita	Taita
Coast	Kilifi	38	Kilifi	Kilifi	Kilifi	Kilifi	Kilifi	Kilifi
							Malindi	Malindi
Coast	Kwale	39	Kwale	Kwale	Kwale	Kwale	Kwale	Kwale
Coast	Mombasa	40	Mombasa	Mombasa	Mombasa	Mombasa	Mombasa	Mombasa
Nairobi	Nairobi	41	Nairobi	Nairobi	Nairobi	Nairobi	Nairobi	Nairobi
Total	**41**		**47**	**52**	**59**	**61**	**65**	**66**

Changing district administrative boundaries also changes crop yields and production reporting on the district level due to change in district areas. Therefore, old administrative boundaries of 41 districts were used during the entire study period, from 1989-1997, to keep the administrative units consistent for reporting annual crop yields and production.

3.4.2 Agro-ecological Zones

Crop Production System Zones (CPSZ) are areas with relatively homogeneous climatic and agricultural characteristics (van Velthuizen, et al, 1995, and FAO, 1978). The CPSZ units were derived by dividing Kenya into 41 districts, and further dividing these 41 polygons into CPSZ units based on agro-climatic conditions.

3.4.3 Length of Growing Period

van Velthuizen, et al, (1995) defines length of growing period for each CPSZ unit by three different methods: climate, crop calendar, and NDVI. The crop calendar method was chosen for running the GIS-based CSWB model since it appeared to more accurately reflect the true length of growing season than the climate and NDVI methodologies (Appendix I, Length of Growing Period (LGP) Images).

3.4.4 Soil Water Holding Capacity

The soil characteristics of each CPSZ unit were determined by quantifying established relationships between soil properties and soil classification names, and developing algorithms to estimate the maximum readily available soil moisture storage, as described by van Velthuizen, et al, (1995). These maximum readily available soil moisture storage data were extracted from the CPSZ database and used in the GIS-based CSWB model with three different resolutions, (Appendix I, Readily Available Soil Moisture Storage and Soil Water Holding Capacity).

In addition, the same soil moisture storage data were used for the three GIS-based CSWB analyses to keep the soil moisture storage variable constant, although images with finer resolutions than CPSZ units could be developed. For example, a soil moisture storage image with 7.6-km resolution could be extracted from the FAO Digital Soil Map of the World (FAO, 1995). Similarly, a soil moisture storage image with 1.1-km resolution could be derived from the soil classification image (1-kilometer resolution), developed from the Kenya AEZ project as shown in Figure 3.7 (Kassam, et al, 1993a). These finer resolution soil images were not used in this study in order to keep the soil

moisture storage constant, but crop yield models developed on a national scale should consider developing soil images with finer resolutions to improve model accuracy.

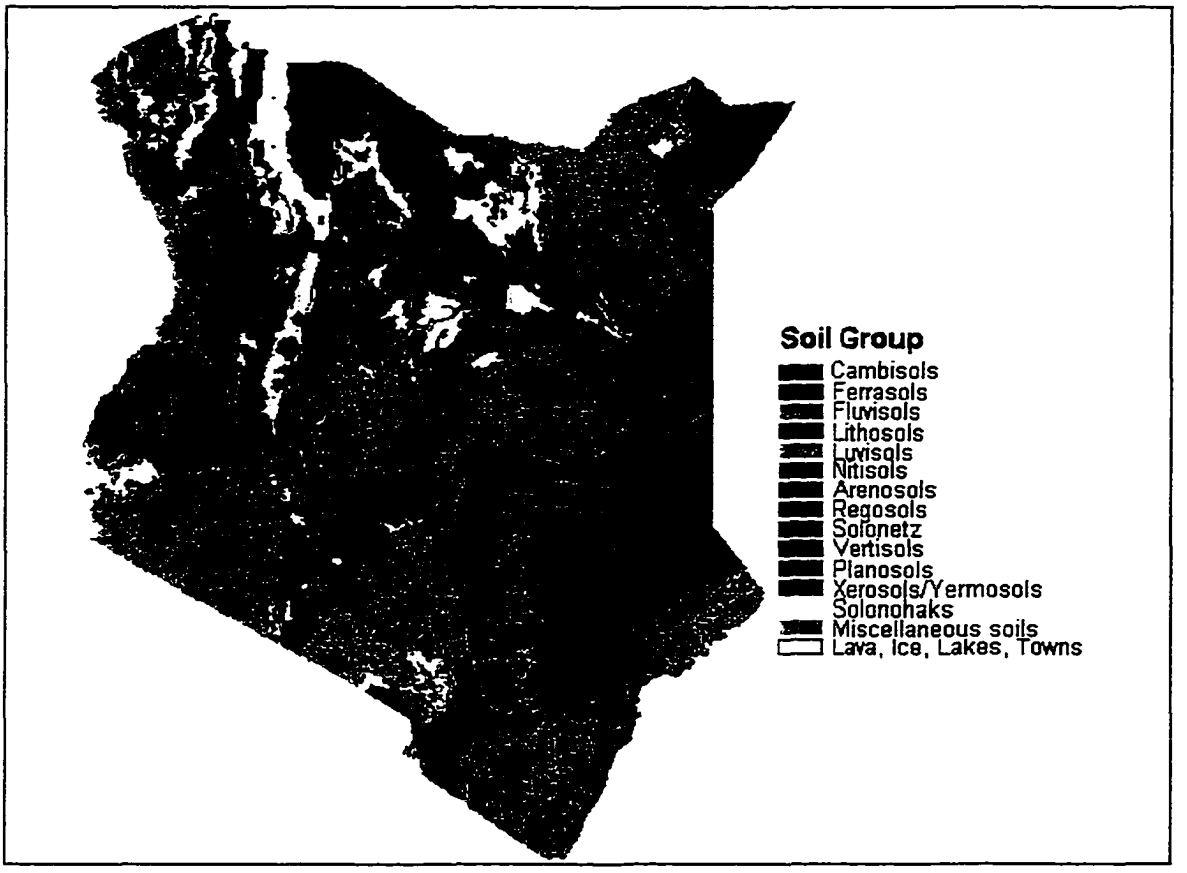

Figure 3.7. Kenya Soils Map at 1:1,000,000 Scale (1-kilometer Resolution), (from Kassam, et al, 1993a).

3.4.5 Historical Crop Yield and Production Reports

The average crop yield data used in the GIS-based CSWB model were exported from the CPSZ database and derived from historical Kenya Ministry of Agriculture reports (van Velthuizen, et al, 1995). These average crop yield data were then multiplied by a factor of 1.2 to approximate maximum yields per each CPSZ for use in equation (2.7). The factor of 1.2 was determined by running a sensitivity analysis on the model which indicated that factors greater than 1.2 tend to over-estimate national production, and factors less than 1.2 under-estimated national production.

Annual crop yield estimates are available from four Government of Kenya ministries: the Ministry of Agriculture (MoA), the Department of Resource Survey and Remote Sensing (DRSRS), the National Cereals and Produce Board (NCPB), and the Central Bureau of Statistics (CBS). Each of these institutions uses different methods in collecting data and estimating crop yield and production.

The MoA uses a subjective method for gathering data where experienced agriculture officers travel through regions and visually estimate area planted and expected yields. Their visual estimates are supplemented by information from local farmers and national research institutes to produce district-level reports, once in mid-

season and finally at the end of the cropping season. The DRSRS uses aerial photography to estimate area planted and estimates yields by using a mid-season radiometric measurement that is augmented with spot visual ground checks. The CBS uses a cluster sampling procedure where a large team of trained individuals approaches a large sample of farmers and asks the farmers to complete questionnaires pertaining to their crops. The NCPB collects data only on sales after harvest provided late in the season, and these data do not account for maize that did not reach the official market.

Only reported crop yield and production reports from the MoA and the DRSRS were utilized for validating the GIS-based CSWB model. Reports from these two agencies were chosen because estimates from the MoA are considered complete and thorough, and area-planted estimates from DRSRS are regarded as reliable because aerial photographic surveys and radiometric techniques are utilized. Unfortunately, the DRSRS crop yield and production database for maize is only from 1989-1993, because funding constraints prevented thorough and adequate surveys after 1993.

3.4.6 Average Rainfall and PET Images

While average rainfall and PET images can be developed and used for forecasting crop yields, they were not developed for this research since the study objective is to validate the GIS-based CSWB model and not to forecast yields.

3.5 Real-time Input Data

As shown in Figure 3.5, the four principle real-time input databases required to run the GIS-based CSWB model include:

1. *Real-time RFE satellite data (from FEWS (1998) home page):* for determining estimated precipitation.
2. *Real-time NDVI satellite data (from FEWS (1998) home page):* for determining the start of the growing season by using the VAST3 computer program.
3. *Real-time ground-based PET data (from the Kenya Meteorological Department):* for determining the dekad water requirements for maize.
4. *Area planted per district (from MoA and DRSRS):* for determining total maize production.

3.5.1 Satellite-Derived RFE and NDVI Products

The two main real-time satellite products used in the GIS-based CSWB model are RFE and NDVI images. These data products were developed by the USAID-sponsored FEWS project, and the images are currently stored at the United States

Geological Survey (USGS) Earth Resources Observation Systems (EROS) Data Center at Sioux Falls, South Dakota. Presently, all archived NDVI and RFE images are available from the Africa Data Dissemination Service from the EDC (Appendix I).

The RFE data begin in 1995 when FEWS contracted the Climate Prediction Center (CPC) of NOAA to produce RFE images. The algorithm for producing RFE images utilizes Cold Cloud Duration (CCD) data from the geo-stationary METEOSAT 5 satellite; Global Telecommunication System (GTS) rain gauge reports from the World Meteorology Organization (WMO); model analyses of wind and relative humidity from the Environmental Modeling Center (EMC); and topography; as described by Herman, et al, (1994) and Herman, et al, (1997). RFE images from FEWS were used by this research from May, 1995 - December, 1997. Because RFE images before May, 1995 are not available from FEWS, RFE images from January, 1989 - May, 1995 were developed by using the IGT software. The Satellite Enhanced Data Interpolation (SEDI) module from IGT interpolates between rain gauges by using CCD images as a background image for correlating rainfall to CCD. (Appendix I, RFE Images).

The NDVI images distributed by the FEWS and ARTEMIS projects are developed and calibrated by the Global Inventory Monitoring and Modeling Studies (GIMMS) group at the

Goddard Space Flight Center (GSFC) of NASA. The raw data to develop these NDVI maps are retrieved from the NOAA-AVHRR series satellite, and after processing the final GAC images have 7.6-kilometer spatial resolution near the equator.

In 1989, spatial resolution of the NOAA-AVHRR data was improved with the introduction of regional Local Area Coverage (LAC) data that has a 1.1-kilometer spatial resolution. However, an automatic method for developing NDVI images with LAC resolution has not been implemented for the entire African continent, as for the GAC data sets, because LAC data are collected regionally making it difficult to coordinate such a system.

In East Africa, raw NOAA-AVHRR data are received by the High Resolution Picture Transmission (HRPT) station at the Kenya Meteorological Department, Figure 3.8. Presently, the Department of Resource Surveys and Remote Sensing (DRSRS) of the Kenya Government develops and calibrates a dekad NDVI product with LAC data received by the HRPT station (Ganzin, 1995). However, the NDVI product from DRSRS only covers the country of Kenya, while the Regional Centre for Services in Surveying, Mapping, and Remote Sensing began in 1998 to develop a dekad NDVI product with LAC resolution covering all of east Africa.

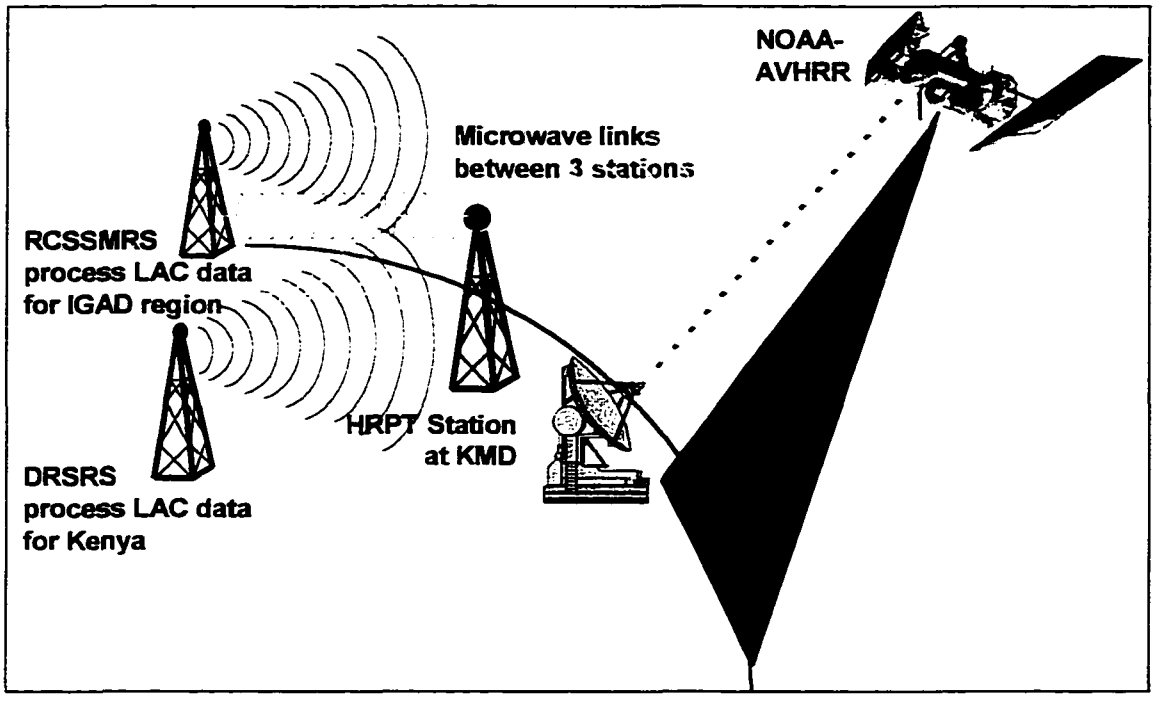

Figure 3.8. Collection, Transmission and Processing LAC data from the HRPT station at Nairobi, Kenya

Traditional *qualitative* vegetation assessments performed by EWS stations do not extensively use LAC data because LAC data do not have a similar 15-year GAC NDVI archive (1981-1997) for making *qualitative* comparisons from historical averages. In making a historical average NDVI image with GAC resolution, the following years should be eliminated when calculating a NDVI long-term average:

- 1982-1983 due to aerosol contamination from Mt. El Chichon, Mexico, volcanic eruption.
- 1991-1992 due aerosol contamination from Mt. Pinatubo, Philippines, volcanic eruption.
- 1995-present due to slight sensor differences with the current NOAA-14 satellite.

In other words, only the calendar years of 1984-1990, 1993, and 1994, are included in calculating the average NDVI image in an effort to eliminate NDVI images contaminated by volcanic aerosols or sensor differences. Therefore, maintaining the GAC data set is difficult due to changes in sensors, radiometric sensor decay, atmospheric changes caused by volcanic eruptions, etc. However, one major appealing aspect of the GIS-based CSWB model is that real-time LAC data can be utilized immediately since inter-annual variation of NDVI data caused by aerosol contamination and sensor decay is not a great concern.

For this research, NDVI images of both GAC and LAC resolution are used to determine the beginning of the growing season, and images of 1991 can be used since NDVI is only used for determining the start of growing season. However, cloud effects with LAC data can cause problems in determining the start of the growing season while the GAC data set are relatively cloud-free.

Both LAC and GAC NDVI images are introduced into the VAST3 program to estimate the start of the growing season (Appendix II, and Lee, 1997) and to initialize the GIS-based CSWB model. The VAST3 program develops a start of the growing season image by analyzing a NDVI time series and detecting a rising NDVI trend of 0.02 for two dekad time

steps. The end of the growing season is determined in a similar manner by detecting a declining NDVI trend, but was not utilized for this study because it could not be assumed maize follows the same greening cycle as the surrounding vegetation during the senescence period. Instead Length of Growing Period (LGP) data was extracted from the CPSZ database to estimate the length and end of the growing seasons (Appendix I: NDVI; Start of Season; and Length Growing Period).

3.5.2 Ground-based PET Images

Actual potential evapotranspiration (PET) images were developed by using the IGT software to interpolate PET measurements between 32 ground-based agrometeorological stations located within Kenya (Figure 3.9). These agro-meteorological stations collect ground-based measurements for minimum and maximum temperature, wind speed, hours of sunshine, and relative humidity to calculate daily and dekad PET estimates by the FAO Penman equation (Doorenbos and Pruitt, 1977).

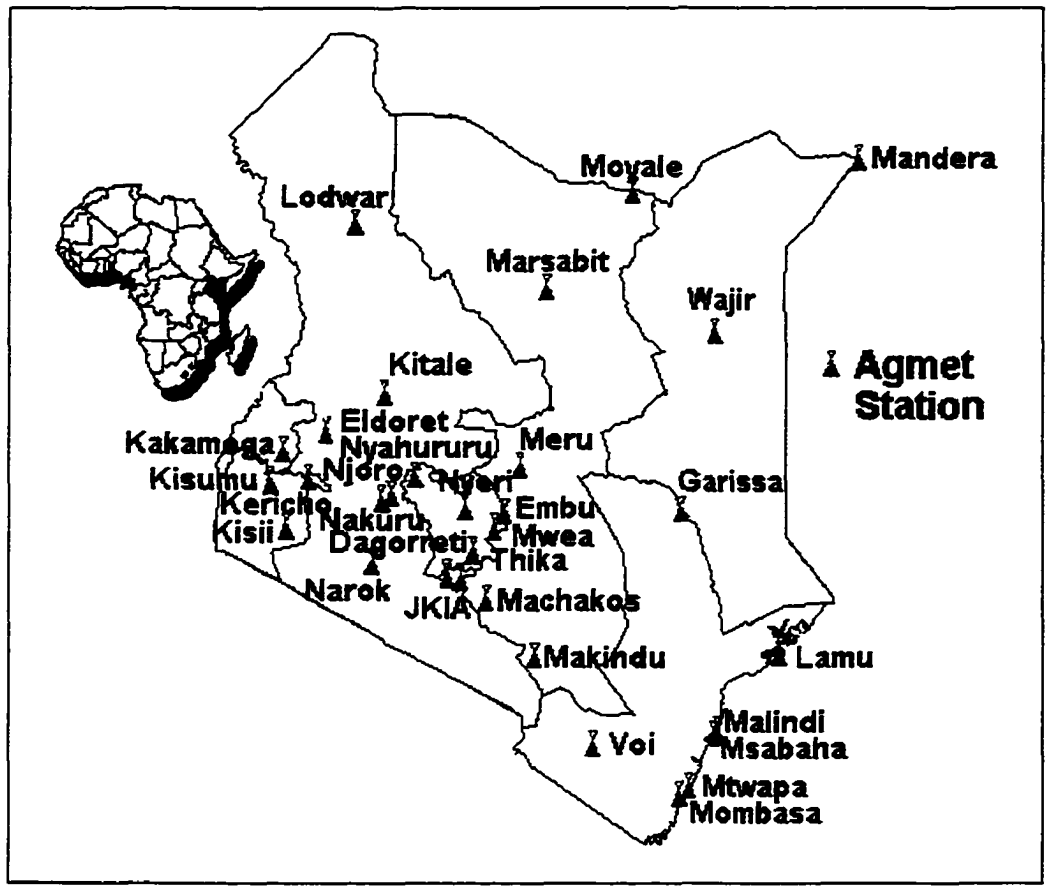

Figure 3.9. Location of agro-meteorological stations maintained by the Kenya Meteorological Department (adapted from FEWS,1997).

The SEDI module from IGT interpolates between PET measurements by using Digital Elevation Models (DEM) (Appendix I, PET and DEM images). The spatial resolutions for the two DEM images are 7.6-km and 1.1-km. Interpolation between PET and elevation is a common GIS procedure because PET has negative correlation with altitude (Eastman, 1997, and Hoefsloot, 1996).

3.5.3 Area Planted

The crop production equation used for estimating regional crop production is:

Production(tons) = Yield(tons/ha) * Area Planted(ha) (3.1)

This research concentrates on developing the "yield" term of equation (3.1) by combining the FAO CSWB model with crop production functions. Determining the exact area planted solely from remote sensing data is beyond the scope of this research because high-resolution images require large amounts of computer memory, expensive aerial surveys, or expensive images from Landsat or SPOT satellite series. Other researchers are exploring how to develop inexpensive and operational methods to identify crops and estimating crop areas, and successful results from their research may be later applied to the GIS-based CSWB model.

For the modified GIS-based CSWB model, "area planted" was estimated from low-altitude flights by the DRSRS or from ground estimates conducted by the MoA at the district level. This data was further divided into CPSZ units by using the raster Biosphere-Atmosphere Transfer Scheme (BATS) image from the 1-KM Global Data Set Project overlaid with the CPSZ vector map from the CPSZ database, as shown in Figure 3.10 (van Velthuizen, et al, 1995, and Eidenshink and Faundeen, 1996).

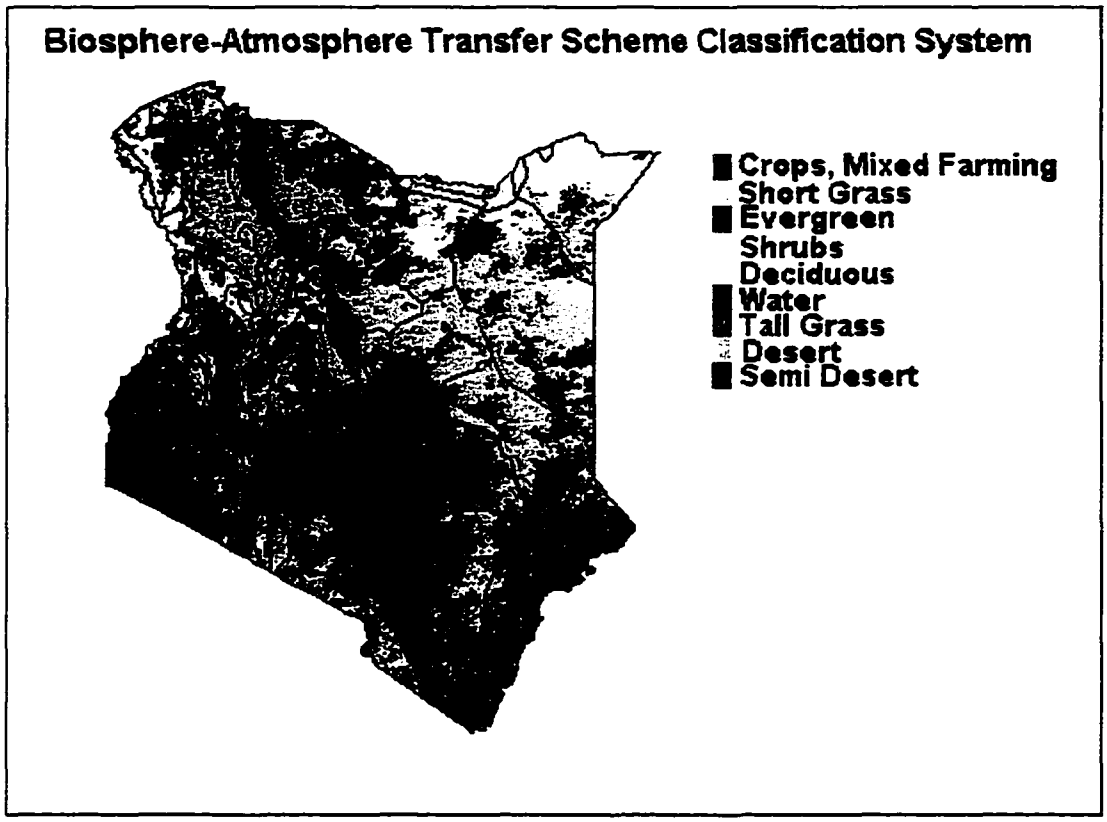

Figure 3.10. Vegetation Classification Image (1-kilometer Resolution) Overlaid with FAO Crop Production System Zones (from Eidenshink and Faundeen, 1996, and van Velthuizen, et al, 1995).

Approximating the average area planted per each CPSZ unit was accomplished by extracting from the BATS image the total area planted for each CPSZ polygon and district polygon. Then the percent of CPSZ area planted per district was calculated by dividing the total CPSZ crop area by the total district crop area. Finally, district area planted estimates from the Government of Kenya were multiplied by the percent of CPSZ area planted per district to estimate the total area planted per CPSZ unit.

3.6 CSWB Model

The GIS-based CSWB model for this research was executed at the following three resolutions:

1. *Agro-Ecological Zone (AEZ) Polygon Analysis:* information from 7.6-kilometer spatial resolution images are extracted based on Crop Production System Zone (CPSZ) polygons as defined by van Velthuizen, et al, (1995).

2. *Pixel-by-Pixel Analysis:* 7.6-kilometer spatial resolution images are overlaid.

3. *Pixel-by-Pixel Analysis:* 1.1-kilometer spatial resolution images are overlaid.

The input GIS databases used for the above three methods were essentially the same, except methods (1) and (2) used a 7.6-km spatial resolution data set and method (3) used a 1.1-km resolution data set.

For the GIS-based CSWB model, real-time satellite-derived RFE data are introduced as actual precipitation, P_a, in the water balance equation (2.3). Real-time satellite derived NDVI data are used to determine the start of the growing season to initialize the model for estimating seasonal crop water requirements. Real-time PET measurements from ground-based agro-meteorological stations are correlated with a DEM to interpolate PET between agro-meteorological stations. These PET images, along with crop coefficients (equation (2.4) derived from starting data and

LGP images, are used to estimate the seasonal crop water requirements and the seasonal Water Requirement Satisfaction Index.

The time fractions of the LGP and the crop coefficients for determining the initial, reproductive, and maturing stages of crop development and water requirements are shown in Table 3.3.

Table 3.3. Critical Crop Coefficient Values (from Gommes, 1983)

Growing Period	Initial	Reproductive	Maturing
LGP Time Fraction	0.16	0.44	0.76
Crop Coefficient, K_c	0.35	1.20	0.60

The WRSI in the CSWB model was changed from a *qualitative* index to a *quantitative* estimate by introducing crop yield functions as defined by Stewart and Hash, (1973) Stewart, et al, (1975); and later developed by the FAO (Doorenbos and Kassam, 1979). Hence, the GIS-based CSWB model provides *quantitative* and *timely* regional yields estimated from real-time RFE and NDVI data images.

A detailed flowchart of the GIS-based CSWB model combined with crop yield functions is shown in Figure 3.11.

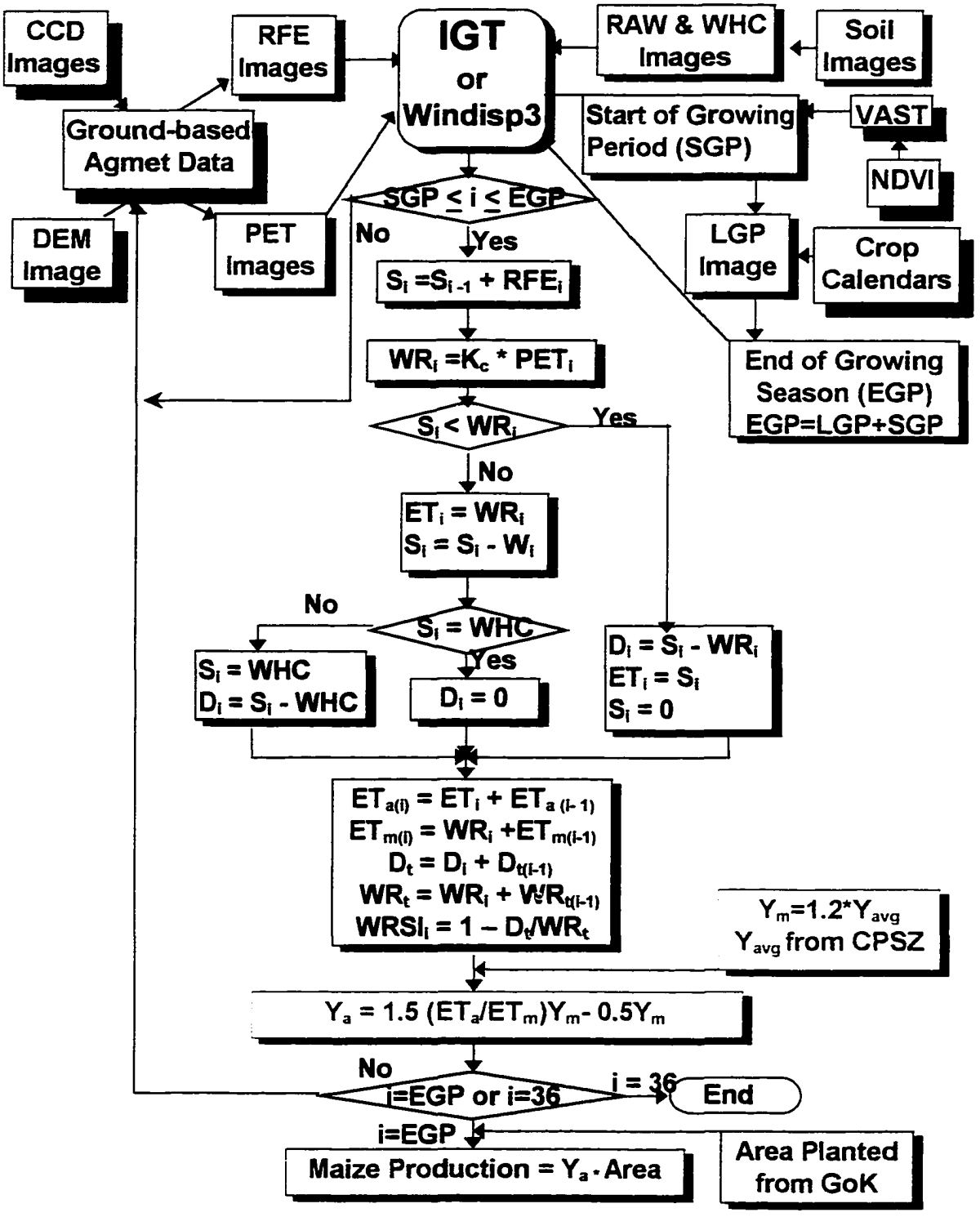

Figure 3.11. Flowchart of GIS-Based CSWB Model (adapted from Gommes, 1983)

The CD-ROM included with this research contains (Appendix IV):

- programs (CPSZ, IGT, IDA, WINDISP3, VAST3, and GISCSWB directories)
- input spatial databases (Kenya1km and Kenya7km directories)
- Government of Kenya ground-based data (GoK directory)
- final results and spatial data (Results directory)

The above information on the CD-ROM allows one to re-run the GIS-based CSWB model for the three different spatial resolutions and compare model results with GoK estimates. All GIS input spatial databases can be re-processed by following the processing steps described in Appendix I or by executing the respective batch files stored on the CD-ROM.

For the AEZ polygon analysis, a FORTRAN program, based on Figure 3.11, was written to run the GIS-based CSWB model, calculate annual crop yield and production for each district, and compare model results with DRSRS and MoA estimates. The input files utilize average rainfall, evapotranspiration, and start of season values extracted for the 206 CPSZ polygons by using the "process\stats\avg" module from the WINDISP3 program (Pfirman and Hogue, 1997). These dekad values were introduced into the FORTRAN program as an array with 36 dekads and 206 CPSZ polygons. Modeled yield values for each CPSZ polygons were then multiplied

with GoK area planted data to calculate crop production for each district.

For the pixel-by-pixel analyses with 7.6- and 1.1-kilometer resolutions, IGT formula files, based on Figure 3.11, were written to run the GIS-based CSWB model by overlaying images. The pixel-by-pixel method differs from the AEZ analysis because GIS (i.e., rainfall and crop water use) images are overlaid to calculate yield images for each dekad. Average annual yields for each CPSZ polygon were extracted from the final yield images by using the "process\stats\avg" module from the WINDISP3 program. Another FORTRAN program was written that multiplies these tabular yield values by GoK area planted data to estimate total maize production for each district, and to compare model results with GoK crop yield and production estimates.

The specific steps for executing the GIS-based CSWB model follow:

Install VAST3, IGT, and WINDISP3 programs on the c: drive.

a. Insert the CD-ROM in the CD-ROM drive (assumed as the d: drive from hereafter).

b. Install the VAST3 program by creating a VAST3 directory on the c: drive and copying the d:\VAST3\vast3.exe file to c:\VAST3.

c. Install the DOS-based IGT program by uncompressing the d:\igt\IGT.zip file into the c:\temp directory and typing install.exe.

d. Install the WINDISP3 program by uncompressing the d:\WINDISP3\wd3setup.zip file into c:\temp directory and running setup.exe from the Run menu in Windows.

For the AEZ Polygon analysis;

a. Run the "Batch\Play" module in WINDISP3 with the d:\WINDISP3\cmd\extraez.cmd batch file. This file extracts average RFE and PET values for each CPSZ polygon; runs the VAST3 program for determining the start of season from a NDVI time series; extracts the average start of season dekad for each CPSZ polygon, and copies these files to the c:\temp directory. These output files are used as arrays within the FORTRAN program in the next step. The statistic output files (*.sta files) used by this research are stored within the d:\WINDISP3\sta\ directory.

b. Run the GIS-based CSWB model for AEZ polygons by typing "cswbazdr" or "cswbazma" at the d:\GISCSWB\AEZ\ directory. These programs calculate district crop yield and production (c:\temp\mp**cswb.val) and compare model results with estimates (c:\temp\mp*GoK.val) from the DRSRS or the MoA. The c:\temp\mp*GoK.val files are similar to original the data from the GoK (d:\GoK\DRSRS\product\pr*drsr.dat and d:\GoK\DRSRS\product\pr*moa.dat), but are reorganized for easy statistical analysis within an Excel spreadsheet. The results for this research are listed in the d:\results\files\MoA\AEZ\ and d:\results\files\ DRSRS\ AEZ\ directories.

For the 7.6-kilometer Pixel-by-Pixel analysis

a. Run the GIS-based CSWB model by executing the "Imgcal\calculate image" module from IGT with the d:\GISCSWB\7km\cswbpx*.fml files. The resultant images for the program will be stored in c:\temp directory and results for this research are stored within the d:\results\yieldimg\7km directory.

b. Extract the average yield for each CPSZ polygon by executing the "Batch\Play" module in WINDISP3 with the d:\GISCSWB\7km \extyd7km.cmd batch file. The resultant yield file will be stored in the c:\temp directory and resultant files for this research are listed as

d:\WINDISP3\sta\yd*avg.sta files. These output files are used as arrays by the FORTRAN program in the next step to calculate crop production.

c. Calculate district production by typing "prod7kdr" or "prod7kma" at the d:\GISCSWB\7km\ directory. Model results (c:\temp\mp*cswb.val) can be compared with crop yield and production estimates (c:\temp\mp*.val) from DRSRS and MoA. The c:\temp\mp*.val files are similar to the original GoK data (d:\GoK\DRSRS\product\pr*drsr.dat and d\GoK\MoA\product\pr**moa.dat), but are reorganized for easy statistical analysis in an Excel spreadsheet. The results for this research are listed in the d:\results\files\MoA\7km\ and d:\results\files\ DRSRS\7km\ directories.

For the 1.1-kilometer Pixel-by-Pixel analysis

a. Run the GIS-based CSWB model by executing the "Imgcal\calculate image" module from IGT with the d:\GISCSWB\1km\cswbpx*.fml files. The resultant images for the program will be stored in c:\temp directory and results for this research are stored within the d:\results\yieldimg\1km directory. Note the final yield images were multiplied by a binary area planted image as described in Section 3.5.3.

b. Extract the average yield for each CPSZ polygon by executing the "Batch\Play" module in WINDISP3 with the d:\GISCSWB\1km\extyd1km.cmd batch file. The resultant yield file will be stored in the c:\temp directory and resultant files for this research are listed as d:\WINDISP3\sta\yd*av1k.sta files. These output files are used as arrays by the FORTRAN program in the next step to calculate crop production.

c. Calculate district production by typing "prod1kma" at the d:\GISCSWB\1km\ directory. Model results (c:\temp\mp*cswb.val) can be compared with crop yield and production estimates (c:\temp\mp*moa.val) from the MoA. The c:\temp\mp*moa.val files are similar to the original MoA data (d:\GoK\MoA\product\pr**moa.dat), but are reorganized for easy statistical analysis in an Excel spreadsheet. The results for this research are listed in the d:\results\files\MoA\1km\ directory.

The DOS-based IGT program was used to prepare the input spatial databases and to run the GIS-based CSWB model for the 7-km and 1-km pixel-by-pixel analyses (Appendix I). However, the IGT program is no longer required to run the GIS-based CSWB model because the new version of WINDISP3 recently integrated the Satellite Enhanced Data Interpolation (SEDI) function (Pfirman, 1998). Thus, WINDISP3 now has the ability to process all real-time input spatial databases and to run the GIS-based model, eliminating the need for the DOS-based IGT program.

WINDISP3 is recommended for future operation of the GIS-based CSWB model because a Windows environment is user-friendly and file variables are easily executed. A batch file in WINDISP3 was recently written to run the GIS-based CSWB model, but this file was not used by this research because SEDI was not yet integrated within WINDISP3. If WINDISP3 is used to run the model for the 1-km and 7-km pixel-by-pixel analyses, perform step (a) by executing the d:\GISCSWB\windcswb\windcswb.cmd batch file with the "Batch\play" module in WINDISP3.

3.7 Crop Yield Functions

The crop yield function of equation (2.8) relates water stress to yield reduction. The factors used for each term are described below.

The maximum evapotranspiration for equation (2.8) was obtained from the CSWB model by summing the maximum water requirement images, WR_i in Figure 3.11, during the entire growing season.

The actual evapotranspiration for equation (2.8) was obtained from the CSWB model by summing the actual evapotranspiration images, ET_a in Figure 3.11, during the entire growing season.

Average crop yield values were obtained from the CPSZ database and these values were multiplied by a factor of 1.2 to estimate the maximum yield value for each CPSZ unit, Y_m for equation (2.7). As discussed in Section 3.4.5, the average CPSZ values were multiplied by a 1.2 factor since the CPSZ values are an average value and a model sensitivity analysis revealed a 1.2 factor closely approximated maximum yields on a district level.

A seasonal Ky value of 1.5 was chosen for equation (2.8) based on recommendations by Gommes and Houssiau (1983) and Stewart and Hash (1982), and confirmed by performing a sensitivity analysis on the model. The same sensitivity

analysis showed a seasonal K_y of 1.5 to be adequate and to have no disadvantage compared to use of phenological K_y values.

3.8 Output Products

The final output derived from the GIS-based CSWB model is a single crop yield image which does not indicate the large amounts of research needed to develop the original CSWB model or the large amounts of empirical experiments conducted to determine the crop yield functions. A single crop yield image also does not indicate the large amounts of information and data integrated into a GIS to run the CSWB model.

Processing the final yield image to determine production per district involves extracting average yield data for each CPSZ polygon, and multiplying these values with area planted data. The final *quantitative* figures provided by the GIS-based model are very useful for helping countries decide how much grain to export or import at the end of the growing season, long before a food shortage has occurred.

Model results from the three different methods were compared with district crop yield and production reports from the MoA during 1989-1997 and from the DRSRS during

1989-1993. Only district results were used in the comparisons since crop yield estimates based on smaller administrative units at the divisional level are not readily available from the GoK for statistical comparison. However, yield images derived by the pixel-by-pixel analyses enable yield and production estimates based on larger (provincial) or smaller (divisional) administrative units to be generated if desired.

In addition, for future operational use, historical yield images could be averaged and subtracted from the current yield image to identify areas with yield anomalies. Such anomaly yield images are useful for identifying surplus and deficit regions for deciding whether to alleviate localized food shortages by transporting grains from a surplus area to a deficit region. This research made no effort to geographically display regional yield anomalies, even though they could be easily generated for operational use in Kenya.

4. RESULTS AND DISCUSSION

The overall objective of the research was to estimate regional crop yields by integrating the CSWB model with real-time satellite data, ground-based ancillary data, and a GIS. The GIS-based CSWB model developed by this research was validated by comparing model crop production estimates based on archived satellite data to historical district maize production reports from two Kenya government agencies, the Ministry of Agriculture (MoA) and the Department of Resource Surveys and Remote Sensing (DRSRS). The MoA maize production reports were from 1989-1997, and the DRSRS maize production reports were from 1989-1993. In addition, the model analyzed real-time satellite data at three different levels of resolution: agro-ecological zone (AEZ) polygons; 7.6-kilometer pixels; and 1.1-kilometer pixels.

Relative crop yield images are the main output from the model, as shown in Figures 4.1 and 4.2. The AEZ polygon method is not consider as useful as the pixel-by-pixel methods because the polygons prevent yield data to be extracted for administrative units smaller than the district level. However, yield data on the divisional or locational levels could be easily extracted from the yield images calculated via the 7.6-km or 1.1-km pixel-by-pixel method.

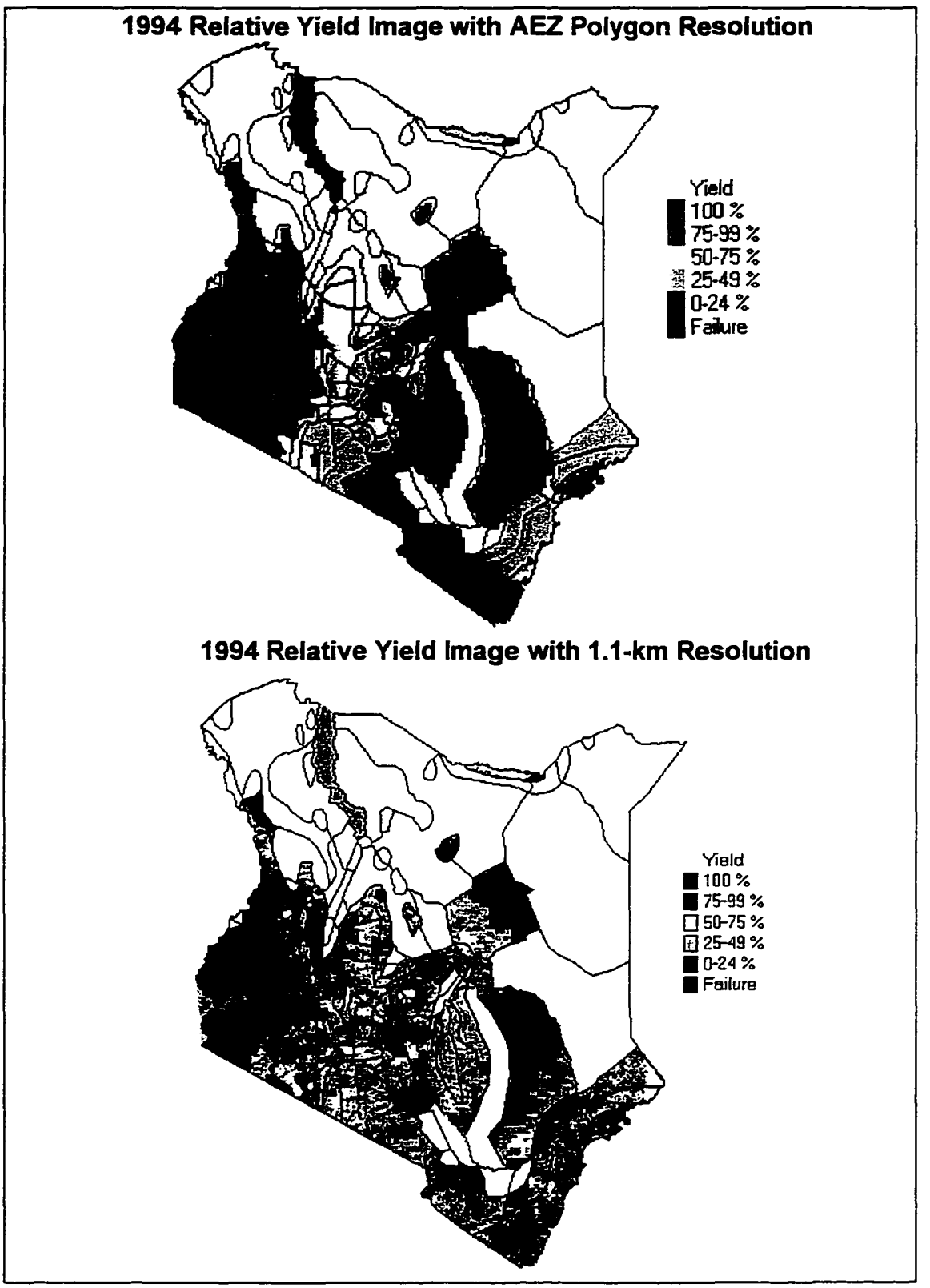

Figure 4.1. Relative Yield Images for 1994

The yield images also show large visual contrasts between poor and bumper year harvests, as indicated by Figure 4.2. These strong contrasts indicate subtracting a current yield image from a 10-year average yield image would create useful anomaly yield images.

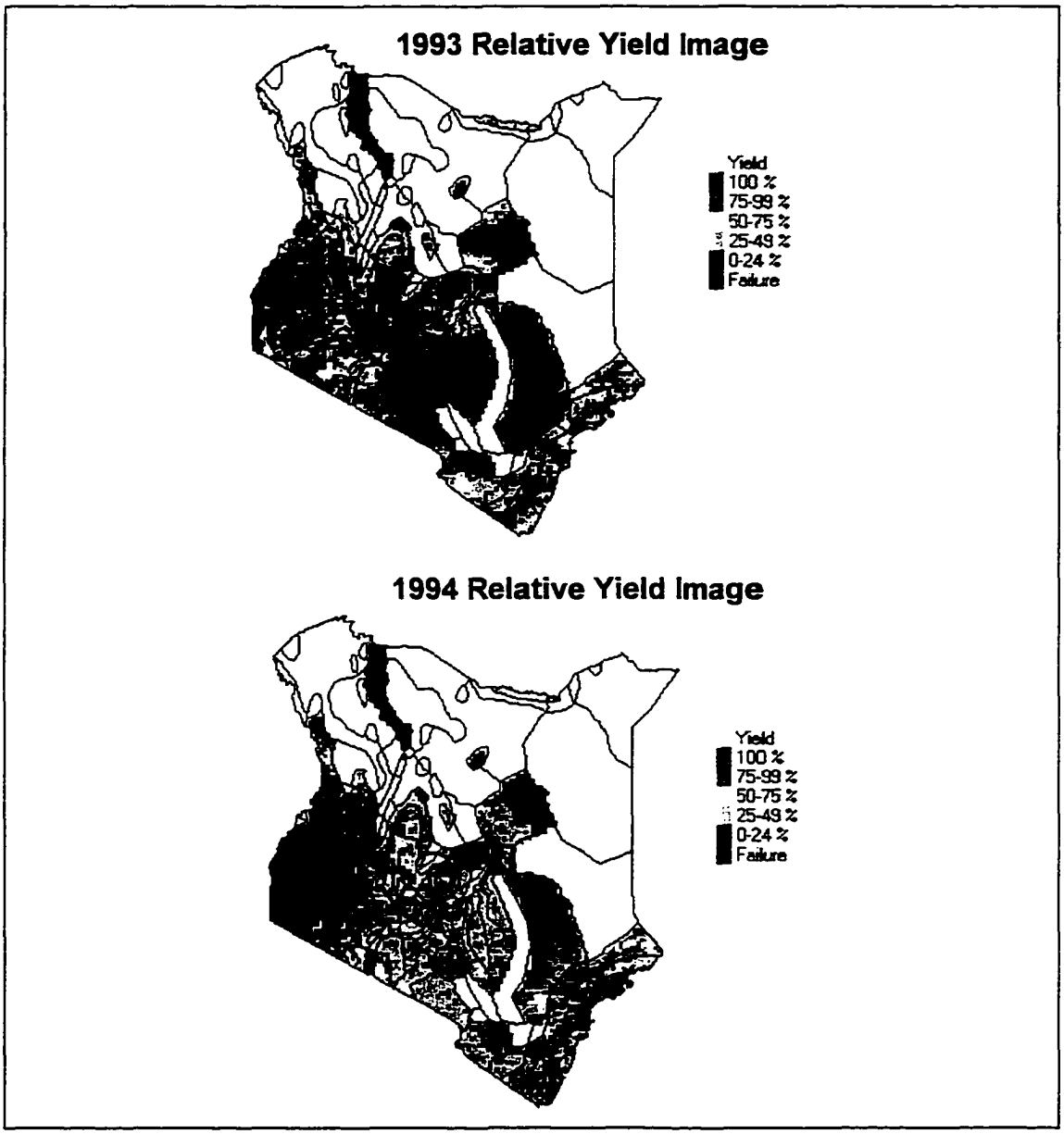

Figure 4.2. Relative Yield Images (7.6-km resolution) for 1993 and 1994.

The relative yield images enable the yield term of the production equation to be estimated. Average yield data from these images were extracted for each district in tabular form by using WINDISP3. The average yield data was multiplied by area-planted data from the respective government agency to estimate district productions.

District production results from the model for three different spatial resolutions were compared to district production estimates from the Kenya Government, as shown by the regression coefficients in Tables 4.1 and 4.2. The scatter diagrams for these district analyses are presented in Figures 4.3 and 4.7.

Table 4.1 Summary of Regression Coefficients (r) by Comparing DRSRS Reported District Maize Production to Model District Production Results with AEZ and 7.6-km Resolutions.

Year	*r from DRSRS District Estimates Compared to AEZ Model District Estimates*	*r from DRSRS District Estimates Compared to 7.6-km Model District Estimates*
1989	0.9570	0.9439
1990	0.9486	0.9565
1991	0.9387	0.9489
1992	0.9528	0.9545
1993	0.9596	0.9648
1989-93	0.9349	0.9430

Table 4.2 Summary of Regression Coefficients (r) by Comparing MoA Reported District Maize Production to Model District Production Results with AEZ, 7.6-km, and 1.1-km Resolutions.

Year	*r from MoA District Estimates Compared to AEZ Model District Estimates*	*r from MoA District Estimates Compared to 7.6-km Model District Estimates*	*r from MoA District Estimates Compared to 1.1-km Model District Estimates*
1989	0.9608	0.9520	*No*
1990	0.9444	0.9463	*LAC*
1991	0.9657	0.9615	*Data*
1992	0.9551	0.9588	*Available*
1993	0.9092	0.9353	0.9356
1994	0.9615	0.9539	0.9575
1995	0.9243	0.9340	0.9552
1996	0.9559	0.9484	0.9593
1997	0.9540	0.9604	0.9597
1989-97	0.9397	0.9447	0.9421

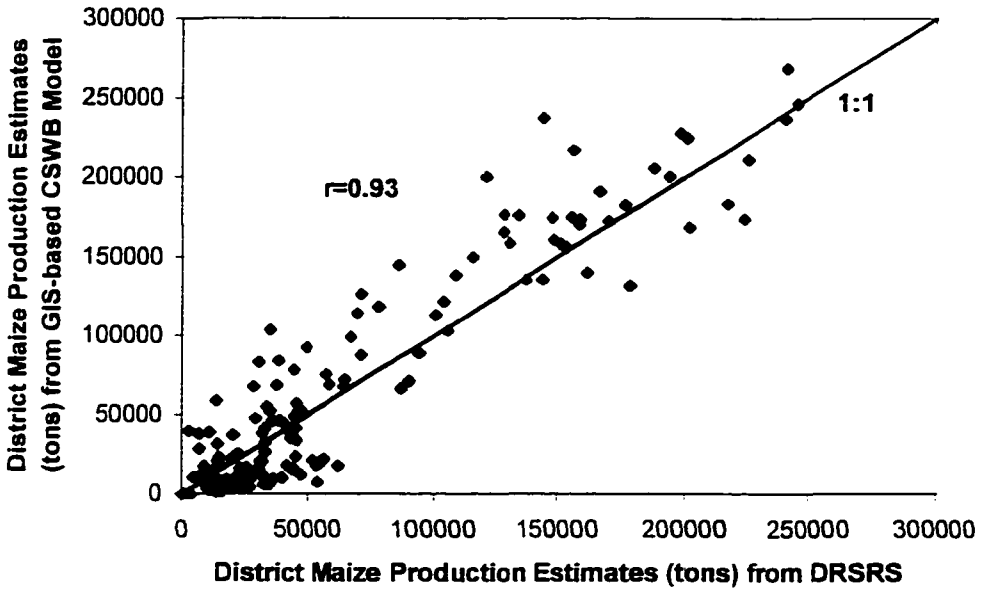

Figure 4.3. GIS-Based CSWB Model Results vs. DRSRS District Maize Production Estimates from 1989-1993 (Agro-Ecological Zone Analysis)

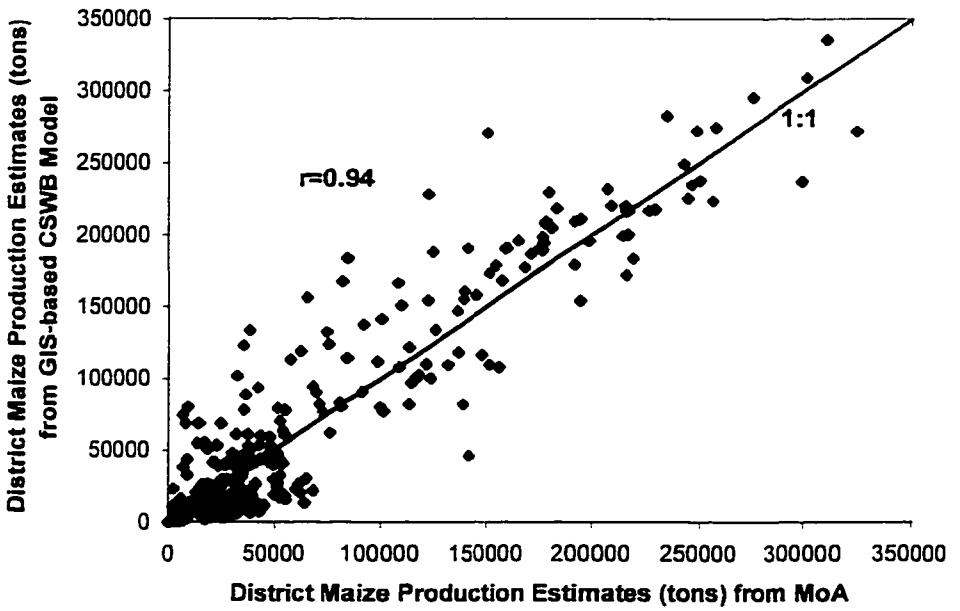

Figure 4.4. GIS-Based CSWB Model Results vs. MoA District Maize Production Estimates from 1989-1997 (Agro-Ecological Zone Analysis)

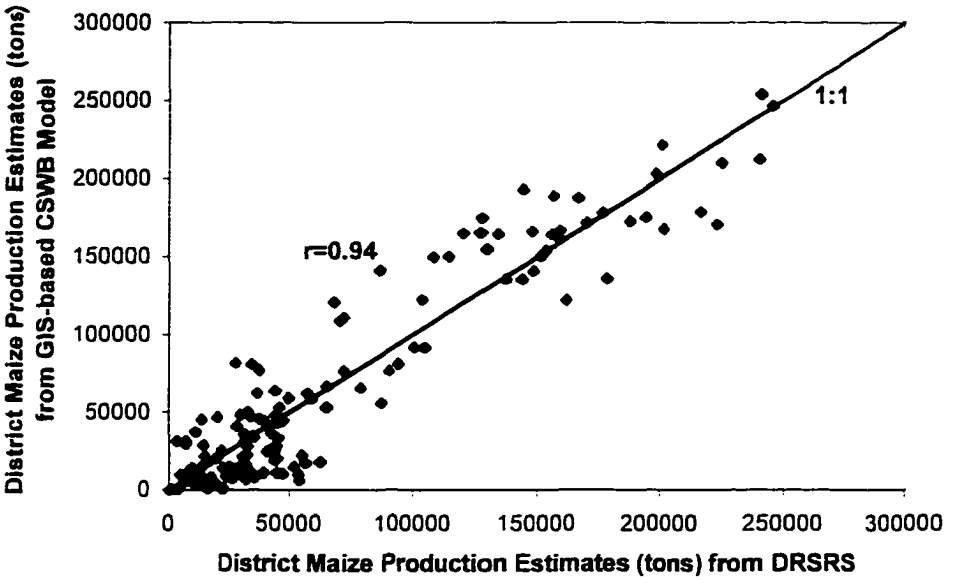

Figure 4.5. GIS-Based CSWB Model Results vs. DRSRS District Maize Production Estimates from 1989-1993 (7.6-kilometer Pixel-by-Pixel Analysis)

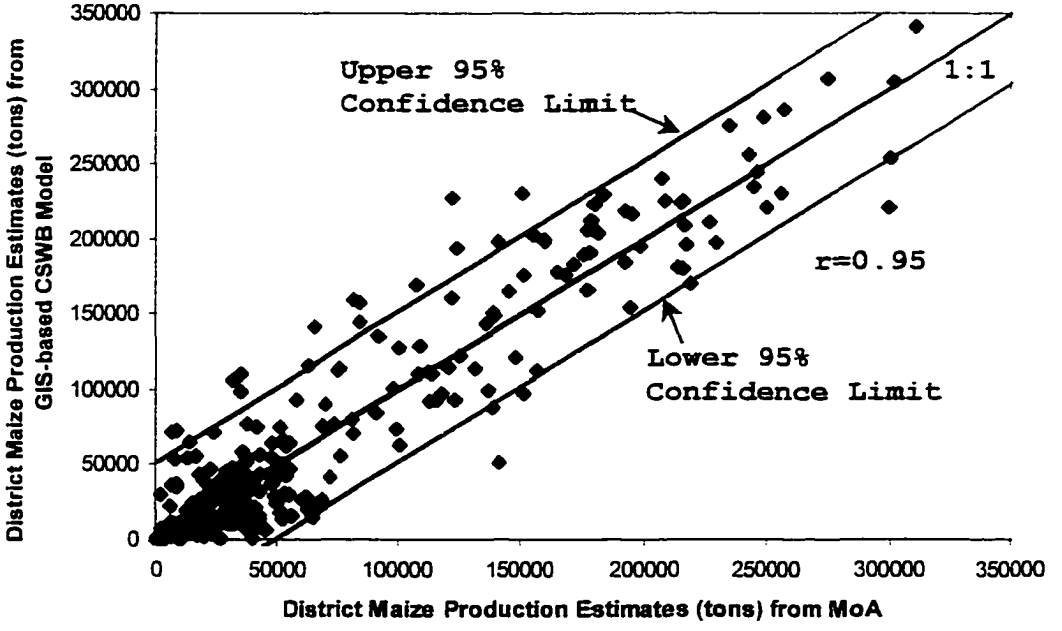

Figure 4.6. GIS-Based CSWB Model Results vs. MoA District Maize Production Estimates from 1989-1997 (7.6-kilometer Pixel-by-Pixel Analysis)

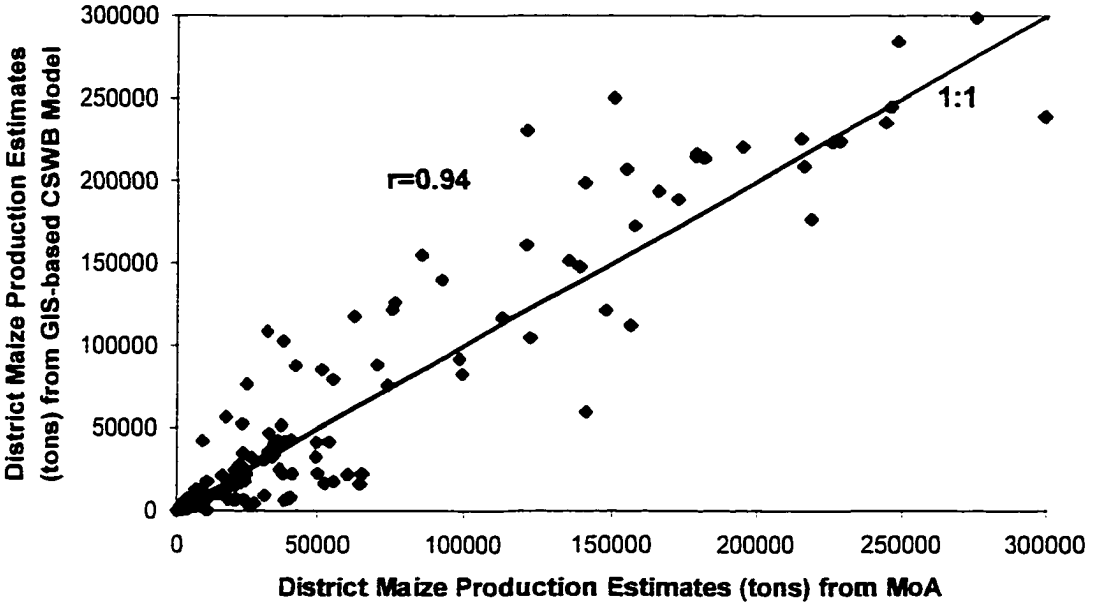

Figure 4.7. GIS-based CSWB Model Results vs. MoA District Maize Production Estimates from 1993-1997 (1.1-kilometer Pixel-by-Pixel Analysis

The above correlation coefficients ranged from 0.91 to 0.96 when comparing model results to district estimates from the Government of Kenya. For the AEZ analysis, model results compared to district maize production estimates from the MoA and the DRSRS revealed correlation coefficients of 0.94 and 0.93, respectively (Table 4.1, and Figures 4.3 and 4.4). For the 7.6-kilometer pixel-by-pixel analysis, the comparison showed correlation coefficients of 0.95 and 0.94, respectively (Table 4.2, and Figures 4.5 and 4.6). For the 1.1-kilometer analysis, the correlation coefficient between

model results and district maize production estimates from the MoA (1993-1997) was 0.94 (Table 4.2 and Figure 4.7).

The scatter diagrams in Figures 4.3-4.7 show the model over-estimates production for each analysis. However, this is common for water balance models because crop yield models cannot always estimate negative events such as pest infestations and disease.

Comparison of district crop production reports from the MoA and DRSRS is shown in the scatter diagram of Figure 4.8. The correlation coefficient between these two data sets is 0.90, indicating the correlation coefficient between the two government data sets is less than correlation coefficients between the GIS-based CSWB model. The better correlation with the GIS-based CSWB model is probably because area-planted data for the GIS-based model is dependent upon area-planted data from the Government of Kenya, while area-planted data from the two government agencies are independent.

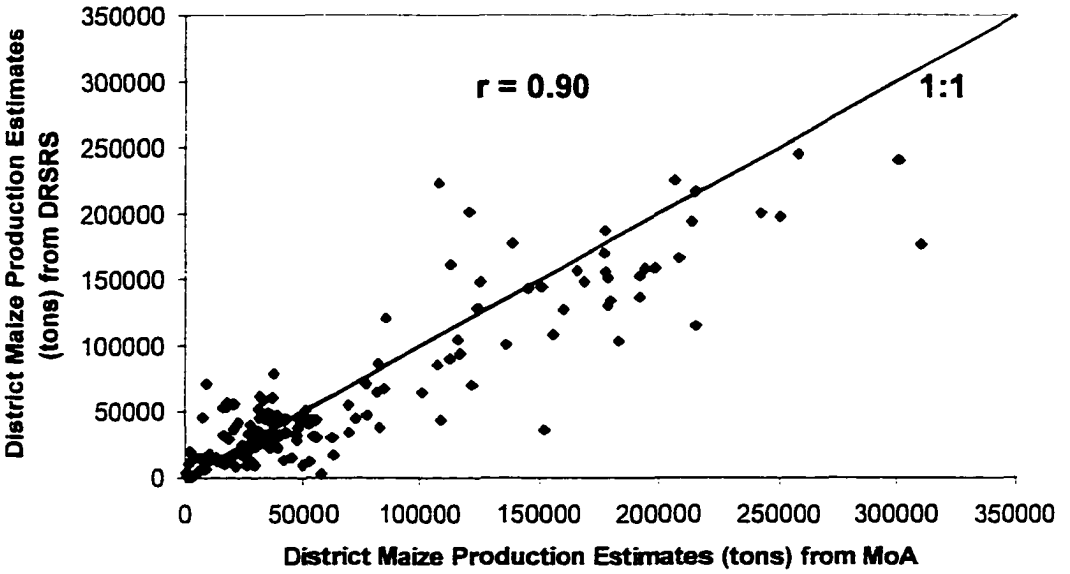

Figure 4.8. Comparison of District Maize Production Estimates from MoA and DRSRS (1989-1993).

District production estimates from the GIS-based CSWB model were summed to obtain the total national maize production for the long rain season, as shown in Tables 4.3 and 4.4. The percent difference columns from these tables show that the GIS-based CSWB model both under- and over-estimates national maize production. The largest discrepancies occurred for years 1993, 1996, and 1997, with all three of these discrepancies showing the model over-estimating production.

The largest error when comparing the model with both government data sets occurred during the drought year of

1993. The MoA and DRSRS estimated national maize production during this year was less than 25-50 percent from the average. However, the FAO estimated maize production for 1993 was 2,089,000 metric tons (Figure 3.4), which indicates the GoK estimates may have been excessively low during this year (FAO, 1997). In addition, model discrepancy for 1997 was probably due to crop reductions caused by water-logging due to the heavy ENSO related rains in late 1997.

Table 4.3 Summary of Annual Maize Production in Kenya (long rains) for DRSRS Reported Estimates vs. GIS-based CSWB Model Results with AEZ and 7.6-km Resolutions.

Year	*DRSRS Maize Production Estimates (tons)*	*AEZ Analysis: Maize Production Estimates (tons)*	*7.6-km Analysis: Maize Production Estimates (tons)*	*Percent Difference*	
				AEZ	*7.6-km*
1989	2,108,000	2,179,000	2,203,000	3.4	4.5
1990	1,947,000	2,005,000	1,813,000	3.0	-6.9
1991	2,236,000	2,221,000	2,046,000	-0.7	-8.5
1992	2,391,000	2,152,000	2,016,000	-10.0	-15.7
1993	1,140,000	1,673,000	1,403,000	46.7	23.1

One should note that the national production figures of the DRSRS and MoA do not agree (Tables 4.3 and 4.4), because DRSRS data did not cover the whole of Kenya and the MoA data includes all maize-producing districts in the republic.

Table 4.4 Summary of Annual Maize Production in Kenya (long rains) for MoA Reported Estimates vs. GIS-based CSWB Model Results with AEZ, 7.6-km, and 1.1-km Resolutions.

Year	*MoA Maize Production Estimates (tons)*	*AEZ Analysis: Maize Production Estimates (tons)*	*7.6-km Analysis: Maize Production Estimates (tons)*	*1.1-km Analysis: Maize Production Estimates (tons)*	*Percent Difference*		
					AEZ	*7.6-km*	*1.1-km*
1989	2,724,000	2,515,000	2,653,000	*No*	-7.7	-2.6	No
1990	2,676,000	2,763,000	2,585,000	*LAC*	3.3	-3.4	LAC
1991	2,184,000	2,279,000	2,191,000	*Data*	4.4	0.3	Data
1992	2,135,000	2,139,000	2,098,000	*Available*	0.2	-1.6	Avail
1993	1,503,000	2,065,000	1,837,000	1,976,000	37.3	22.2	31.4
1994	2,593,000	2,490,000	2,473,000	2,508,000	-4.0	-4.6	-3.3
1995	2,083,000	1,933,000	1,852,000	2,083,000	-7.2	-11.1	-12.5
1996	2,053,000	2,303,000	2,320,000	2,053,000	12.1	13.0	13.6
1997	2,258,000	2,539,000	2,498,000	2,576,000	12.5	10.6	14.1
r		0.77	0.88	0.80			

Regression coefficients were calculated between model results and national production estimates from the MoA, even though the sample size is only nine years (Table 4.4). National production regressions were not calculated for the DRSRS data because only five years of data were available. The national regression coefficients for the MoA data are less than the district regressions because the larger scale probably caused more errors.

The best national level regression occurred for the 7.6-kilometer analysis, and the best method at the district level was also the 7.6-km analysis (Table 4.2). Therefore, 95% confidence intervals were calculated for the 7.6-kilometer analysis at both the national and district levels (Figures 4.9 and 4.6). The 95% confidence intervals for national and district level production estimates were $\pm$350,000 and $\pm$52,000 tons, respectively.

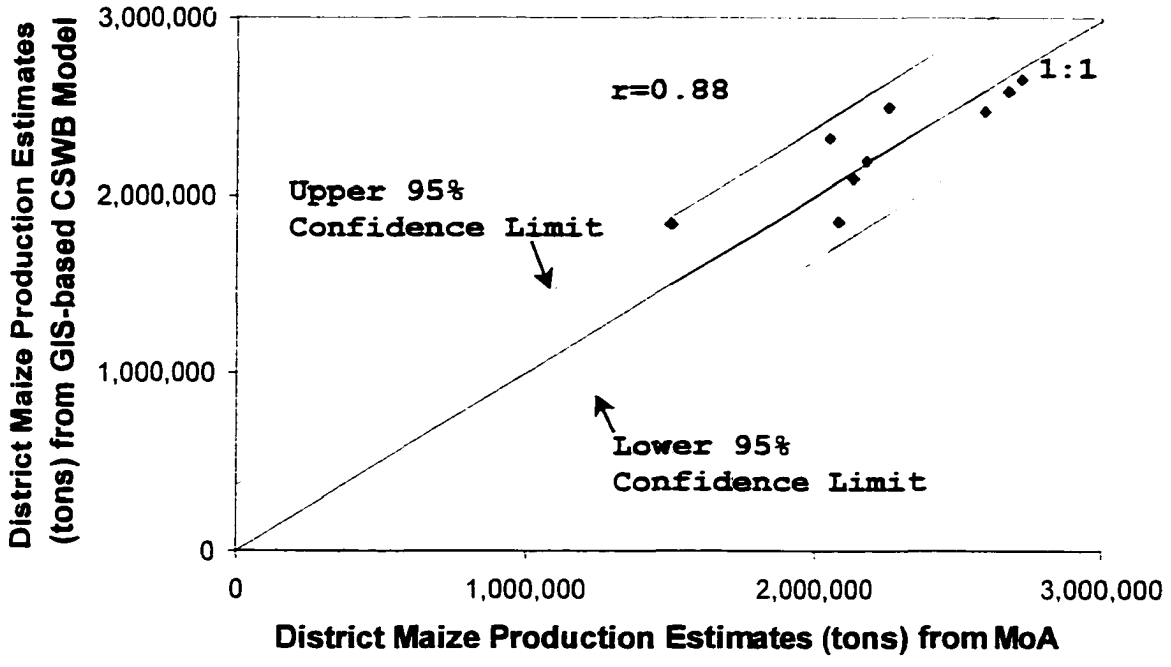

Figure 4.9. MoA National Production Estimates (1989-1997) Compared to GIS-based Model Results (7.6-km Pixel-by-Pixel Analysis).

Other major differences between the three model resolutions include: computer run time, method of estimating the soil water holding capacity, method of obtaining the area planted, and smallest administrative units for reporting final results. A summary of model differences for the different model resolutions is presented in Table 4.5.

Table 4.5 Summary of the GIS-based Model with Three Different Resolutions.

Parameter	*AEZ Resolution*	*7.6-km Resolution*	*1.1-km Resolution*
Computer (Pentium 80-MHz) Run Time	5 seconds	2.5 hours	60 hours
Area planted	District Tables	District Tables	District Tables/Digital
Readily Available Soil Moisture Storage	Average for AEZ polygon	7-km pixel (FAO,1995)	1-km pixel (Kassam,1993a)
Smallest Admin. Unit For Reporting Yields or Production	District	Division or Smaller	Division or Smaller

Both area planted and soil moisture storage images could have been improved as the resolution of the GIS-based model improved. Better resolution soil moisture storage images are expected to improve estimates for a finer resolution analysis, but these improvements were not made by this research to keep the soil input databases consistent. Accordingly, area-planted data on the district-level and a soil moisture storage image with AEZ resolution were used for all three analyses. However, better resolution soil moisture storage images and area-planted data are expected to improve estimates for a finer resolution analysis.

4.1 GIS-based CSWB Model Results

As previously stated, the GIS-based CSWB model used 1989 district boundaries for all years from 1989-1997 in order to keep the district boundaries consistent for this study. Changing boundaries will cause problems with the AEZ analysis, because each CPSZ unit was based on the 1989 district boundaries. However, new and changing district boundaries will not pose any problems with the pixel-by-pixel analyses because average yield data can still be extracted with different polygon shapes or political boundaries.

The GIS-based model with AEZ resolution can monitor the variability in maize production both temporally and spatially, but slight accuracy is lost. However, one of the benefits with the AEZ method is that significantly less computer time is needed to estimate yields and production, Table 4.5.

The 7.6-kilometer pixel-by-pixel analysis indicates model estimates are slightly better than estimates by the AEZ method, but computer processing time also increases. However, longer computer time for a Pentium 80-MHz computer is not a disadvantage for real-time operation, since the model, under normal real-time operation conditions, will be executed in 10-day increments. Thus, 2.5 hours run time to

process a year of 7.6-kilometer images would be 150 hours divided by 36 dekads, or slightly over 4 minutes for each dekad.

Surprisingly, the finer resolution 1.1-kilometer pixel-by-pixel analysis did not significantly improve crop production estimates, and processing time for one year of data was 60 hours. No improvement of accuracy can probably be attributed to the coarse resolution of the input data such as the RFE images with 7.6-kilometer resolution, soil moisture storage image with an AEZ polygon resolution, and area-planted data at the district level. Due to the above resolution limitations for the input data and increased computer processing time (60 hours), the 1.1-kilometer analysis is not recommended at the present. However, finer resolution analysis will be beneficial in the future, especially after the resolution of soil moisture storage, area-planted data, and RFE images improve.

In summary, the ground-based CSWB model was refined and improved by introducing real-time satellite data and by using a GIS to manage the spatial data. The research results indicate that the model has the ability to objectively monitor the seasonal variability of rainfall and crop production at the national and district levels. The model also can be enlarged to estimate crop yields and

production for other countries because most of the input data is already available for all of Africa and Kenya was windowed-out for this study. The model could also be extended to monitor other crops because the soil water balance method and principals are applicable to other crops.

Comparison of model results based from archived satellite data with historical crop yield reports indicates the model can be used in the future with relative confidence with all three resolutions. The pixel-by-pixel method allows crop production to be monitored at even smaller administrative units such as at the divisional or locational level. Accordingly, the AEZ analysis is not recommended due to the difficulty in reporting in smaller administrative units, and the 1.1-kilometer analysis is not recommended at present due to coarse resolution input data and no improvement in model accuracy. Therefore, crop production estimates using the 7.6-km pixel-by-pixel analysis is recommended at present. Finer resolution pixel-by-pixel analysis at the 1-kilometer scale can be attempted in the future after the resolution of soil moisture storage, area planted, and RFE images are improved.

4.2 Specific Problems and Future Improvements

The various problems associated with each of the five components of the GIS-based CSWB model and software are discussed below. Recommendations for improving each of these model deficiencies are suggested for future work.

4.2.1 Real-time Input Database Problems

Developing real-time PET images is a major concern for future real-time operation of the model since PET is acquired from national ground-based agrometeorological stations and not by remote sensing methods. Presently, obtaining real-time PET values is a problem in Kenya, and obtaining real-time PET values is difficult in most parts of Africa, making PET data a major drawback in operating a national crop yield model based on the water balance method. However, because crop yield estimation is usually done at a national level, obtaining PET data on a real-time basis should not be a major problem provided the national meteorological departments cooperate in providing real-time PET data.

For Kenya, acquiring PET data is difficult because the Kenya Meteorological Department (KMD) calculates PET values at the end of the year, preventing use of real-time PET values. In order to have reliable crop yield estimates for

Kenya in the future, KMD needs to modify their policy and calculate real-time PET values at the end of each dekad. Average or normal PET images can be used in the absence of real-time values, but use of these normal values will tend to under estimate crop yield during dry periods (FAO, 1986a).

While interpolating PET values between agro-meteorological stations has traditionally been a spatial problem, using the IGT software and a DEM as a background image produced relatively good interpolations.

Development of digital area-planted images is another improvement that is needed, because only tabular area-planted data on a district level could be obtained for this study. Area-planted images with district level resolution ultimately defined the final spatial resolution of the analysis, resulting in little improvement with finer resolution analysis. For better model accuracy, digital area-planted images are needed to indicate exactly which pixels should be used for calculating production, instead of estimating yields by averaging all the pixels within a given district or agro-ecological region.

Area-planted images are also limited by 8-bit images which allow IDA software to store 0-255 (2^8=256) classes of "real world" information per pixel. A total of 255 classes

of stored information is large enough to run the GIS-based CSWB model for calculating yields, but developing area-planted images on a district level is more complex because the number of hectares planted per district can easily exceed 255.

Currently, IGT software is able to develop an area-planted image with values larger than 255 by selecting a 200 IDA image type, and defining the slope and intercept. However, large rounding errors are produced by the IGT method, and unreasonable errors occur for those pixels located along a district boundary. These problems could be avoided by developing digital area maps with 1.1-kilometer resolution or less. The best method to develop digital area images with this type of resolution is to introduce area-planted images derived from aerial digital videography, LANDSAT, or the soon to be launched MODIS satellite series from NASA (Appendix III, MODIS).

Future recommendations:

1. Make the GIS-based CSWB model operational in Kenya. A User's Manual also needs to be written.

2. Develop the Kenya GIS-based CSWB model for the Kenya short rains season and several other crops.

3. Modify the present KMD policy to calculate PET values at the end of every dekad so that dekad PET data are readily available on a real-time basis.

4. Develop the GIS-based CSWB model for other countries and crops.

5. Develop on a real-time basis digital area planted images with 1.1-kilometer resolution or better.

   a) Advances in determining area planted should be possible with the launch of MODIS in June, 1998. MODIS will have 250-meter resolution for dekad vegetation index images, and the daily temporal frequency will allow crop area-planted estimates to be developed similar to the algorithm used by the Global 1-KM Project to distinguish crop area planted. The 1-KM Global Project gave good crop area estimates for Kenya with most misclassifications occurring along the coast.

4.2.2 Reference Database Problems

It was not possible to readily derive soil moisture storage images with 1-kilometer resolution due to the lack of soil depth and soil texture images with similar resolution. Global soil texture and soil depth images with 1-kilometer resolution are required to complement the Global 1-KM Land Data project. However, a soil moisture storage image with 1-kilometer resolution is not required for the model until area-planted images are produced with 1-kilometer resolution or better.

Future recommendations:

1. Develop soil moisture storage images with 1-km resolution by first developing soil depth and soil texture images with 1-km resolution. Soil water

holding capacity images can then be derived by the same methodology described by FAO (1995).

4.2.3 CSWB model and Crop Yield Function Problems

The ground-based and GIS-based CSWB models do not account for reduced yields caused by excess precipitation Efforts to incorporate a water-logging factor in these models should be undertaken, because excess water can reduce yields significantly, as demonstrated by the heavy 1997/98 short rains induced by El Niño. Polynomial crop production functions, as described by Solomon (1985), could be easily introduced into the CSWB model to correct for excess rainfall.

In addition, regional variations caused by such non-weather factors as soil fertility, pests, disease, etc. are not accounted for in the crop yield model, and crop damage caused by pests and disease cannot be modeled effectively. However, the crop yield function indirectly accounts for farm inputs and other factors by the maximum crop yield factor, Y_m from equation (2.8). Y_m, therefore, is critical for reasonable estimates and should be constantly monitored to maintain the model's accuracy.

The major weakness of the ground-based and GIS-based CSWB models, which could be corrected with minor effort, is estimating the length of growing period (LGP) from thermal

days and not from calendar days. The FAO method of estimating crop coefficients from average LGP crop calendar data is not advisable when using a GIS because LGP is better estimated by using thermal days. Thermal days is a common procedure used by most water balance and irrigation scheduling models because crop growth is better monitored by measuring thermal units, rather than from an average time period.

Thermal days or Growing Degree Days, GDD, is a much better way to estimate LGP, where GDD are defined as:

$$\mathbf{GDD = \Sigma\{(T_{max}-T_{min})/2 - T_{base}\}} \qquad \mathbf{(4.1)}$$

where, T_{max} = daily max. temperature, °C
T_{min} = daily min. temperature, °C
T_{base} = minimum air temperature required for crop growth, °C

Equation (4.1) is valid for $T_{base} \leq (T_{max}-T_{min})/2 \leq TG_{max}$ where TG_{max} is the maximum air temperature for which crop growth is constant. Allen (1976) describes how to calculate GDD by a modified sine wave curve. A T_{base} of 10°C and a TG_{max} of 30°C is recommended for calculating GDD for maize in most agro-ecological zones (Sammis, et al, 1985, and Stegman, 1988).

A GIS makes it easy to incorporate the GDD function into the CSWB model since T_{max} and T_{min} images are measured daily by the geo-stationary METEOSAT satellite. Ten-day GDD

images for Africa could be distributed by the FEWS or ARTEMIS projects and would be a very useful data set for estimating the actual LGP on a regional scale.

Future recommendations:

1. Estimate LGP, crop coefficients, and water use from Growing Degree Days, instead of calendar days.
2. Develop ten-day GDD images derived from the METEOSAT for determining the LGP and regional crop water use.
3. Estimate crop yield reductions due to excess rainfall by introducing polynomial crop yield functions.

4.2.4 Software Problems

IGT software permitted the development of a user-friendly GIS-based CSWB model due to IDA compatibility, and allowing one archive in IDA format. The compatibility of different input data sources is a major concern because the GIS-based CSWB model integrates large amounts of data. Fortunately, IGT permitted all input data to be easily transferred into an IDA format and to run the GIS-based CSWB model.

Despite the above advantages, problems with the IGT software include:

- DOS environment is not user-friendly.

- Batch files with different variables cannot be executed.
- Errors are generated for pixels located along district boundaries when developing area planted images.
- Large rounding errors are created when producing area planted maps.

Recently, the SEDI function was integrated into WINDISP3, which now allows WINDISP3 to run the GIS-based CSWB model. The only features that IGT can perform and WINDISP3 cannot are:

- Overlay images with complex functions (exponential, square root, log, etc.).
- Import tabular data into IDA format images.
- Replace missing values from IGT images with any numerical value.

The use of complex functions is not presently required to run the GIS-based CSWB model, but it may be required in the future when introducing crop coefficients calculated from thermal days instead of calendar days. Also, importing tabular data into spatial images is not a critical function to run the model, but the equivalent of an "assign" feature within other GIS software is especially useful when importing crop yield estimates from governments or importing tabular data from the CPSZ database.

Cloud cover for finer resolution LAC data is another problem when determining start of season images from the

VAST3 program and a LAC-NDVI time series data set. The VAST3 program smoothes images to a certain degree, but more processing must be done by WINDISP3 software to produce better cloud-free images from the real-time LAC data sets (Appendix II, Start of Season; and Appendix III, VAST3 and WINDISP3 software). Averaging every other dekad or filtering pixels could assist in reducing cloud effects with LAC data, but none of these options were performed for this research in order to keep the methodologies between the GAC and LAC data sets similar.

Another solution for creating a cloud-free start of season image, would be to incorporate RFE images within the VAST3 program. Using RFE images in the VAST3 program would also be beneficial to compare difference of onset of growing season by an NDVI and RFE analysis. Hassan (1997) suggest a rainfall accumulation of 80 mm is the best indication of the start of growing season, while FAO (1986) and Stewart (1988) suggest a rainfall value of 30 mm accumulated in one dekad. Regardless of the methodology, it probably would be better to use RFE images in combination with NDVI images to determine the start of the season and use a thermal day calendar to determine the length and end of the growing seasons.

Future recommendations:

1. Incorporate the few missing features from IGT into WINDISP3.

2. Add a new feature to VAST where the start of growing season is determined by RFE images, and isolate pixels with large discrepancies between the NDVI and RFE start of season estimates.

5. CONCLUSIONS

This research introduces real-time satellite data into the ground-based CSWB model to provide *timely* and *quantitative* crop yield and crop production estimates. Integrating real-time satellite data into a GIS-based crop yield model enables crop yield estimates to be made at the end of the growing season, several months before food supplies might be depleted. Quantitative estimates of regional crop yields and production should serve as valuable information for government decision-makers who determine how much grain to export or import annually. This information should be particularly beneficial to IGAD countries because the region has a grain deficit even during years of good rains.

The research methodology integrates several FAO and EWS models, data, and software, such as:

- ground-based crop yield model (Frère and Popov, 1979 and FAO, 1986a),
- crop production functions (Doorenbos and Kassam, 1979),
- real-time satellite data (FAO, 1994 and Snijders, 1995),
- spatial agriculture database (van Velthuizen, et al, 1995), and
- Early Warning System software and tools (Hoefsloot, 1996, Lee, 1997, and Pfirman and Hogue, 1997).

Many of these methods and tools are already commonly used by several agro-meteorological and Early Warning System

stations in Africa, but they have not yet been combined together by a GIS model to estimate crop yields.

Kenya was the trial area for developing the model, but results from this model can be applied elsewhere because most of the input data cover all of Africa, and Kenya was windowed-out for this study. The FAO CSWB method is also a universal method for estimating crop yields which requires small amounts of local data. Correspondingly, the GIS-based CSWB model could be expanded to serve other countries or extended to estimate yields for other crops.

The GIS-based CSWB model utilized three different resolutions: agro-ecological zone (AEZ) polygon analysis, 7.6-kilometer and 1.1-kilometer pixel-by-pixel analysis. When comparing model results to historical district crop production reports from two Government of Kenya departments, the correlation coefficients for the model at the three different resolutions ranged from 0.91 to 0.96. These results indicate that real-time satellite data with ground-based measurements is a reasonable and objective method to estimate crop yields, and that future crop production estimates can be made with relative confidence.

The results further showed the 7.6-kilometer pixel-by-pixel analysis to be the most favorable method due to model accuracy, availability of input data, less computer

processing time, and ability to monitor crop yields for small administrative units at the district level or smaller (i.e., divisions, locations). The 1.1-kilometer pixel-by-pixel analysis had little advantage over the agro-ecological zone analysis due to lack of digital area-planted, soil moisture storage, and RFE images with 1.1-kiolmeter resolution.

IDA GIS Tools (IGT) was used as the primary GIS software to manage and integrate the input data and to run the GIS-based CSWB model. All input spatial images were stored in IDA format and the time step for the model was ten-day increments for monitoring temporal and spatial variability of the model parameters.

The model utilizes four real-time input data sets:

- dekad RFE and NDVI satellite-derived products downloaded from FEWS home page (1998),
- dekad PET images and seasonal area-planted estimates from the Government of Kenya.

These real-time data input requirements for the GIS-based CSWB model are flexible enough so that the model can run on a minimum budget (free real-time data from FEWS) or run with more advanced and expensive data sets using LANDSAT or SPOT imagery for estimating crop area planted. Model crop production estimates should also improve in the future as satellite technologies improve with time.

Another benefit of the GIS-based CSWB model is that current and future moderate resolution satellite data, such as Local Area Coverage (LAC) data with 1-kilometer spatial resolution or the soon to be launched Moderate Resolution Spectroradiometer (MODIS) with 250-meter resolution, can be immediately used by the model. Traditional *qualitative* crop condition tools cannot immediately use LAC or MODIS data because a historical archive of five years or more is needed for determining *qualitative* anomalies from average values. In contrast, the GIS-based CSWB model does not require historical archives of moderate satellite images to estimate seasonal crop yields because NDVI is only used for determining the start of season.

In real-time operation, the GIS-based CSWB model could also produce crop yield anomaly images or be used for crop forecasting yields by running the model in advance of harvest with normal rainfall and PET values. Climate models based on ENSO forecasts could also be integrated into the GIS-Based CSWB model to forecast crop yields one or two growing seasons in advance.

Model improvements recommended in the future include (in order of priority):

1. Make the GIS-based CSWB model operational in Kenya at the DRSRS or at the DMC.

2. Enlarge the model to estimate seasonal maize yields and production for other countries.

3. Expand the model to estimate seasonal yields and production for other crops.

4. Incorporate the few missing features from IGT into WINDISP3, and add a new RFE feature to VAST3 that estimates start of season from both RFE and NDVI images.

5. Improve the CSWB model by estimating:

   a) crop water use from Growing Degree Days (GDD)

   b) crop yield reductions from excess rainfall by introducing polynomial crop yield functions.

6. Introduce MODIS data products after the launch date of June, 1998.

   a) Use dekad vegetation index images with 250-meter resolution for determining:

      i) start of the growing season.
      ii) crop area planted.

   b) Use the MODIS GDD product if developing a METEOSAT GDD product is not undertaken. However, a GDD product from the geo-stationary METEOSAT satellite would be more accurate than a GDD from the polar-orbiting MODIS satellite.

7. Develop digital area-planted images with 1.1-kilometer resolution and automate the final methodology so that an area-planted image can be produced seasonally.

   a) Develop soil moisture storage images with 1.1-kilometer resolution to complement the Global 1-KM Land Data Set

8. Introduce ENSO forecasts into the GIS-based CSWB model.

APPENDIX I. METADATA FOR SPATIAL DATABASES

Dekad NDVI Images with Global Area Coverage (GAC) (7.6-km Resolution)

Description:

The Normalized Difference Vegetation Index (NDVI) measures the amount and vigor of vegetation. In general, NDVI values range from -1.0 to 1.0, with negative values indicating clouds and water and the positive values indicating soil and vegetation. The higher positive values of NDVI indicate greater vigor and amounts of vegetation, and the value of 0.67 is the maximum amount of vegetation greenness.

Purpose: Dekad NDVI images are used to estimate the start or beginning of the growing season.

Source: NDVI is derived from data collected from the Advanced High Resolution Radiometer (AVHRR) sensor placed on-board the National Oceanic and Atmospheric Administration (NOAA) satellite series. Raw digital data from the red and near-infrared (NIR) channels are collected and processed by the Global Environmental Monitoring and Modeling Studies (GIMMS) group from the National Aeronautics and Space Administration (NASA) and distributed every ten days to organizations such as the FEWS and ARTEMIS projects.

1. Dekad NDVI composites from 1989-1992 were obtained from FAO ARTEMIS CD-ROM (1994).

2. Dekad NDVI composites from 1993-1997 were downloaded from the Africa Data Dissemination Service at the EDC, URL:http://edcintl.cr.usgs.gov/adds/adds.html

Processing Steps:

A summary of processing steps performed by GIMMS to develop dekad NDVI composites with 7.6-km resolution follows:

1. Store Level 1B format GAC data for channels 1 (visible), 2 (near-infrared) and 5 (thermal infrared) per orbit over each continent.
2. Eliminate off-nadir and cloudy pixels.

3. Apply preflight radiometric calibration to channels 1 and 2, but sensor degradation is not considered.
4. Calculate NDVI.
5. Resample the 4-kilometer image to 7.638-km with Hammer-Aitoff projection.
6. Geo-register image using NOAA orbital parameters. Shift entire image to vector database if necessary.
7. Apply Maximum Value Composite (MVC) technique to develop a dekad (ten-day) NDVI composite image.
8. Adjust NDVI data for sensor degradation that occurred over time during the operation of NOAA-7, -9, and -11 satellites.
9. Scale 10-bit image to 8-bit image for use with personal computers.

Spatial Resolution:

At the equator, one pixel is equal to 7.638-kilometers.

Projection:

Hammer-Aitoff

Scale: 1:5,000,000

Steps for Importing into Model:

A summary of steps for importing GAC images into the GIS-based CSWB model follows:

1. Download a binary image from the EDC by selecting Greater Horn of Africa region.
2. Uncompress the file into the c:\temp directory.
3. Import the binary image from the EDC by using the "Process\Import\Binary" module from WINDISP3.
3. Geo-reference the image by changing the IDA header with the "Process\header" module in WINDISP3. Ensure IDA header type is "13, ARTEMIS FEWS NDVI" so NDVI ocean values of 0.68 are not included in calculations along the coast.
4. Window-out Kenya and change projection from Hammer-Aitoff to a geographic projection by using the "IMG->IMG" module from IGT or the "Process/Reproject" module from WINDISP3.

CD-ROM Directory:

WINDISP3 Batch File Function:

Import real-time NDVI dekad images (binary format) from FEWS into the GIS-CSWB model (IDA format).

WINDISP3 Batch File Name:

d:\WINDISP3\cmd\importrf.cmd

GIS-based CSWB Model Archive:

d:\kenya7km\ndvi\

Dekad NDVI with Local Area Coverage (LAC) (1.1-km Resolution):

Sources:

1. Dekad NDVI composites from the one-kilometer AVHRR Global Land Data Set were used for years 1993 and 1995. These images were downloaded from the EDC, URL:http://edcwww.cr.usgs.gov/landdaac/1km/10compd.html

2. Dekad NDVI composites from DRSRS were used for years 1994, 1996, and 1997. Raw LAC data are currently received daily by the HRPT station at the Kenya Meteorological Department and the DRSRS processes NDVI dekad composites for Kenya on a real-time basis (Ganzin, 1995).

Spatial Resolution:

At the equator, one pixel is equal to approximately 1.1-kilometers.

Projection:

NDVI images from EDC have Goode Homolosine projection.
NDVI images from DRSRS have geographic projection.

Scale: 1:1,000,000

Steps for Importing into Model:

A summary of steps for importing NDVI-LAC composites from the EDC follows:

1. Download the NDVI composite file from EDC by selecting (5,33,-5,43) as the coordinates.
2. Import the binary file into IDA format by using the "Process\Import\Binary" module in WINDISP3.

3. Geo-reference the image by changing the IDA header with the "Process\Header" module in WINDISP3. Also, classify the image type as a "EROS NDVI".
4. Re-project the image for use by the GIS-based CSWB model.

Steps for Importing into Model:

A summary of steps for importing NDVI-LAC composites from the DRSRS follows:

1. Strip the 128-byte header from the image by using the "Pare" module from IDRISI. A sample pare macro file (*.iml) in IDRISI follows:
   pare x dr3dec93.nvi n1k93123 128 1024 1024
   latlong degrees 1.0 33.0 43.0 -5.0 5.0 b
2. Import the binary file into IDA format by using the "Process\Import\Binary" module in WINDISP3.
3. Geo-reference the image by changing the IDA header with the "Process\Header" module in WINDISP3. Also, classify the image type as a "ARTEMIS FEWS Diff" type.

CD-ROM Directory:

WINDISP3 Batch File Function:

Import NDVI composites (binary format) from EDC into the GIS-based CSWB model (IDA format).

WINDISP3 Batch File Name:

d:\WINDISP3\cmd\imporedc.cmd

GIS-based CSWB Model Archive:

d:\kenya1km\ndvi\1993 & 1995

WINDISP3 Batch File Function:

Import NDVI composites (binary format with 128 byte header) from DRSRS into the GIS-based CSWB model (IDA format).

WINDISP3 Batch File Name:

d:\WINDISP3\cmd\importdr.cmd or imporlac.cmd

GIS-based CSWB Model Archive:

d:\kenya1km\ndvi\1994, 1996, 1997

Dekad RFE Images (January, 1989 - May,1995)

Description:

RFE Images from May,1995-December,1997:

Dekad rainfall estimate (RFE) images are derived by utilizing METEOSAT 5 satellite data, ground-based Global Telecommunication Systems (GTS) rain gauge reports, model analyses of wind and relative humidity, and a digital elevation model (DEM) (Herman, et. al., 1997). These RFE images are developed by the Climate Prediction Center (CPC) of the National Oceanic and Atmospheric Administration (NOAA).

RFE Images from January,1989-April,1995:

Dekad RFE images were developed by using the IGT software, Cold Cloud Duration (CCD) images, and ground-based rain gauge measurements. IGT empirically interpolates between ground-based rainfall point data by using a CCD image as the "background" variable. CCD images help to interpolate between ground-based rainfall stations since CCD is positively correlated with rainfall. In other words, rainfall increases over areas with higher CCD values and decreases with lower CCD values.

IGT interpolates rainfall between stations by first calculating the rainfall/CCD ratio over each ground-based rain station and then using the "inverse distance" squared gridding method to interpolate the ratio between points. A RFE image is then created by multiplying a estimated rainfall/CCD ratio at a particular pixel with the CCD value at that point (Hoefsloot, 1996).

Purpose: Dekad RFE images were used to estimate the amount of rainfall during each growing season from 1989-1997.

Sources:

1. Dekad RFE images (May,1995-December,1997) were downloaded from the Africa Data Dissemination Service at the EDC, URL:http://edcintl.cr.usgs.gov/adds/adds.html

2. Dekad rainfall data for 1989-1992 were downloaded from the EDC, URL:http://edcintl.cr.usgs.gov/adds/rain/rain.html, and data from 1992-1997 were collected from the Kenya Meteorology Department (KMD).

3. Dekad CCD images from 1989-1995 were obtained from the RCSSMRS through the FAO ARTEMIS program.

Processing Steps:

A summary of processing steps performed by CAC to develop real-time RFE images (Herman, et al, 1997) follows:

1. Form CCD images for a dekad by using a threshold temperature of -38°C.
2. Convert CCD images to rainfall estimates by applying the Global Precipitation Index (GPI) of x millimeters for each hour of CCD.
3. Collect daily rain gauge data from the Global Telecommunication System (GTS) and sum on a dekadal basis for stations all over Africa
4. Model the relationship between CCD and rain gauge values for a given dekad by a regression equation.
5. Use the regression equation to adjust the GPI estimate by giving precedence to those actual points where GTS rain gauge measurements are collected.
6. Create a "warm cloud" correction for those locations where there is rain in the rain gauge, but zero values within the CCD images. For these instances, it is believed that rain comes from warm clouds and another regression equation is formed using a CCD threshold of +2°C. This is combined with parameters obtained from a DEM and the NOAA-predictive models for relative humidity and wind direction.

A summary of steps to develop RFE images from the IGT or WINDISP3 programs, CCD images, and ground-based rainfall measurements follows:

1. Obtain dekad rainfall data in IGAD file format (d:\GoK\agmet\rain\kewx*ra.dat) for 32 agro-

meteorological stations in Kenya from the KMD (1992-1997) and the EDC (1989-1992).
2. Use FORTRAN sub-routine (faorain.exe) to create point files in Surfer format.
3. Extract rainfall values from the background image and calculate ratios by using the "SEDI-Create SEDI Ration File" module of IGT or "Process\SEDI" module in WINDISP3.
4. Create a grid file by using "SEDI-Create SEDI Grid" module of IGT or "Process\SEDI" module in WINDISP3.
5. Interpolate rainfall images from CCD images by using the "SEDI-Create SEDI Image" module of IGT or the "Process\SEDI" module in WINDISP3.

Caveat: RFE images developed by IGT may have errors in high altitude areas and coastal areas. Mountainous regions tend to have errors due to fewer rainfall gauges, and thin cirrus clouds can be colder than the threshold temperature but not produce rain. Rainfall estimates in coastal regions may underestimate rainfall because clouds near coastal regions can be warmer than the threshold temperature and still produce rain.

Resolution:
One pixel is approximately equal to 7.6-kilometers.

Projection:
Hammer-Aitoff

Steps for Importing into Model:
A summary of steps to import RFE images from the EDC into the GIS-based CSWB model follows:

1. Download the dekad RFE image from the Africa Data Dissemination Service at the EDC.
2. Uncompress the file into the c:\temp directory.
3. Import the binary image by using the "Process\Import" module in WINDISP3.
4. Window-out Kenya from the Africa image by using the "Process\Window" module in WINDISP3.
5. Re-project the image by using the "Process\Reproject" module in WINDISP3.

CD-ROM Directory:

WINDISP3 Batch File Function:

Import RFE images (binary format) from FEWS into the GIS-based CSWB model (IDA format).

WINDISP3 Batch File Name:

d:\WINDISP3\cmd\importrf.cmd

GIS-based CSWB Model Archive:

d:\kenya7km\rfe\1995-1997
d:\kenya1km\rfe\1995-1997

WINDISP3 Batch File Function:

Develop RFE images (IDA format) from the WINDISP3/SEDI program, CCD images, and ground-based rainfall measurements.

WINDISP3 Batch File Name:

d:\WINDISP3\cmd\

GIS-based CSWB Model Archive:

d:\kenya7km\rfe\1989-1994
d:\kenya1km\rfe\1989-1994

IGT Batch File Function:

Develop RFE images (IDA format) from the WINDISP3/SEDI program, CCD images, and ground-based rainfall measurements.

IGT Batch File Name:

d:\igt\cmd\rfe89011.cmd

GIS-based CSWB Model Archive:

d:\kenya7km\rfe\1989-1994
d:\kenya1km\rfe\1989-1994

Dekad CCD Images (January,1989-May,1995)

Description:

In the tropics, rainfall is to a large extent related to the occurrence of convective cloud systems. Researchers have found that the tops of these convective cloud systems with temperatures of -70°C and colder have a high probability of rain, while the tops of clouds with temperatures warmer than -30°C have a low probability of rain. Based on this statistical relationship, the occurrence of cold cloud temperatures is monitored and measured to estimate rainfall.

Cold cloud duration (CCD) images are processed by collecting thermal infrared images every hour from the geostationary METEOSAT satellite. These images are compared to a reference temperature threshold image (-40°C for ARTEMIS CCD images) and every pixel which is lower than the reference threshold image is classified as a cold cloud. A counter image is then updated to generate a final CCD image every ten days.

Purpose: CCD images are integrated with ground-based rainfall (and other variables for some models such as the RFE images developed by CAC) to estimate rainfall.

Source: CCD images are processed by the FAO ARTEMIS project for the continent of Africa on a real-time dekad and monthly basis. ARTEMIS disseminates CCD and NDVI images over Africa through the regional remote sensing projects in IGAD (RCSSMRS at Nairobi, Kenya) and SADC (Harare, Zimbabwe) regions.

Caveats:

1. CCD images are based on the statistical or empirical assumption that cold clouds coincide with rainfall-producing clouds.
2. One pixel represents an area of 58 km^2 and rainfall variability within such a large area can be quite high.
3. CCD images are based on a discontinuous sampling procedure at regular intervals whereas a continuous sampling procedure would be a better measure of cold cloud duration.
4. High and thin cirrus clouds, especially in mountainous areas, can be cold but do not produce rain.
5. Clouds near coastal regions can be warmer than the threshold temperature and still produce rain.

Resolution:

5-kilometer METEOSAT pixels are re-sampled to approximately 7.6-kilometer pixels at the equator.

Projection:

Hammer-Aitoff projection

CD-ROM Directory:

GIS-based CSWB Model Archive:

d:\kenya7km\ccd\

PET (Potential Evapotranspiration) with 7.6-km and 1.1-km Resolution: from January 1989 - December 1997

Description:

Dekad potential evaporation (PET) images were derived from the IGT software. The IGT software facilitates the empirical interpolation between ground-based PET point data by using a DEM (Digital Elevation Models) as the "background" variable. A DEM is used to interpolate PET measurements between agro-meteorological stations because PET is negatively correlated with altitude. In other words, PET decreases with increasing elevations and increases with decreasing elevations.

PET is calculated by using the FAO-Penman equation from agro-meteorological data collected by Kenya Meteorology Department (KMD) from 32 ground-based agro-meteorological stations. PET is interpolated between stations by calculating the PET/elevation ratio over each station and then using the "inverse distance" squared gridding method to interpolate the ratio for each pixel. A PET image is finally created by multiplying an estimated PET/elevation pixel ratio with the elevation value at that point (Hoefsloot, 1996).

Purpose: Dekad PET images were used to estimate the crop water use for each dekad during the main growing seasons from 1989-1997.

Source: IGT was used to create PET images for Kenya from 1989-1997. A 7.6-kilometer resolution digital elevation model (DEM) was obtained from the FEWS project, a 1.1-kilometer resolution DEM image was obtained from the EDC, and ground-based agro-meteorological (PET) data were purchased from the KMD.

Resolution:

7.6- and 1.1-kilometer pixels.

Projection:

Geographic

Processing Steps:

A summary of steps to develop PET images for the GIS-based CSWB model follows:

1. Obtain dekad PET data in IGAD file format (d:\GoK\agmet\pet\kewx*ea.dat) for thirty-two agro-meteorological stations in Kenya.
2. Use FORTRAN sub-routine (d:\GoK\agmet\pet\faopet.exe) to create point files in Surfer format.
3. Extract PET values from the background image and calculated ratios by using the "SEDI-Create SEDI Ration File" module of IGT or WINDISP3.
4. Create a grid file by using "SEDI-Create SEDI Grid" module of IGT or WINDISP3.
5. Interpolate PET images were created from a DEM image by using the "SEDI-Create SEDI Image" module of IGT or WINDISP3.

CD-ROM Directory:

WINDISP3 Batch File Function:

Develop PET images (IDA format) by using a DEM (IDA format) to interpolate between agro-meteorological stations.

WINDISP3 Batch File Name:

d:\WINDISP3\cmd\sedipet.cmd

GIS-based CSWB Model Archive:

d:\kenya7km\pet\
d:\kenya1km\pet\

IGT Batch File Function:

Develop PET images (IDA format) by using a DEM (IDA format) to interpolate between agro-meteorological stations.

IGT Batch File Name:

d:\igt\cmd\pet97011.cmd

GIS-based CSWB Model Archive:

d:\kenya7km\pet\
d:\kenya1km\pet\

Start of Season Images

Description:

Several researchers have shown a correlation between the start of growing season and crop yield in east Africa. An early start of growing season tends to give a longer growing season and better crop yields, while a late start of growing season tends to produce a short growing season and reduced yields (Stewart, 1988, and Henricksen and Durkin, 1985 and 1986).

The start of season images for this research were derived from the VAST3 program by determining when a NDVI time series first increases by an NDVI value of 0.02. The theory is an increase of NDVI indicates an increase of biomass caused by rainfall.

Purpose: The start of the growing season image initializes the GIS-based CSWB model and begins to calculate the water balance (i.e., difference between rainfall and maximum crop water use) during the growing season.

Source: Output image from the VAST3 program by analyzing NDVI time series.

Resolution:

Approximately 7.6- and 1.1-kilometers

Scale: 1:5,000,000 (7.6-kilometer pixels) and 1:1,000,000 (1.0-kilometer pixels)

Projection:

Geographic

Processing Steps:

A summary of steps to develop start of season images follows:

1. Transfer NDVI time series into a sub-directory.
2. Run the VAST3 program with the following command line:

VAST3 <cc> <yr> [inpath] [outpath] [ext] [st mon] [ed mon] [pbase] [ptol]

where,
yr = 2 digit year
inpath = up to 15 characters input data path
outpath = up to 15 characters output data path
ext = up to 3 characters file extension
st mon = starting month; the first dekad
en mon = ending month; the third dekad is used
pbase = base NDVI pixel value (default=107)
ptol = minimum NDVI increase (default=5)

An example command line for NDVI-LAC composites from the DRSRS follows:

VAST3 dv 97 c:\VAST3 c:\VAST3\out img 2 6 140 3

An example command line for NDVI-LAC composites from the EDC follows:

VAST3 dv 97 c:\VAST3 c:\VAST3\out img 2 6 110 2

3. For the 1-km pixel-by-pixel analysis, cloud cover produces numerous blank pixels. These blank pixels were replaced with average start of season values obtained from the CPSZ database.

Caveat: The command lines for step (2) use different base and tolerance values than the VAST3 default values because the VAST3 default is set for GAC images from FEWS. However, NDVI images from DRSRS are scaled differently, with digital numbers less than 128 represented as negative NDVI values and digital numbers greater than 128 represented as positive NDVI values. In a similar fashion, NDVI images from EDC are scaled with digital numbers less than 100 represented as negative NDVI values and greater than 100 represented as positive NDVI values. Correspondingly, the base and tolerance values from the above examples are scaled to approximate the VAST3 default values.

CD-ROM Directory:

WINDISP3 Batch File Function:

Develop start of season images (IDA format) by using the VAST3 program to analyze NDVI time series.

WINDISP3 Batch File Name:

d:\WINDISP3\cmd\vastsdat.cmd

GIS-based CSWB Model Model Archive:

d:\kenya7km\lgp\start*.img
d:\kenya1km\lgp\start*.img

DEM (Digital Elevation Model) with 7.6-km and 1-km Resolution

Description:

A Digital Elevation Model (DEM) provides a digital representation of elevation over a two dimensional surface. A DEM is normally generated from topographic maps, aerial photographs, or satellite images. The most common DEM is a simple rectangular grid with each pixel representing average elevation.

Purpose: DEM images for Kenya with 1-km and 7.6-km resolutions were used to develop PET maps with 1-km and 7.6-km resolutions, respectively, by correlating PET to altitude.

Source: Global Coverage Digital Elevation Models at 30-arc Seconds (approximately 1-kilometer) are available at http://edcwww.cr.usgs.gov/landdaac/1km/gtopo30/gtopo30.html.

A 16-bit DEM for Africa with 1.1-kilometer resolution, IDRISI format, and a Geographic Projection was obtained from FEWS, 1997. Kenya was windowed-out from the Africa DEM, and the 16-bit window image was converted into 8-bit image in IDRISI before importing into IDA format.

An 8-bit DEM for Africa with 7.6-kilometer resolution, IDA format, and a Lambert-Azimuthal projection was obtained from FEWS, 1997. Kenya was windowed-out from the Africa DEM and the image was converted into a geographic projection.

Resolution:

Approximately 1.1- and 7.6-kilometers

Projection:

Lambert-Azimuthal (7.6-kilometer pixels) and Geographic (1.1-kilometer pixels)

Scale: 1:5,000,00 (7.6 kilometer pixels) and 1:1,000,000 (1.1-kilometer pixels).

Steps for Importing into Model:

A summary of steps to import DEM images into the GIS-based CSWB model follows:

Africa DEM in IDRISI format, with 1-km resolution and Geographic Projection

1. Window-out Kenya from the Africa DEM image.
2. Use the "reclass" module from IDRISI to convert the 16-bit DEM image into a 8-bit image.
3. Reclassify the original 1-meter pixel values into 25-meter intervals by creating 3 sets of reclass (*.rcl) files.
4. Import the final reclass image into IDA by using the WINDISP3 commands, "Process/Import/IDRISI image".
5. Re-project the imported 8-bit image to a standard 1.1-kilometer image for use by the GIS-based CSWB model.

Africa DEM in IDA format, with 7.6-km resolution and Lambert-Azimuthal Projection

1. Window-out Kenya and change to a geographic projection by using the IGT "IMG->IMG" function or the WINDISP3 command, "Process/Reproject".

CD-ROM Directory:

GIS-based CSWB Model Archive:

d:\kenya7km\DEM\dem.img (IDA format)
d:\kenya1km\DEM\kendem16.img(16-bit IDRISI format)
d:\kenya1km\DEM\ken1kdem.img (IDA format)

Soil Water Holding Capacity

Description:

The soil water holding capacity is the average available water multiplied by the maximum root depth, where available water is the soil's field capacity less the permanent wilting point of the soil. Estimated available water value is derived from soil classification, soil texture, and soil depth of the area covered by the pixel. A digital image was developed where each pixel represents the amount of water stored in the plant's root zone.

Purpose: Multiplying the soil water holding capacity by a water management value will approximate the maximum readily available water for plant extraction.

Source: Soil water holding capacity images developed by the FAO (1995).

Resolution:

Approximately 7.6-kilometer pixels

Scale: 1:5,000,000

Projection:

Geographic

Processing Steps:

A summary of steps to develop soil water holding capacity image from the FAO (1995) follows:

1. Window-out Kenya and extract the soil water holding capacity image as a bmp file.
2. Import the bmp file into IDRISI.
3. Geo-reference the bmp image and reclassify the image according to the legend.
4. Re-project the image so use by the GIS-based CSWB model.

CD-ROM Directory:

IGT Batch File Function:

Import tabular data from the CPSZ database into IDA format.

IGT Batch File Name:

d:\igt\cmd\raw.cmd

GIS-based CSWB Model Archive:

d:\kenay7km\soils\faowhc.img
d:\kenay1km\soils\faowhc.img

Readily Available Soil Moisture Storage

Description:

The maximum readily available soil moisture storage is the available water multiplied by the maximum root depth and a water management factor for easy extraction of water by the plant. A digital image was developed where each pixel represents the maximum amount of water stored in the plant's root zone *that can be readily extracted by the plant.*

Purpose: If rainfall is greater than the estimated maximum readily available soil moisture storage capacity, the soil has a surplus of water, causing deep percolation or runoff. If rainfall is less than the water requirement, the soil has a deficit, causing reduction in crop yield.

Source: FAO-CPSZ database developed by van Velthuizen, et al (1995).

Resolution:

Crop production systems zones (CPSZ) polygons.

Projection:

Not applicable, can be imported as any projection.

Processing Steps:

A summary of steps to develop a maximum readily available soil moisture storage image extracted from the CPSZ database follows:

From CPSZ program,

1. Select "CPSZ Data/Map Data/Kenya CPSZ Map Boundaries".
2. Export Kenya CPSZ bna file.
3. Select "CPSZ Data/Physical Information/Readily Available Soil Moisture".
4. Export soil data file.

From DOS editor or Windows Word Pad editor,

1. Delete first four lines from the soil data file
2. Delete all lines which do not start with "KE"
3. Delete all quotation marks and KE by using the replace command.
4. Replace all commas with a blank space by using the replace command.
5. Save file with a .val extension.

From IGT program,

1. Use the "BNA>IMG/BNA>MSK" function to create a mask file.
2. Use the "BNA>IMG/MSK>IMG" function to create the image from the values file.

CD-ROM Directory:

GIS-based CSWB Model Archive:

d:\kenya7km\soils\rawcview.img
d:\kenya1km\soils\rawcview.img

Global Land Cover Characteristics

Description:

Seasonal land cover characteristics are derived from monthly NDVI composites processed from the 1-kilometer AVHRR Global Land Data Set from April, 1992 through March, 1993. Several thematic land cover classification systems were derived from the AVHRR data set, and the Biosphere-Atmosphere Transfer Scheme (BATS) was chosen because cropland pixels were classified as one separate category.

Purpose: The BATS classification system was used to calculate the percent of cropland within each Crop Production System Zone (CPSZ) per district.

Projection:

Lambert Azimuthal

Resolution:

Approximately 1-kilometer

Scale: 1:1,000,000

Source: Africa Land Cover Characteristics derived from the One-kilometer AVHRR Global Land Data Project were downloaded from the EDC, URL:http://edcwww.cr.usgs.gov/landdaac/glcc/glcc.html

Derived Data:

Biosphere-Atmosphere Transfer Scheme (BATS)

Steps for Importing into Model:

A summary of steps for importing a BATS image into the GIS-based CSWB model follows:

1. Download the BATS file from the EDC by selecting (5,33,-5,43) as the coordinates.
2. Import the binary file into IDA format by using the "Process\Import\Binary" module in WINDISP3.
3. Geo-reference the image by changing the IDA header with the "Process\Header" module in WINDISP3.
4. Re-project the image into the GIS-based CSWB model by using the "Process\Reproject" module from WINDISP3.

CD-ROM Directory:

GIS-based CSWB Model Archive:

d:\kenya1km\veg\kenbats.img

Length of Growing Period (LGP) Images

Description:

Several methods can be used to estimate the length of growing period such as average climate data, average NDVI time series images, crop calendars, or growing degree days (thermal units). The crop calendar method from the CPSZ database program was used for determining LGP images for this research.

Purpose: A length of growing period image assists in determining the end of the growing season by adding the LGP image to the start of growing season.

Source: FAO-CPSZ database developed by van Velthuizen, et al (1995).

Resolution:

Crop production systems zones (or agro-ecological zone) polygons.

Projection:

Not applicable, can be imported as any projection.

Processing Steps:

A summary of steps to develop a LGP image from data extracted from the CPSZ database follows:

From CVIEW program,

1. Select "CPSZ Data/Map Data/Kenya CPSZ Map Boundaries".
2. Export Kenya CPSZ bna file.
3. Select "CPSZ Data/Physical Information/Length of Growing Period (calendar)".
4. Export LGP data file.

From DOS editor or Windows Word Pad editor,

1. Delete first for lines from the LGP data file
2. Delete all lines which do not start with "KE"
3. Delete all quotation marks and KE by using the replace command.
4. Replace all commas with a blank space by using the replace command.
5. Save file with a .val extension.

From IGT program,

1. Use the "BNA>IMG/BNA>MSK" function to create a mask file.
2. Use the "BNA>IMG/MSK>IMG" function to create the image from the values file.

CD-ROM Directory:

GIS-based CSWB Model Archive:

d:\kenya7km\lgp\lgp.img
d:\kenya1km\lgp\lgp.img

APPENDIX II. SOFTWARE

IDA (Image Display Analysis) is a DOS-based program used for displaying, processing, and analyzing of remote sensing time-series images commonly used by EWS (Early Warning Systems) stations. IDA goes beyond displaying NDVI, RFE, and CCD images by providing tools for processing and analyzing time-series satellite images such as extracting statistics from these images, comparing differences between current and average (historical) images, converting images into different file formats, etc. IDA is easily automated for routine image processing by running on batch mode and by defining different temporal variables (Pfirman and Hoefsloot, 1995).

WINDISP3 is the Window-based successor of IDA. In addition to transferring all IDA functions to Windows, many additional features have been added to provide a simpler, yet more powerful interface within a Windows environment. Batch file functions were also extended to include if/then, for/next, and goto/label statements (Pfirman and Hogue, 1997). Both WINDISP3 and IGT softwares will soon be upgraded by incorporating the DOS-based IGT software into WINDISP3.

IGT (IDA GIS Tools) was developed by the SADC (Southern African Development Community) Regional Remote Sensing Project based in Harare to increase the GIS abilities of IDA. This software greatly facilitates the empirical interpolation of point data by using satellite imagery or DEM (Digital Elevation Models) as the "background" variable. For example, given rainfall data from several rainfall stations, IGT will use CCD (Cold Cloud Duration) images to

interpolate rainfall between stations by correlating CCD values to rain gauge measurements. Another application is interpolating PET (potential evapotranspiration) between stations by using a DEM as the background variable to correlate PET with altitude. IGT also allows digital maps, satellite images, point data, and tabular data to be integrated for spatial analysis and IGT provides an image calculation function which allows IDA images to be reclassed by if-then statements, etc., (Hoefsloot, 1996).

VAST (Vegetation Analysis in Space and Time-Version 4) is a DOS-based program developed by FEWS to analyze a series of NDVI images for agricultural monitoring. In particular, it monitors NDVI changes during the growing season by determining the start of season, maximum vegetation growth, etc., rather than relying on simply predetermined calendar dates. The program automatically smoothes NDVI images to get meaningful results, and final images produced by VAST are presented in IDA format. Statistics can be extracted from output VAST images by using the threshold and statistics modules from WINDISP3 (Lee, 1997).

CPSZ (Crop Production System Zones) Viewer is a computerized database providing detailed information on actual agriculture conditions in the IGAD (Intergovernmental Authority on Development) region for the Horn of Africa. Agro-ecological zones are divided within each administration unit to make 1220 polygons, or crop production system zones. More than 500 variables were collected or calculated which include main crops grown; agronomic data such as crop phenology, yields, common pests and diseases; physical environment parameters such as rainfall, PET (potential

evapotranspiration), elevation, slope, soil water holding capacity, length of growing season, crop calendars defining when the average growing season starts and ends, etc. (van Velthuizen, et al., 1995).

A **FORTRAN (Visual Workbench)** compiler was used to develop a FORTRAN program for performing the Agro-Ecological Zone (AEZ) polygon analysis. The agro-ecological zones in Kenya were defined by 206 polygons from the CPSZ database. RFE, PET, NDVI data were extracted from each of these polygons by using WINDISP3 and their average values were introduced into the FORTRAN program as an array. The FORTRAN program was initially tested by using point input data and comparing these results with results from the ground-based CSWB program called FAOINDEX (Gommes, 1993). The filenames for the AEZ program and source codes are \fortran\cswb.*

SOURCES OF SOFTWARE PROGRAMS

IDA, WINDISP3, and IGT
ftp.fao.org, anonymous login and change to sub-directory /SDRN. (Hoefsloot, 1997; Pfirman and Hoefsloot, 1995; and Pfirman and Hogue, 1997)

WINDISP and IDA:
http://www.arizona.edu/~epfirman/WINDISP3.html

VAST3: e-mail: info@fews.org (Lee, 1997)

CVIEW: e-mail: agromet@fao.org and ask to purchase FAO Agrometeorology Series Working Paper No. 10 (van Velthuizen, et al, 1995).

IDRISI for Windows: http://www.idrisi.clarku.edu/ (Eastman, 1997)

APPENDIX III. SATELLITE SERIES

NOAA-AVHRR series

The NOAA satellite series are meteorological satellite which operate in a near-polar sun synchronous orbit at a height of about 850 km and provide global coverage at least once daily. These satellites incorporate visible and thermal sensors with a very coarse spatial resolution. Thus, these systems are useful for studies that do not require high spatial resolution, but frequent imaging. Presently, NOAA-12 (D) and NOAA-14 (J) are in operation and carry the AVHRR (Advance Very High-Resolution Radiometer) sensor onboard.

The present AVHRR sensor is a radiation detection imager used for remotely determining cloud cover, surface temperature, and vegetation condition. The scanning radiometer uses five detectors that collect five different bands of radiation wavelengths which can later be processed for multi-spectral analysis and archived for multi-temporal analysis. Channel one monitors energy in the visible band (wavelength 0.58-0.68 μm), and channel two monitors the near-infrared portion of the energy electromagnetic spectrum with wavelengths of 0.725-1.10 μm to observe vegetation, clouds, lakes, shorelines, snow, and ice. The other three channels operate entirely within the thermal or infrared bands (3.55-3.93 μm, 10.3-11.3 μm, and 11.5-12.5 μm wavelength) to detect the heat radiation and hence the temperature of land, water, sea surfaces, and the clouds above them.

The AVHRR has a 1.1-km field of view at nadir and AVHRR data are acquired in three formats:

1. HRPT are full resolution image data transmitted to a ground station with resolution of approximately 1.1 km at the satellite nadir orbit.

2. LAC are full resolution image data that are recorded on tape for subsequent transmission during a station overpass. The resolution is approximately 1.1 km at the satellite nadir orbit.
3. GAC data are derived from an onboard sample averaging of the full resolution LAC data yielding a 1.1-km by 4-km resolution image at nadir.

NOAA-K, -L, and -M will be much like the NOAA-AVHRR predecessors, but represent a new generation of NOAA polar orbiting satellites since they will have larger solar arrays and more technologically advanced sensor instrumentation. NOAA-15 (K) is scheduled for launch in February, 1998, with NOAA-16 (L) and NOAA-17 (M) scheduled for launch in December, 1999, and April, 2001, respectively. The main difference with this new generation of Polar-Orbiting Operational Environmental Satellites (POES) will be the Advanced Very High Resolution Radiometer (AVHRR) sensor will be modified and improved by adding more channels.

METEOSAT

The European METEOSAT satellite series is in geo-stationary orbit at 36,000-kilometer altitude. It is always located at zero degrees longitude, over the equator, and monitors the Eastern Hemisphere. Scene views are updated every thirty minutes and METEOSAT -5, and -7 are currently operational, with METEOSAT -6 on standby.

The radiometer has the following spectral bands: visible (0.5 - 0.9 μm), near infrared or water band (5.7 - 7.1 μm), and infrared or thermal band (10.5 - 12.5 μm). The visible band has a 2.5-km resolution at nadir, and the near-infrared and infrared bands have a 5-km resolution at nadir. The visible spectra give an indication of surface albedo (reflectance), and the image resembles that of a normal

photograph. The infrared (thermal) views are an indication of energy radiance from the surface and cloud tops, and hence surface temperature and cloud top temperature. The infrared (water vapor) image gives an indication of total water vapor present in the atmospheric column.

The analysis of cloud top temperatures CCD (Cold Cloud Duration) can give an indication of rainfall, as there is a statistical relationship between CCD and the actual rainfall measured at the ground.

EOS-MODIS

NASA's Earth Observing System (EOS) initiative will launch a series of polar orbiting satellites in the next 15 years to monitor the earth's land, ocean, and atmospheric processes and their interactions. The first satellite, EOS AM-1, will be launched in June, 1998. "AM" means the satellite will fly in a sun-synchronous polar orbit, descending southward across the equator in the morning. In the year 2000, EOS PM-1 will be launched into a sun-synchronous polar orbit ascending northward across the equator in the afternoon. Afterwards, EOS AM-2 and EOS PM-2 will be launched before the year 2006.

The main sensor carried abroad the EOS AM and PM satellites is the Moderate Imaging Spectroradiometer (MODIS). The objective of MODIS is to take measurements in the spectral regions that have been and currently are being measured by other satellite sensors in order to extend current data sets. However, the MODIS sensor will also be a state-of-the-art sensor that exceeds capabilities of current sensors such as the Advanced Very High Resolution Radiometer (AVHRR) sensor used to monitor sea surface temperatures, sea ice, and vegetation.

MODIS will have a viewing swath width of 2330 km and will view the earth in 36 spectral bands, sampling the electromagnetic spectrum from 0.14 to 14 μm with a spatial resolution ranging from 250 to 1000 meters. The two bands, red and near-infrared, are imaged at a nominal resolution of 250 m at nadir, with five bands at 500 meter resolution, and the remaining 29 bands at 1,000 meters. Raw data will be processed in high-speed computers, using theoretically and empirically derived algorithms, to yield over 40 global data products to analyze global change.

Some of the land data products from MODIS will include spectral albedo, land cover, spectral vegetation indices, snow and ice cover, surface (and fire) temperature, and a number of biophysical variables such as leaf area index, fraction of absorbed photosynthetically active radiation, surface photosynthesis, evapo-transpiration, net primary production, etc..

APPENDIX IV. CD-ROM DATA SET

The CD ROM attached includes: 1.1-kilometer and 7.6-kilometer spatial data sets; freeware programs (VAST3, IGT, WINDISP3, and IDA); and source codes for the customized utility programs from this research. These data sets and programs have been collected from a variety of sources, and have been included for replication of this study or for other research applications. All images are in IDA format and have a geographic projection. The meta-data for processing these images are described in Appendix I.

Note that compressed files have a .zip file extension and can be uncompressed by using pkunzip, WIN-Zip, or any other similar decompression software for personal computers.

The following is a list of directories and sub-directories on the CD-ROM:

CPSZ
- LGP
- yield

GISCSWB
- 1km
- 7km
- AEZ
  - GoK
  - DRSRS
- windcswb

GoK
- agmet
  - PET
  - rain
- DRSRS
  - areapl
  - product
- MoA

```
    ├areapl
    ├product
IDA
IGT
    ├cmd
    ├lut
kenya7km
  ├ccd
    ├1989
    ├1990
    ├1991
    ├1992
    ├1993
    ├1994
    ├1995
    ├1996
  ├dem
  ├lgp
  ├ndvi
    ├1989
    ├1990
    ├1991
    ├1992
    ├1993
    ├1994
    ├1995
    ├1996
    ├1997
    ├1998
    ├mean
  ├pet
    ├1989
    ├1990
    ├1991
    ├1992
    ├1993
    ├1994
    ├1995
    ├1996
    ├1997
    ├mean
  ├rfe
    ├1989
    ├1990
    ├1991
    ├1992
    ├1993
```

- 1994
- 1995
- 1996
- 1997
- 1998
- mean
- soils
- veg

kenya1km

- dem
- lgp
- pet
  - 1993
  - 1994
  - 1995
  - 1996
  - 1997
  - mean
- rfe
  - 1993
  - 1994
  - 1995
  - 1996
  - 1997
  - mean
- soils
- veg

Results

- files
  - DRSRS
    - 7km
    - AEZ
  - MoA
    - 1km
    - 7km
    - AEZ
- yieldimg
  - 1km
  - 7km
  - AEZ

VAST3

WINDISP3

- bna
- clr
- cmd
- lst
- sta

APPENDIX V. SOURCE CODES FOR THE GIS-BASED CSWB MODEL

Sample source codes for the pixel-by-pixel analyses (WINDISP3 and DOS-based IGT) are stored on the CD-ROM within the following directories:

1. WINDISP3 batch file for the pixel-by-pixel analysis, d:\GISCSWB\windpix\giscswb.cmd

2. DOS-based IGT formula file for the pixel-by-pixel analysis, d:\GISCSWB\7km\cswbpx**.fml

Brief versions of the above files are presented below.

WINDISP3 batch file for the GIS-based CSWB model stored within the d:\GISCSWB\windcswb\ directory on the CD-ROM.

```
#Batch Variable Prompt, "country,Enter desired
country,Kenya"

# Process the 7-km or 1-km database on CD-ROM
  Batch Variable Prompt, "scale,Enter desired scale,7km"
  Batch Variable Prompt, "year,Enter desired year,89"

#Initialize for long rain season by adding lgp image (from
   CPSZ database) to the start of season image (from VAST3).
   Process Images Algebra, "plt+lgp,C:\TEMP\harv.IMG,plt,D:\
   KENYA%scale%\lgp\start%year%.IMG,lgp,D:\KENYA%scale%\lgp\
   lgp.IMG"

 #Calculate crop coefficients
  Process Images Algebra, "@IF(plt<=1& plt>0,@IF(lgp>0,(1-
  plt+1)*100/lgp,0),0),c:\temp\xaxis.img,plt,D:\KENYA%scale%
  \LGP\START%year%.IMG,lgp,D:\KENYA%scale%\LGP\LGP.IMG"
 #Off-season and establishment phase
  Process Images Algebra, "@IF((x=0|x>100),0,@IF((x<=16 &
  x>0),35,0)),c:\temp\kcpps.img,x,C:\TEMP\XAXIS.IMG"
 #Initial or Vegetative phase
  Process Images Algebra, "@IF((x<=44 & x>16),(35+((120-
  35)/(44-16))*(x-
  16)),0),c:\temp\kcv.img,x,c:\temp\xaxis.img"
 #Reproductive and Maturing (senescence) phase
   Process Images Algebra, "@IF((x<=76 &
   x>44),120,@IF((x<=100 & x>76),(120+((60-120)/(100-
   76))*(x-76)),0)),c:\temp\kcrep.img,x,c:\temp\xaxis.img"
```

```
#Calculate max crop water requirements
 Process Images Algebra,
 "(kcpps+kcv+kcrep)*(pet1/100),c:\temp\w1.img,kcpps,c:\temp
 \kcpps.img,kcv,c:\temp\kcv.img,kcrep,c:\temp\kcrep.img,
 pet1, d:\kenya%scale%\pet\19%year%\dp%year%011.img"

#Calculate soil moisture for first dekad of January
  Process Images Algebra, "@IF(plt=1, si,
  @IF((si+rfe1)<w1,0,@IF((si+rfe1-w1)<raw,si+rfe1-
  w1,raw))),c:\temp\s1.img,plt,D:\KENYA%scale%\lgp\start%ye
  ar%.IMG,si,d:\kenya%scale%\soils\si.img,rfe1,d:\kenya%sca
  le%\rfe\19%year%\dr%year%011.img,w1,c:\temp\w1.img,raw,d:
  \kenya%scale%\soils\rawcview.img"

#Calculate soil deficit image
  Process Images Algebra, "@IF((si+rfe1)<w1,w1-si-rfe1,0),
  c:\temp\d1.img,si,d:\kenya%scale%\soils\si.img,rfe1,
  d:\kenya%scale%\rfe\19%year%\dr%year%011.img,w1,
  c:\temp\w1.img"

#Calculate evaporation image
  Process Images
  Algebra,"@IF((si+rfe1)<w1,si+rfe1,w1),c:\temp\
  e1.img,si,d:\kenya%scale%\soils\si.img,rfe1,d:\kenya%scal
  e%\rfe\19%year%\dr%year%011.img,w1,c:\temp\w1.img"

#Calculate cumulative plant water needs
  Process Images Algebra, "@IF((x>0 &
  x<=100),(pwneedi+w1/10),0), c:\temp\pwneed1.img, x,
  c:\temp\xaxis.img, pwneedi,
  d:\kenya%scale%\soils\pwneedi.img ,w1, c:\temp\w1.img"

#Calculate cumulative evaporation image
  Process Images Algebra, "@IF((x>0 & x<=100),
  (evapi+e1/10),0), c:\temp\evap1.img, x,
  c:\temp\xaxis.img, evapi,
  d:\kenya%scale%\soils\evapi.img, e1, c:\temp\e1.img"

#Calculate cumulative soil deficit image
 Process Images Algebra, "@IF((x>0 & x<=100),
  (deficti+d1/10),0), c:\temp\defict1.img, x,
  c:\temp\xaxis.img, deficti,
  d:\kenya%scale%\soils\deficti.img, d1, c:\temp\d1.img"

#Calculate WRSI image
  Process Images Algebra, "si * 0, c:\temp\index1.img, si,
  d:\kenya%scale%\soils\si.img"
```

```
 #Calculate yield image
  Process Images Algebra, "si * 0, c:\temp\yld1.img, si,
  d:\kenya%scale%\soils\si.img"

 #Copy initial images to c:\temp for faster processing
  File Run, "xcopy D:\kenya%scale%\soils\ c:\temp"
  Batch Pause


#Loop the model for dekads 2-36.

#Fix the month
Batch For Begin, "month,1,12,1"
        Batch If Begin, "%month%<10"
                Batch Variable Set, "mon,0%month%"
        Batch If Else
                Batch Variable Set, "mon,%month%"
        Batch If End

  #Loop the model for dekads 2-3
  Batch If Begin, "%month%=1"
        Batch For Begin, "dekad, 2,3,1"
           Batch Variable Set, "count,  (3*(%month%-
           1)+%dekad%)"
           Batch Variable Set, "down, (3*(%month%-
           1)+%dekad%-1)"
           Batch Variable Set, "up, (3*(%month%-
           1)+%dekad%+1)"

  Batch If Else

  #Loop the model for dekads 4-36
        Batch For Begin, "dekad, 1,3,1"
           Batch Variable Set, "count,  (3*(%month%-
           1)+%dekad%)"
           Batch Variable Set, "down, (3*(%month%-
           1)+%dekad%-1)"
           Batch Variable Set, "up, (3*(%month%-
           1)+%dekad%+1)"
  Batch If End

 #Calculate crop coefficients
  Process Images Algebra, "@IF(plt<=%count% &
  plt>0,@IF(lgp>0,(%count%-
  plt+1)*100/lgp,0),0),c:\temp\xaxis.img,plt,D:\KENYA%scale
  %\LGP\START%year%.IMG,lgp,D:\KENYA%scale%\LGP\LGP.IMG"
  #Off-season and establishment phase
```

```
 Process Images Algebra, "@IF((x=0|x>100),0,@IF((x<=16 &
 x>0),35,0)),c:\temp\kcpps.img,x,C:\TEMP\XAXIS.IMG"
#Initial or Vegetative phase
 Process Images Algebra, "@IF((x<=44 & x>16),(35+((120-
 35)/(44-16))*(x-
 16)),0),c:\temp\kcv.img,x,c:\temp\xaxis.img"
#Reproductive and Maturing (senescense) phase
 Process Images Algebra, "@IF((x<=76 &
 x>44),120,@IF((x<=100 & x>76),(120+((60-120)/(100-
 76))*(x-76)),0)),c:\temp\kcrep.img,x,c:\temp\xaxis.img"
#Develop a dekad crop coefficent image by adding the 3
 phases together.
 Process Images Algebra, "(kcpps+kcv+kcrep),
 c:\temp\kc%count%.img,kcpps,c:\temp\kcpps.img,kcv,c:\temp
 \kcv.img,kcrep,c:\temp\kcrep.img"

#Calculate max crop water requirements
 Process Images Algebra,
 "(kcpps+kcv+kcrep)*(pet%count%/100),
 c:\temp\w%count%.img,kcpps,c:\temp\kcpps.img,kcv,c:\temp\
 kcv.img,kcrep,c:\temp\kcrep.img, pet%count%,
 d:\kenya%scale%\pet\19%year%\ dp%year%%mon%%dekad%.img"

#Calculate soil mositure
 Process Images Algebra,
 "@IF(plt=%count%,si,@IF((s%down%+rfe%count%)
 <w%count%,0,@IF((s%down%+rfe%count%-
 w%count%)<raw,s%down%+rfe%count%-
 w%count%,raw))),c:\temp\s%count%.img,plt,d:\kenya%scale%\
 lgp\start89.IMG,si,c:\temp\si.img,
 s%down%,c:\temp\s%down%.img,rfe%count%,
 d:\kenya%scale%\rfe\19%year%\dr%year%%mon%%dekad%.img,w%c
 ount%,c:\temp\w%count%.img,raw,c:\temp\rawcview.img"

#Calculate soil deficit image
 Process Images Algebra,
 "@IF((s%down%+rfe%count%)<w%count%,w%count%-s%down%-
 rfe%count%,0), c:\temp\d%count%.img,
 s%down%,c:\temp\s%down%.img,rfe%count%,d:\kenya%scale%\rf
 e\19%year%\dr%year%%mon%%dekad%.img,w%count%,c:\temp\w%co
 unt%.img"

#Calculate an evaporation image
 Process Images Algebra,
 "@IF((s%down%+rfe%count%)<w%count%,
 s%down%+rfe%count%,w%count%),c:\temp\e%count%.img,s%down%
 ,c:\temp\s%down%.img,rfe%count%,d:\kenya%scale%\rfe\19%ye
```

```
  ar%\dr%year%%mon%%dekad%.img,w%count%,
  c:\temp\w%count%.img"

 #Calculate cumulative plant water needs
    Process Images Algebra, "@IF((x>0 &
  x<=100),pwneed%down%+(w%count%/10),0),
  c:\temp\pwneed%count%.img, x, c:\temp\xaxis.img,
  pwneed%down%, c:\temp\pwneed%down%.img ,w%count%,
  c:\temp\w%count%.img"

 #Calculate cumulative soil deficit image
  Process Images Algebra, "@IF((x>0 & x<=100), defict%down%+
  (d%count%/10),0), c:\temp\defict%count%.img, x,
  c:\temp\xaxis.img, defict%down%,
  c:\temp\defict%down%.img, d%count%, c:\temp\d%count%.img"

 #Calculate cumulative evaporation image
    Process Images Algebra, "@IF((x>0  &  x<=100),
  evap%down% + (e%count%/10), 0), c:\temp\evap%count%.img,
  x, c:\temp\xaxis.img, e%count%, c:\temp\e%count%.img,
  evap%down%, c:\temp\evap%down%.img"

 #Calculate WRSI image
  Process Images Algebra, "@IF(lgp>0 & harv=%up%, 100 -100*
  defict%count%/pwneed%count%,index%down%),
  c:\temp\index%count%.img, pwneed%count%,
  c:\temp\pwneed%count%.img, lgp,
  d:\kenya%scale%\lgp\lgp.img, harv, c:\temp\harv.img,
  defict%count%, c:\temp\defict%count%.img, index%down%,
  c:\temp\index%down%.img"

 #Calculate yield image by assuming yield reduction
factor=1.5.
  Process Images
  Algebra,"@IF(lgp>0&harv=%up%,@IF(100*evap%count%
  /pwneed%count%<=33,254,150*evap%count%/pwneed%count%-
  50),yld%down%),c:\temp\yld%count%.img,pwneed%count%,c:\te
  mp\pwneed%count%.img,lgp,d:\kenya%scale%\lgp\lgp.img,harv
  ,c:\temp\harv.img,evap%count%,c:\temp\evap%count%.img,yld
  %down%,c:\temp\yld%down%.img"

  Batch For End
Batch For End
```

DOS-based IGT formula file for the GIS-based CSWB model stored within the d:\GISCSWB\7km\ directory on the CD-ROM.

```
Pixel-by-Pixel CSWB Model
************************************************************
Note: Start of Season Images from VAST created by
c:\windisp3\cmd\CSWBPOLY.cmd batch file and then *sdat
images are moved to d:\kenya*km\lgp  directory.
************************************************************

************************************************************
Start of Season image from VAST (sdat) may have unrealistic
zero values. The section below replaces these zero values
with average Start of Season values from CVIEW.  The new
images are stored in d:\kenya*km\lgp directory and are named
as start*.img.
************************************************************
Calculate a Reverse Binary Image for Start of Season image
from VAST4. Reverse means pixels with values are set to zero
and zero values are set to one.

//#a:FILENAME=d:\kenya7km\lgp\dv89sdat.img
//#b:FILENAME=c:\temp\rbinary.img
//#b:IMGTYPE =200
//#b:TITLE = Binary Start of Season
//#b:LUT =d:\igt\lut\universe.lut
//#b:BNA =d:\windisp3\bna\cpsz.bna
//#b:SLOPE = 1
//#b:INTERCEPT = 0

FORMULA
//?b=if(a>=1,0,1)

Multiply the reverse binary file times the start of season
file from CVIEW.
//#c:FILENAME=c:\temp\startcv.img
//#c:IMGTYPE =200
//#c:TITLE = CVIEW Start of Season
//#c:LUT =d:\igt\lut\universe.lut
//#c:BNA =d:\windisp3\bna\cpsz.bna
//#c:SLOPE = 1
//#c:INTERCEPT = 0
//#d:FILENAME=d:\kenya7km\lgp\start.img

FORMULA
//?c=b*d
```

```
Add CVIEW start of season plus VAST start of Season
//#e:FILENAME=c:\temp\start89.img
//#e:IMGTYPE =200
//#e:TITLE = Start of Season (CVIEW + VAST4)
//#e:LUT =d:\igt\lut\universe.lut
//#e:BNA =d:\windisp3\bna\cpsz.bna
//#e:SLOPE = 1
//#e:INTERCEPT = 0

FORMULA
//?e=a+c

*******************
Define files
*******************
#pet1:FILENAME=d:\kenya7km\pet\1989\dp89011.img
#pet1:REPL_MISSING=0
#pet2:FILENAME=d:\kenya7km\pet\1989\dp89012.img
#pet2:REPL_MISSING=0
#pet3:FILENAME=d:\kenya7km\pet\1989\dp89013.img
#pet3:REPL_MISSING=0
#pet4:FILENAME=d:\kenya7km\pet\1989\dp89021.img
#pet4:REPL_MISSING=0
#pet5:FILENAME=d:\kenya7km\pet\1989\dp89022.img
#pet5:REPL_MISSING=0
#pet6:FILENAME=d:\kenya7km\pet\1989\dp89023.img
#pet6:REPL_MISSING=0
#pet7:FILENAME=d:\kenya7km\pet\1989\dp89031.img
#pet7:REPL_MISSING=0
#pet8:FILENAME=d:\kenya7km\pet\1989\dp89032.img
#pet8:REPL_MISSING=0
#pet9:FILENAME=d:\kenya7km\pet\1989\dp89033.img
#pet9:REPL_MISSING=0
#pet10:FILENAME=d:\kenya7km\pet\1989\dp89041.img
#pet10:REPL_MISSING=0
#pet11:FILENAME=d:\kenya7km\pet\1989\dp89042.img
#pet11:REPL_MISSING=0
#pet12:FILENAME=d:\kenya7km\pet\1989\dp89043.img
#pet12:REPL_MISSING=0
#pet13:FILENAME=d:\kenya7km\pet\1989\dp89051.img
#pet13:REPL_MISSING=0
#pet14:FILENAME=d:\kenya7km\pet\1989\dp89052.img
#pet14:REPL_MISSING=0
#pet15:FILENAME=d:\kenya7km\pet\1989\dp89053.img
#pet15:REPL_MISSING=0
#pet16:FILENAME=d:\kenya7km\pet\1989\dp89061.img
#pet16:REPL_MISSING=0
```

```
#pet17:FILENAME=d:\kenya7km\pet\1989\dp89062.img
#pet17:REPL_MISSING=0
#pet18:FILENAME=d:\kenya7km\pet\1989\dp89063.img
#pet18:REPL_MISSING=0
#pet19:FILENAME=d:\kenya7km\pet\1989\dp89071.img
#pet19:REPL_MISSING=0
#pet20:FILENAME=d:\kenya7km\pet\1989\dp89072.img
#pet20:REPL_MISSING=0
#pet21:FILENAME=d:\kenya7km\pet\1989\dp89073.img
#pet21:REPL_MISSING=0
#pet22:FILENAME=d:\kenya7km\pet\1989\dp89081.img
#pet22:REPL_MISSING=0
#pet23:FILENAME=d:\kenya7km\pet\1989\dp89082.img
#pet23:REPL_MISSING=0
#pet24:FILENAME=d:\kenya7km\pet\1989\dp89083.img
#pet24:REPL_MISSING=0
#pet25:FILENAME=d:\kenya7km\pet\1989\dp89091.img
#pet25:REPL_MISSING=0
#pet26:FILENAME=d:\kenya7km\pet\1989\dp89092.img
#pet26:REPL_MISSING=0
#pet27:FILENAME=d:\kenya7km\pet\1989\dp89093.img
#pet27:REPL_MISSING=0
#pet28:FILENAME=d:\kenya7km\pet\1989\dp89101.img
#pet28:REPL_MISSING=0
#pet29:FILENAME=d:\kenya7km\pet\1989\dp89102.img
#pet29:REPL_MISSING=0
#pet30:FILENAME=d:\kenya7km\pet\1989\dp89103.img
#pet30:REPL_MISSING=0
#pet31:FILENAME=d:\kenya7km\pet\1989\dp89111.img
#pet31:REPL_MISSING=0
#pet32:FILENAME=d:\kenya7km\pet\1989\dp89112.img
#pet32:REPL_MISSING=0
#pet33:FILENAME=d:\kenya7km\pet\1989\dp89113.img
#pet33:REPL_MISSING=0
#pet34:FILENAME=d:\kenya7km\pet\1989\dp89121.img
#pet34:REPL_MISSING=0
#pet35:FILENAME=d:\kenya7km\pet\1989\dp89122.img
#pet35:REPL_MISSING=0
#pet36:FILENAME=d:\kenya7km\pet\1989\dp89123.img
#pet36:REPL_MISSING=0
#rfe1:FILENAME=d:\kenya7km\rfe\1989\dr89011.img
#rfe1:REPL_MISSING=0
#rfe2:FILENAME=d:\kenya7km\rfe\1989\dr89012.img
#rfe2:REPL_MISSING=0
#rfe3:FILENAME=d:\kenya7km\rfe\1989\dr89013.img
#rfe3:REPL_MISSING=0
#rfe4:FILENAME=d:\kenya7km\rfe\1989\dr89021.img
#rfe4:REPL_MISSING=0
```

```
#rfe5:FILENAME=d:\kenya7km\rfe\1989\dr89022.img
#rfe5:REPL_MISSING=0
#rfe6:FILENAME=d:\kenya7km\rfe\1989\dr89023.img
#rfe6:REPL_MISSING=0
#rfe7:FILENAME=d:\kenya7km\rfe\1989\dr89031.img
#rfe7:REPL_MISSING=0
#rfe8:FILENAME=d:\kenya7km\rfe\1989\dr89032.img
#rfe8:REPL_MISSING=0
#rfe9:FILENAME=d:\kenya7km\rfe\1989\dr89033.img
#rfe9:REPL_MISSING=0
#rfe10:FILENAME=d:\kenya7km\rfe\1989\dr89041.img
#rfe10:REPL_MISSING=0
#rfe11:FILENAME=d:\kenya7km\rfe\1989\dr89042.img
#rfe11:REPL_MISSING=0
#rfe12:FILENAME=d:\kenya7km\rfe\1989\dr89043.img
#rfe12:REPL_MISSING=0
#rfe13:FILENAME=d:\kenya7km\rfe\1989\dr89051.img
#rfe13:REPL_MISSING=0
#rfe14:FILENAME=d:\kenya7km\rfe\1989\dr89052.img
#rfe14:REPL_MISSING=0
#rfe15:FILENAME=d:\kenya7km\rfe\1989\dr89053.img
#rfe15:REPL_MISSING=0
#rfe16:FILENAME=d:\kenya7km\rfe\1989\dr89061.img
#rfe16:REPL_MISSING=0
#rfe17:FILENAME=d:\kenya7km\rfe\1989\dr89062.img
#rfe17:REPL_MISSING=0
#rfe18:FILENAME=d:\kenya7km\rfe\1989\dr89063.img
#rfe18:REPL_MISSING=0
#rfe19:FILENAME=d:\kenya7km\rfe\1989\dr89071.img
#rfe19:REPL_MISSING=0
#rfe20:FILENAME=d:\kenya7km\rfe\1989\dr89072.img
#rfe20:REPL_MISSING=0
#rfe21:FILENAME=d:\kenya7km\rfe\1989\dr89073.img
#rfe21:REPL_MISSING=0
#rfe22:FILENAME=d:\kenya7km\rfe\1989\dr89081.img
#rfe22:REPL_MISSING=0
#rfe23:FILENAME=d:\kenya7km\rfe\1989\dr89082.img
#rfe23:REPL_MISSING=0
#rfe24:FILENAME=d:\kenya7km\rfe\1989\dr89083.img
#rfe24:REPL_MISSING=0
#rfe25:FILENAME=d:\kenya7km\rfe\1989\dr89091.img
#rfe25:REPL_MISSING=0
#rfe26:FILENAME=d:\kenya7km\rfe\1989\dr89092.img
#rfe26:REPL_MISSING=0
#rfe27:FILENAME=d:\kenya7km\rfe\1989\dr89093.img
#rfe27:REPL_MISSING=0
#rfe28:FILENAME=d:\kenya7km\rfe\1989\dr89101.img
#rfe28:REPL_MISSING=0
```

```
#rfe29:FILENAME=d:\kenya7km\rfe\1989\dr89102.img
#rfe29:REPL_MISSING=0
#rfe30:FILENAME=d:\kenya7km\rfe\1989\dr89103.img
#rfe30:REPL_MISSING=0
#rfe31:FILENAME=d:\kenya7km\rfe\1989\dr89111.img
#rfe31:REPL_MISSING=0
#rfe32:FILENAME=d:\kenya7km\rfe\1989\dr89112.img
#rfe32:REPL_MISSING=0
#rfe33:FILENAME=d:\kenya7km\rfe\1989\dr89113.img
#rfe33:REPL_MISSING=0
#rfe34:FILENAME=d:\kenya7km\rfe\1989\dr89121.img
#rfe34:REPL_MISSING=0
#rfe35:FILENAME=d:\kenya7km\rfe\1989\dr89122.img
#rfe35:REPL_MISSING=0
#rfe36:FILENAME=d:\kenya7km\rfe\1989\dr89123.img
#rfe36:REPL_MISSING=0
#raw:FILENAME=d:\kenya7km\soils\rawcview.img
#plt:FILENAME=d:\kenya7km\lgp\start89.img
//#plt:FILENAME=c:\igt\cswb\dr1989\plt.img//
//?plt=p-2//
#lgp:FILENAME=d:\kenya7km\lgp\lgp.img
#harv:FILENAME=c:\temp\harv.img
#harv:IMGTYPE= 200
#harv:TITLE = End of Season
******
Calculate end of season by adding start* + lgp.
******
?harv=lgp+plt
**************************************************
Initialize model:
**************************************************
  soil water content (si)
  plant water needs (pwneedi)
  evapotranspiration (evapi)
  soil deficit (defici)
 *****
  Assume initial soil water content is 50mm or less.
 *****
#si:FILENAME=d:\kenya7km\soils\si.img
//#si:SLOPE=1
//#si:INTERCEPT =0
//#si:LUT=d:\igt\lut\universe.lut
//?si=if(raw>50,50,raw)
  **********
  Assume plant water needs, evap, and soil deficit are zero
at beggining of the year
  **********
#pwneedi:FILENAME=d:\kenya7km\soils\pwneedi.img
```

```
//#pwneedi:SLOPE=1
//#pwneedi:INTERCEPT =0
//#pwneedi:LUT=d:\igt\lut\universe.lut
//?pwneedi=0*si

#evapi:FILENAME=d:\kenya7km\soils\evapi.img
//#evapi:SLOPE=1
//#evapi:INTERCEPT =0
//#evapi:LUT=d:\igt\lut\universe.lut
//?evapi=0*si

#deficti:FILENAME=d:\kenya7km\soils\deficti.img
//#deficti:SLOPE=1
//#deficti:INTERCEPT =0
//#deficti:LUT=d:\igt\lut\universe.lut
//?deficti=0*si
**************************************************************
Divide main growing season into five parts for calculating
crop coefficient:
1. Pre-season.
2. Initial and vegetative phase.
3. Reproductive phase.
4. Maturing phase.
5. Post-season.
f1=0.16
f2=0.44
f3=0.76
k1=0.35
k2=1.20
k3=0.60

**************************************************************
DEKAD 1
**************************************************************
#xaxis:FILENAME=c:\temp\xaxis.img
#xaxis:IMGTYPE = 0
#xaxis:LUT =d:\igt\lut\universe.lut
#xaxis:BNA =d:\windisp3\bna\cpsz.bna
  ***
  Ensure no pixel=254 values (none) are present-i.e.,when
xaxis is negativeor lgp = 0.
  ***
?xaxis=if(plt<=1.and.plt>0,if(lgp>0,(1-plt+1)*100/lgp,0),0)
 *****
 Calculate plant water needs.
 *****
   Kc pre-season  and post season = 0.0 and Kc Initial
 *****
```

```
#kcpps:FILENAME=c:\temp\kcpps.img
#kcpps:IMGTYPE = 0
#kcpps:LUT =d:\igt\lut\universe.lut
kcpps:BNA =d:\windisp3\bna\cpsz.bna
?kcpps=if((xaxis=0.or.xaxis>100),0,if((xaxis<=16).and.(xaxis
>0),35,0))
 *****
   Kc Vegetative
 *****
#kcv:FILENAME=c:\temp\kcv.img
#kcv:IMGTYPE = 0
#kcv:LUT=d:\igt\lut\universe.lut
kcv:BNA=d:\windisp3\bna\cpsz.bna
?kcv=if((xaxis<=44.and.xaxis>16),(35+((120-35)/(44-
16))*(xaxis-16)),0)
 *****
   Kc Reproductive  and Kc Maturity
 *****
#kcrep:FILENAME=c:\temp\kcrep.img
#kcrep:IMGTYPE = 0
#kcrep:LUT=d:\igt\lut\universe.lut
kcrep:BNA=d:\windisp3\bna\cpsz.bna
?kcrep=if((xaxis<=76.and.xaxis>44),120,if((xaxis<=100.and.xa
xis>76),(120+((60-120)/(100-76))*(xaxis-76)),0))
 *****
   Add together all phases of the growing season.
 *****
#kc:FILENAME=\igt\cswb\dr1994\kc.img
#kc:IMGTYPE = 0
#kc:LUT =d:\igt\lut\universe.lut
kc:BNA =d:\windisp3\bna\cpsz.bna

FORMULA
kc=(kcpps+kcv+kcrep)

#w1:FILENAME=c:\temp\w1.img
#w1:IMGTYPE = 200
#w1:SLOPE = 1
#w1:INTERCEPT=0
#w1:REPL_MISSING=0
#w1:LUT=d:\igt\lut\universe.lut
w1:BNA=d:\windisp3\bna\cpsz.bna
?w1=(kcpps+kcv+kcrep)*pet1/100
  *****
  Calculate soil water balance.
  *****
#s1:FILENAME=c:\temp\S1.IMG
#s1:IMGTYPE = 200
```

```
#s1:SLOPE=1
#s1:INTERCEPT=0

#s1:REPL_MISSING=0
#s1:LUT=d:\igt\lut\universe.lut
s1:BNA=d:\windisp3\bna\cpsz.bna
#d1:FILENAME=c:\temp\D1.IMG
#d1:IMGTYPE = 200
#d1:SLOPE=1
#d1:INTERCEPT=0
#d1:REPL_MISSING=0
#d1:LUT=d:\igt\lut\universe.lut
d1:BNA=d:\windisp3\bna\cpsz.bna
#e1:FILENAME=c:\temp\E1.IMG
#e1:IMGTYPE =200
#e1:SLOPE=1
#e1:INTERCEPT=0
#e1:REPL_MISSING=0
#e1:LUT=d:\igt\lut\universe.lut
e1:BNA=d:\windisp3\bna\cpsz.bna
?s1=if(plt=1,si,if((si+rfe1)<w1,0,if((si+rfe1-
w1)<raw,si+rfe1-w1,raw)))
?d1=if((si+rfe1)<w1,w1-si-rfe1,0)
?e1=if((si+rfe1)<w1,si+rfe1,w1)
  ******
  Calculate index.
  ******
#pwneed1:FILENAME=c:\temp\pwneed1.img
#pwneed1:IMGTYPE =200
#pwneed1:SLOPE=1
#pwneed1:INTERCEPT = 0
#pwneed1:LUT=d:\igt\lut\universe.lut
pwneed1:BNA=d:\windisp3\bna\cpsz.bna
?pwneed1=if((xaxis>0.and.xaxis<=100),pwneedi+round(w1/10,1),
0)

#evap1:FILENAME=c:\temp\evap1.img
#evap1:IMGTYPE = 200
#evap1:SLOPE=1
#evap1:INTERCEPT = 0
#evap1:LUT=d:\igt\lut\universe.lut
evap1:BNA=d:\windisp3\bna\cpsz.bna
?evap1=if((xaxis>0.and.xaxis<=100),evapi+round(e1/10,1),0)

#defict1:FILENAME=c:\temp\defict1.img
#defict1:IMGTYPE = 200
#defict1:SLOPE=1
#defict1:INTERCEPT = 0
```

```
#defict1:LUT=d:\igt\lut\universe.lut
defict1:BNA=d:\windisp3\bna\cpsz.bna
?defict1=if((xaxis>0.and.xaxis<=100),deficti+round(d1/10,1),
0)

#index1:FILENAME=c:\temp\index1.img
#index1:IMGTYPE = 200
#index1:SLOPE=1
#index1:INTERCEPT = 0
#index1:LUT=d:\igt\lut\universe.lut
index1:BNA=d:\windisp3\bna\cpsz.bna
?index1=0*si


  *****
  Calulate yield. Assume YRR=1.5
  *****
#yld1:FILENAME=c:\temp\yld1.img
#yld1:IMGTYPE = 200
#yld1:SLOPE=1
#yld1:INTERCEPT = 0
#yld1:LUT=d:\igt\lut\universe.lut
yld1:BNA=d:\windisp3\bna\cpsz.bna
?yld1=0*si


************************************************************
DEKAD 2
************************************************************
#xaxis:FILENAME=c:\temp\xaxis.img
#xaxis:IMGTYPE = 0
#xaxis:LUT =d:\igt\lut\universe.lut
xaxis:BNA =d:\windisp3\bna\cpsz.bna
  ***
  Ensure no pixel=254 values (none) are present-i.e.,when
xaxis is negative
  or lgp = 0.
  ***
?xaxis=if(plt<=2.and.plt>0,if(lgp>0,(2-plt+1)*100/lgp,0),0)
 *****
 Calculate plant water needs.
 *****
   Kc pre-season  and post season = 0.0 and Kc Initial
 *****
#kcpps:FILENAME=c:\temp\kcpps.img
#kcpps:IMGTYPE = 0
#kcpps:LUT =d:\igt\lut\universe.lut
kcpps:BNA =d:\windisp3\bna\cpsz.bna
```

```
?kcpps=if((xaxis=0.or.xaxis>100),0,if((xaxis<=16).and.(xaxis
>0),35,0))
 *****
   Kc Vegetative
 *****
#kcv:FILENAME=c:\temp\kcv.img
#kcv:IMGTYPE = 0
#kcv:LUT=d:\igt\lut\universe.lut
kcv:BNA=d:\windisp3\bna\cpsz.bna
?kcv=if((xaxis<=44.and.xaxis>16),(35+((120-35)/(44-
16))*(xaxis-16)),0)
 *****
   Kc Reproductive  and Kc Maturity
 *****
#kcrep:FILENAME=c:\temp\kcrep.img
#kcrep:IMGTYPE = 0
#kcrep:LUT=d:\igt\lut\universe.lut
kcrep:BNA=d:\windisp3\bna\cpsz.bna
?kcrep=if((xaxis<=76.and.xaxis>44),120,if((xaxis<=100.and.xa
xis>76),(120+((60-120)/(100-76))*(xaxis-76)),0))
 *****
   Add together all phases of the growing season.
 *****
#kc:FILENAME=c:\temp\kc.img
#kc:IMGTYPE = 0
#kc:LUT =d:\igt\lut\universe.lut
kc:BNA =d:\windisp3\bna\cpsz.bna

FORMULA
kc=kcpps+kcv+kcrep

#w2:FILENAME=c:\temp\w2.img
#w2:IMGTYPE = 200
#w2:SLOPE=1
#w2:INTERCEPT=0
#w2:REPL_MISSING=0
#w2:LUT=d:\igt\lut\universe.lut
w2:BNA=d:\windisp3\bna\cpsz.bna
?w2=(kcpps+kcv+kcrep)*pet2/100
  *****
  Calculate soil water balance.
  *****
#s2:FILENAME=c:\temp\S2.IMG
#s2:IMGTYPE = 200
#s2:SLOPE=1
#s2:INTERCEPT=0
#s2:REPL_MISSING=0
#s2:LUT=d:\igt\lut\universe.lut
```

```
s2:BNA=d:\windisp3\bna\cpsz.bna
#d2:FILENAME=c:\temp\D2.IMG
#d2:IMGTYPE = 200
#d2:SLOPE=1
#d2:INTERCEPT=0
#d2:REPL_MISSING=0
#d2:LUT=d:\igt\lut\universe.lut
d2:BNA=d:\windisp3\bna\cpsz.bna
#e2:FILENAME=c:\temp\E2.IMG
#e2:IMGTYPE = 200
#e2:SLOPE=1
#e2:INTERCEPT=0
#e2:REPL_MISSING=0
#e2:LUT=d:\igt\lut\universe.lut
e2:BNA=d:\windisp3\bna\cpsz.bna
?s2=if(plt=2,si,if((s1+rfe2)<w2,0,if((s1+rfe2-
w2)<raw,s1+rfe2-w2,raw)))
Below is the old formula.
s2=if(plt=2,si,if((s1+rfe2)<w2,0,if((s1+rfe2-
w2)<raw,s1+rfe2-w2,raw)))

?d2=if((s1+rfe2)<w2,w2-s1-rfe2,0)
The formula below can be manipulated to develop a surplus
image if desired.
d2=if((s1+rfe2)<w2,w2-s1-rfe2,if((s1+rfe2-w2)<raw,0,s1+rfe2-
w2-raw))
?e2=if((s1+rfe2)<w2,s1+rfe2,w2)
  ******
  Calculate index.
  ******
#pwneed2:FILENAME=c:\temp\pwneed2.IMG
#pwneed:IMGTYPE =200
#pwneed:SLOPE=1
#pwneed:INTERCEPT = 0
#pwneed2:LUT=d:\igt\lut\universe.lut
pwneed2:BNA=d:\windisp3\bna\cpsz.bna
?pwneed2=if((xaxis>0.and.xaxis<=100),pwneed1+round(w2/10,1),
0)

#evap2:FILENAME=c:\temp\evap2.IMG
#evap2:IMGTYPE = 200
#evap2:SLOPE=1
#evap2:INTERCEPT = 0
#evap2:LUT=d:\igt\lut\universe.lut
evap2:BNA=d:\windisp3\bna\cpsz.bna
?evap2=if((xaxis>0.and.xaxis<=100),evap1+round(e2/10,1),0)

#defict2:FILENAME=c:\temp\defict2.img
```

```
#defict2:IMGTYPE = 200
#defict2:SLOPE=1
#defict2:INTERCEPT = 0
#defict2:LUT=d:\igt\lut\universe.lut
#defict2:BNA=d:\windisp3\bna\cpsz.bna
?defict2=if((xaxis>0.and.xaxis<=100),defict1+round(d2/10,1),
0)

#index2:FILENAME=c:\temp\index2.img
#index2:IMGTYPE = 200
#index2:SLOPE=1
#index2:INTERCEPT = 0
#index2:LUT=d:\igt\lut\universe.lut
index2:BNA=d:\windisp3\bna\cpsz.bna
?index2=if(pwneed2=0,0,if(lgp>0.and.harv=3,100*(1-
defict2/pwneed2),index1))

  *****
  Calulate yield. Assume YRR=1.5
  *****
#yld2:FILENAME=c:\temp\yld2.img
#yld2:IMGTYPE = 200
#yld2:SLOPE=1
#yld2:INTERCEPT = 0
#yld2:LUT=d:\igt\lut\universe.lut
yld2:BNA=d:\windisp3\bna\cpsz.bna
?yld2=if(pwneed2=0,0,if(lgp>0.and.harv=3,if(evap2/pwneed2<=1
/3,254,100-150*(1-evap2/pwneed2)),yld1))


**************************************************************
REPEAT SECOND DEKAD STEP FOR DEKADS 3-36.
**************************************************************
```

REFERENCES

Allen, J.C. 1976. A Modified Sine Wave Method for Calculating Degree Days. Environmental Entomology. 5(3):338-396.

Barret, C. 1979. Crop Monitoring and Prediction Using Satellite Data Inputs. Satellite Remote Sensing Application in Agroclimatology and Agrometeorology. European Space Agency, pp. 149-163.

Baier, W. 1977. Crop-Weather Models and Their Use in Yield Assessments. World Meteorological Organization. Technical Report No. 151.

Baier, W. and G.W. Robertson. 1968. The Performance of Soil Moisture Estimates as Compared with the Direct Use of Climatological Data for Estimating Crop Yields. Agricultural Meteorology, 5:17-31.

Boatwright, G.O. and V.S. Whitehead. 1986. Early Warning and Crop Condition Assessment Research. IEEE Transactions on Geoscience and Remote Sensing. GE-24(1);54-64.

Davenport, M.L. and S.E. Nicholson. 1993. On the Relation between Rainfall and the Normalized Difference Index for Diverse Vegetation Types in East Africa. International Journal of Remote Sensing. 14(12);2369-2389.

Doorenbos, J. and W.O. Pruitt. 1977. Guidelines for Predicting Crop Water Requirements. FAO Irrigation and Drainage Paper No. 24., Rome, Italy.

Doorenbos, J. and A.H. Kassam. 1979. Yield Response to Water. FAO Irrigation and Drainage Paper No. 33. Rome, Italy.

Eastman, J. R. 1997. IDRISI for Windows User's Guide and Tutorial Exercises. Version 2.0. IDRISI Production, Clark University, Worcester, MA.

Eiden, G., C. Dreiser, G. Gesell, and T. König. 1991. Large Scale Monitoring of Rangeland Vegetation Using NOAA/11 AVHRR LAC Data. Application to the Rainy Seasons 1989/90 in Northern Kenya. GTZ Range Management Handbook of Kenya, Volume III/4, Nairobi, Kenya/Oberpfaffenhofen, Germany.

Eilerts, G.S. 1993. Information Presentation and Targeting for Early Warning and Global Food Security. Proceedings of the Twenty-Fifth International Symposium, Remote Sensing and Global Environmental Change, Graz, Austria, April 4-8, pp. I-24-I-34.

Eidenshink, J.C., and J.L. Faundeen. 1996. The 1-Kilometer AVHRR Global Land Data Set: First Stages in Implementation. International Journal of Remote Sensing. URL:http://edcwww.cr.usgs.gov/landdaac/1km/1kmhomepage.html

FAO. 1978. Report on the Agro-Ecological Zones Project. Vol. 1, Methodology and Results for Africa. Rome, Italy.

FAO. 1986. Early Agrometeorological Crop Yield Assessment. FAO Plant Production and Protection Paper No. 73. Rome, Italy.

FAO. 1989. The Use of Agrometeorological Models for Crop Monitoring and Yield Forecasting. Workshop on Strengthening National Early Warning and Food Information Systems in Africa. October 23-26, Accra, Ghana.

FAO. 1994. ARTEMIS NDVI CD-ROM.

FAO. 1995. FAO Digital Soil Map of the World and Derived Soil Properties, Version 3.5, FAO, Rome, Italy.

FAO. 1997. FAOSTAT Statistics Database URL:http://apps.fao.org/default.htm

FEWS. 1997. Data from FEWS-Nairobi Office. Unpublished.

FEWS. 1998. FEWS Home Page. URL:http//www.info.usaid.gov/fews/fews.html

Frère, M. and G.F. Popov. 1979. Agrometeorological Crop Monitoring and Forecasting. FAO Plant Production and Protection Paper No. 17. Rome, Italy.

Gallo, K.P. and T.K. Flesch. 1989. Large-Area Crop Monitoring with the NOAA AVHRR: Estimating the Silking Stage of Maize Development. Remote Sensing of the Environment. 27:73-80.

Ganzin, Nicolas. 1995. Satellite Monitoring of Arid Rangelands, SMAR Version 1.2, Internal User's Guide, Biomass Monitoring Unit of the Department of Resource Surveys and Remote Sensing, Republic of Kenya, July, 1995.

Gommes, R.A. 1983. Pocket Computers in Agrometeorology. FAO Plant Production and Protection Paper No. 45. Rome, Italy.

Gommes, R. 1993. FAOINDEX, Version 2.1m, Agrometeorology Group, FAO, Rome, Italy.

Gommes, R. and M. Houssiau. 1983 Rainfall Variability of Growing Seasons and Cereal Yields in Tanzania. Crop Monitoring and Early Warning Project, pp. 312-324.

Hassan, R.M. 1997. New Tools and Emerging Challenges for Agriculture Research: Methods and Results from a GIS Application to Maize in Kenya", In Press.

Hatfield, J.L. 1983. Remote Sensing Estimators of Potential and Actual Crop Yield. Remote Sensing of the Environment. 13;301-311.

Henricksen, B.L. and J.W. Durkin. 1985. Moisture Availability, Cropping Period, and the Prospects for Early Warning of Famine in Ethiopia. ILCA Bulletin 21. January, pp. 2-9.

Henricksen, B.L. and J.W. Durkin. 1986. Growing Period and Drought Early Warning in Africa Using Satellite Data. International Journal of Remote Sensing. 7(11);1583-1608.

Herman, A., P. Arkin, D. Miskus. 1994. Ten Day Rainfall Estimates for the African Sahel Using the Combination of High Resolution Meteosat Infared and Rain Gauge Data for the 1993 Growing Season. Seventh Conference Satellite Meteorology and Oceanography. American Meteorological Society.

Herman, A., V.B. Kumar, P.A. Arkin, and J.V. Kousky. 1997. Objectively Determined 10-Day African Rainfall Estimates Created for Famine Early Warning Systems. International Journal of Remote Sensing. Submitted for publication with the International Journal of Remote Sensing. URL:http://edcintl.cr.usgs.gov/adds/data/rfed/

Hielkema, J.U., J.A. Howard, C.J. Tucker, and H.A. van Ingen Schenau. 1986. The FAO/NASA/NLR ARTEMIS System: An Integrated Concept for Environmental Monitoring by Satellite in Support of Food/Feed Security and Desert Locust Surveillance. Proceedings at the Twentieth International Symposium on Remote Sensing of Environment, Nairobi, Kenya, December 4-10, pp. I47-I59.

Hielkema, J.U. 1991. Operational Environmental Satellite Remote Sensing for Food Security and Locust Control by FAO. Paper presented at the International Training Course on Remote Sensing Applications for Environmental Assessment and Monitoring. Sioux Falls, South Dakota, USA, September 9-October 4, 1991.

Hoefsloot, P. 1996. IGT Manual for Version 1.10. Working Paper Series No. 5, SADC Regional Remote Sensing Project.

Horie, T., M. Yajima, and H. Nakagawa. 1992. Yield Forecasting. Agricultural Systems. 40;211-236.

Hutchinson, C.F. 1991. Uses of Satellite Data for Famine Early Warning in sub-Saharan Africa. International Journal of Remote Sensing, 12(6);1405-1421.

Hutchinson, C.F., S.E. Marsh, E.S. Pfirman, and C.A.J. van der Harten. 1993. Information Technology and Famine Early Warning. Proceedings of the Twenty-Fifth International Symposium, Remote Sensing and Global Environmental Change, Graz, Austria, April 4-8, pp. I13-I23.

Johnson, G.E., C.M. Sakamoto, S.K. LeDuc, and S.L. Callis. 1987. The Application of Drought Early Warning in Africa. Proceedings of the Twenty-First International Symposium on Remote Sensing of Environment. Ann Arbor, Michigan. October 26-30, pp. 361-379.

Johnson, G.E., A. van Dijk, and C.M. Sakamoto. 1987. The Use of AVHRR Data in Operational Agricultural Assessment in Africa. Geocarto International. 1;41-60.

Justice, C.O., B.N. Holben, and M.D. Gwynne. 1986. Monitoring East African Vegetation Using AVHRR Data. International Journal of Remote Sensing. 7;1475-1497.

Justice, C.O., G. Dugdale, J.R.G. Townshend, A.S. Narrocott, and M. Kumar. 1991. Synergism between NOAA-AVHRR and Meteosat Data for Studying Vegetation Development in Semi-Arid West Africa. International Journal of Remote Sensing. 12(6);1349-1368.

Kassam, A.H., H.T. van Velthuizen, G.W. Fisher, and M.M. Shah. 1993a. Agro-Ecological Assessments for National Planning: The Example of Kenya. FAO Soils Bulletin 67.

Kassam, A.H., H.T. van Velthuizen, G.W. Fisher, and M.M. Shah. 1993b. Agro-ecological Land Resources Assessment for Agricultural Development Plan: A Case Study of Kenya. Main Report and Technical Annex 1-9, World Resources Report No. 71/1-9.

LeCompte, D. 1989. Using AVHRR for Early Warning of Famine in Africa. Photogrammetric Engineering and Remote Sensing. 55;168-169

Lee, F.F. 1997. VAST: Vegetation Analysis in Space and Time. Version, 4.0, Famine Early Warning System Project, Arlington, VA, USA.

Malo, A.R. and S.E. Nicholson. 1990. A Study of Rainfall and Vegetation Dynamics in the African Sahel Using Normalized Difference Vegetation Index. Journal of Arid Environments. 19;1-24.

Motha, R.P. and T.R. Heddinghaus. 1986. The Joint Agricultural Weather Facility's Operational Assessment Program. Bulletin American Meteorological Society. September, 67(9);1114-1122.

Negre, T. 1994. An Assessment of the State of Agrometeorological Monitoring and Yield Forecasting in the SADC Regional Early Warning. FAO SADC Early Warning System Working Paper. Rome, Italy.

Philipson, W.R. and W.L. Teng. 1988. Operational Interpretation of AVHRR Vegetation Indexes for World Crop Information. Photogrammetric Engineering and Remote Sensing. January, 54(1);55-59.

Pfirman, E. 1998. SEDI Combined with WINDISP3. E-mail announcement. March.

Pfirman, E. and P. Hoefsloot. 1995. IDA for DOS v.4.2 User Manuel. FAO Technical Report GCP/INT/578/NET, Rome, Italy.

Pfirman, E. and J. Hogue. 1997. WINDISP3 Users Manual. Unpublished.

Quarmby, N.A., M. Milnes, T.L. Hindle, and N. Silleos. 1993. The Use of Multitemporal NDVI Measurements from AVHRR Data for Crop Yield Estimation and Prediction. International Journal of Remote Sensing. 14(2);199-210.

Ropelewski. C. and Halpert, M. 1987. Global and Regional Scale Precipitation Patterns Associated with El Niño/Southern Oscillation. Monthly Weather Review, 115:2352-2362.

Rosema, A., R. A. Roebeling, A. van Dijk, G.A.J. Nieuwenhuis, J. Huygen, and D.A. Kashasa. 1996. ACMP: Agromet and Crop Monitoring Project in the SADC Region. Unpublished Draft Report.

Sakamoto, C.M. and L.T. Steyaert. 1987. International Drought Early Warning Program of NOAA/NESDIC/AISC. P-lanning for Drought: Toward a Reduction of Societal Vulnerability, edited by D.A. Wilhite, et al., Westview Press, Boulder, Colorado, Chap. 16, pp. 247-272.

Sammis, T.W., C.L. Mapel, D.G. Lugg, R.R. Lansford, and J.T. McGuckin. 1985. Evapotranspiration Crop Coefficients Predicted Using Growing Degree Days. Trans. Amer. Soc. Agric. Engrs. 28:773-780.

Snijders, F.L. 1995. ARTEMIS and the Outside World File Formats and Naming Conventions. . FAO Agrometeorology Series Working Paper, No. 13, "Coordination and Harmonisation of Database of Databases and Software for Agroclimatic Applications", FAO, Rome Italy.

Solomon, K.H. 1985. Typical Crop Water Production Functions. ASAE Paper No. 85-2596.

Stegman, E.C. 1988. Corn Crop Curve Comparisons for the Central and Northern Plains of the U.S. Applied Engineering in Agriculture. 4(3):226-233.

Stewart, J.I. 1988. Response Farming in Rainfed Agriculture. The WHARF Foundation Press. Davis, California.

Stewart, J.I. and R.H. Hagan. 1973. Functions to Predict Effects of Crop Water Deficits. ASCE Journal of the Irrigation and Drainage Division. December, 99(IR4);421-439.

Stewart, J.I. and C.H. Hash. 1982. Impact of Weather Analysis on Agricultural Production and Planning Decisions for the Semiarid Areas of Kenya. Journal of Applied Meteorology. April, 21;477-494.

Stewart, J.I., R.D. Misra, W.O. Pruitt, and R.M. Hagan. 1975. Irrigating Maize and Grain Sorghum with a Deficient Water Supply. Transactions of the ASAE, pp. 270-290.

Thornton, P.K., W.T. Bowen, A.C. Ravelo, P.W. Wilkens, G. Farmer, J. Brock, and J.E. Brink. 1997. Estimating Millet Production for Famine Early Warning: An Application of Crop Simulation Modelling Using Satellite and Ground-based Data in Burkina Faso. Agricultural and Forest Meteorology. Elsevier Science, Amesterdam, The Netherlands. 83(1997); 95-112.

Thornton, P.K., A.R. Saka, U. Singh, J.D.T. Kumwenda, J.E. Brink, and J.B. Dents. 1995. Application of a Maize Crop Simulation Model in the Central Region of Malawi. Experimental Agriculture. 32(1995); 213-226.

Wiegand, C.L., A.J. Richardson, R.D. Jackson, P.J. Pinter Jr., J.K. Aase, D.E. Smika, L.F. Lautenschlager, and J.E. McMurtrey III. 1986. Development of Agrometeorological Crop Model Inputs from Remotely Sensed Information. IEEE Transactions on Geoscience and Remote Sensing. January, GE-24(1);90-98.

van Velthuizen, H., L. Verelst, and P. Santacroce. 1995. Crop Production System Zones of the IGADD Sub-Region. Agrometeorology Working Paper Series No. 10, FAO, Rome, Italy.

Vossen, P. and D. Ruks. 1995. Early Crop Yield Assessment of the EU Countries: The System Implemented by the Joint Research Centre. Office for Official Publications of the European Communities, Brussels.

IMAGE EVALUATION TEST TARGET (QA-3)

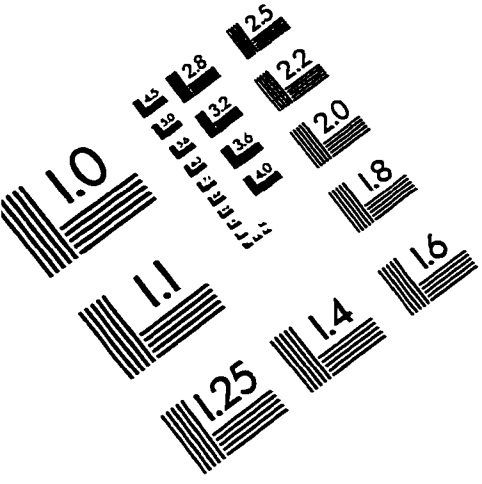

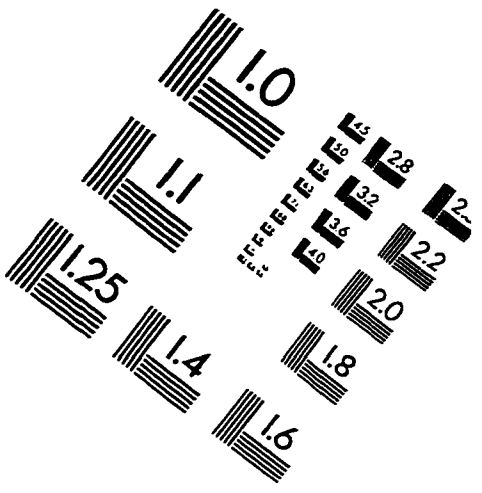

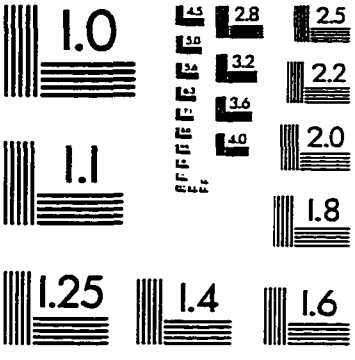

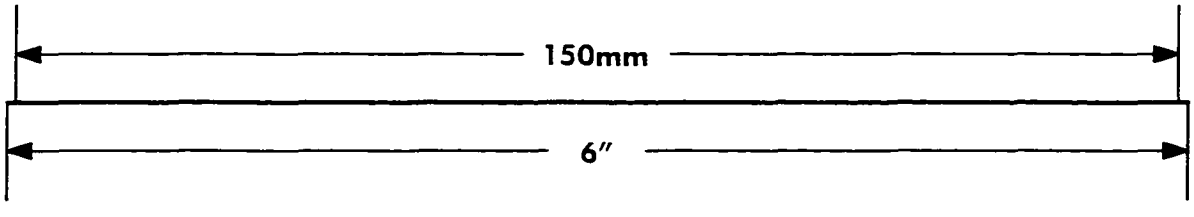

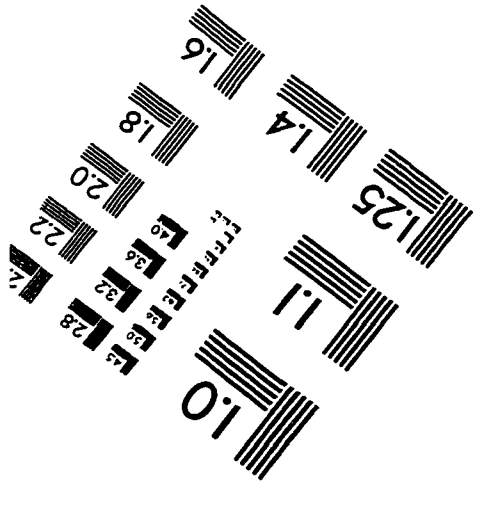

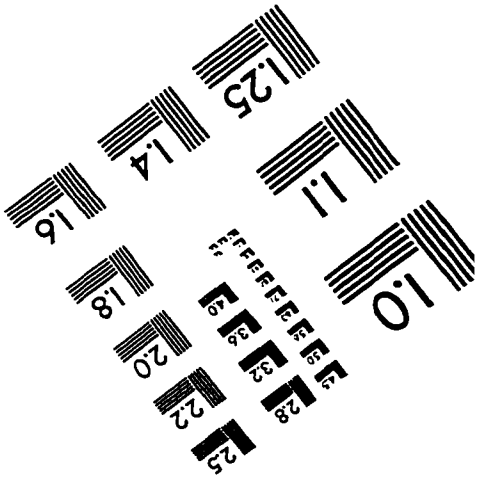

APPLIED IMAGE, Inc
1653 East Main Street
Rochester, NY 14609 USA
Phone: 716/482-0300
Fax: 716/288-5989